A COMPARATIVE ASSESSMENT OF MECHANISTIC LOAD EQUIVALENCE FACTORS FOR FLEXIBLE PAVEMENTS

MARIUS-ADRIAN OANCEA

A COMPARATIVE ASSESSMENT OF MECHANISTIC LOAD EQUIVALENCE FACTORS FOR FLEXIBLE PAVEMENTS

BY

(c) Marius-Adrian Oancea

A thesis submitted in partial fulfillment
of the requirements for the degree of
Master of Engineering

Faculty of Engineering and Applied Science
Memorial University of Newfoundland
June 1991

St. John's Newfoundland Canada

ISBN 0-315-68228-0

Canada

ABSTRACT

This study deals with mechanistic Load Equivalence Factors (LEF) for flexible pavements. It addresses two sets of objectives. First, a theoretical investigation of cycle counting methodologies used for mechanistic LEF's calculation was carried out. Second, a number of these methods were used for calculating LEF's from in-situ strains.

The study includes an extensive literature review, starting with the empirical approach proposed by the AASHO Road Test (AASHO, 1961). Mechanistic methods for LEF's calculation are subsequently introduced and discussed.

Next, the concept of fatigue cycle, as defined by the ASTM standard E 1049-85, is introduced and its applicability to flexible pavements is investigated. As a result of the comparison of all the fatigue cycle counting methods proposed by the standard, the Range-Pair Counting Method was selected for LEF's calculation.

The experiment undertaken in order to obtain strain versus time histories included two experimental trucks, namely a 3-axle configuration and a 5-axle configuration. The experiment involved 3 levels of speed, 3 levels of loading and 2 replicate runs of the experimental vehicles for each speed and load combination. Each set of 2 replicate runs of the experimental

trucks were followed by an equal speed run of the Benkelman Beam truck.

Resulting strain versus time histories were evaluated in terms of the quality of the lateral placement. Those corresponding to the best lateral placements were processed by the proposed ASTM Range-Pair Cycle Counting method, by the mechanistic method employed during the RTAC 1986 study, and the results were compared to the empirical AASHO LEF's. A new integral approach, based on the cycle definition provided by the selected ASTM method for cycle counting, was also introduced.

Comparative assessment of LEF's calculated by different methods was made in order to validate numerically and investigate the suitability of each method for LEF's calculation.

ACKNOWLEDGEMENTS

I would like to express my deep gratitude to my supervisor, Dr. A.T. Papagiannakis for his continuous guidance, valuable suggestions, moral and material support during the entire period of this work.

The author is also grateful to Dr. T.R. Chari, Associated Dean of Graduate Studies, Faculty of Engineering and Applied Science, for the understanding and support received.

The financial assistance received from the Memorial University of Newfoundland is thankfully acknowledged.

Table of Contents

Abstract	i
Acknowledgements	iii
Table of Contents	iv
Table of Figures	vi
Table of Tables	x
Chapter 1 INTRODUCTION AND BACKGROUND	1
Chapter 2 OBJECTIVES	4
Chapter 3 LITERATURE REVIEW	6
3.1 AASHO Road Test (1962)	6
3.2 Study by Deacon (1969)	12
3.3 Study by Ramsamooj et al. (1972)	16
3.4 Study by Christison et al. (1978)	19
3.5 Study by Treybig (1983)	25
3.6 Study by Southgate et al. (1985)	29
3.7 ASTM E 1049-85 Standard Practices for Cycle Counting in Fatigue Analysis (1985)	34
3.7.1 Level-Crossing Counting	36
3.7.2 Peak Counting	37
3.7.3 Simple-Range Counting	38
3.7.4 Range-Pair Counting	39
3.7.5 Rainflow Counting	40
3.8 RTAC Vehicle Weights and Dimensions Study (1986)	41
3.9 AASHO Interim Guide for the Design of Flexible Pavements (1986)	46
3.10 Study by Hutchinson et al. (1987)	47
3.11 Study by Majidzadeh et al. (1988)	52
3.12 Study by Hajek et al. (1989)	54
3.13 Study by Govind et al. (1990)	56
3.14 Study by Tseng and Lytton (1990)	60
3.15 Summary of Methods for LEF's calculation	66
Chapter 4 CRITICAL OVERVIEW OF LITERATURE	70
4.1 The AASHO Road Test	70
4.2 Mechanistic Methods for LEF's Determination	72
4.3 The Methods for Cycle Counting by the ASTM 1049-85 Standard	78
4.3.1 The Simple Range Counting Method	82
4.3.2 The Peak Counting Method	84
4.3.3 The Rainflow Counting Method	87
4.3.4 The Range-Pair Counting Method	88
Chapter 5 THE EXPERIMENTAL PROGRAM	93
5.1 The Experimental Site	93
5.2 The Experiment	96
Chapter 6 METHODOLOGY	10-
6.1 Selection of Runs and Strain Gauge Responses to Analyze	10/

6.2 Selection of the Values Characterizing the Strain Cycles 116
Chapter 7 RESULTS AND DISCUSSION 122
7.1 LEF's Obtained by the ASTM Range-Pair Counting Method 123
7.1.1 LEF's for Individual Axles and Axle Groups 123
7.1.2 Vehicle LEF's 132
7.2 Comparison of the ASTM LEF's to the RTAC LEF's 136
7.3 Comparison of the ASTM LEF's to the AASHO LEF's 145
7.4 LEF's Obtained by Integrating the Strain Cycles 154
7.4.1 Trough-Peak-Trough Integrals 155
Chapter 8 CONCLUSIONS 164
REFERENCES 167
Appendix A Strain Peaks and Integrals versus Vehicle Lateral Placement 172
Appendix B Software for Processing Experimental Data 185
Appendix C Load Equivalency Factors' Tables 194
C.1 LEF's Obtained by the ASTM Range-Pair Counting and the RTAC Method 194
C.2 Comparison between LEF's Obtained by Discrete Methods 199
C.3 LEF's Obtained by Integrating the Strain Cycles 207

Table of Figures

Nr.	Title	Page
3.1	Plane View of Load Arrangement for Stress Computations, (After Deacon, 1969)	14
3.2	Strain Distribution for 36-kip Tandem Axle, (After Deacon, 1969)	15
3.3	LEF Calculation for Tandem Axles, (After Ramsamooj et al., 1972)	18
3.4	Strain Peaks Extraction from Response Curve	21
3.5	Deflection Peaks Extraction from Response Curve	23
3.6	Typical Strain Profile under an 80 kN Single Axle, (After Christison et al., 1978)	24
3.7	Strain Extraction Based on the Curvature Method for a Subgrade Vertical Strain Pattern	27
3.8	Development of Load Equivalency Factors Based on Tensile Strain Using the Curvature Method, for SN=5.51, (After Treybig, 1983)	28
3.9	Comparison of LEF's Based on Compressive Strain, Curvature Method versus AASHO, (After Treybig, 1983)	29
3.10	Tensile Strain versus Work Strain, (After Southgate et al., 1985)	32
3.11	Variation of Damage Factors for selected Axle Groups as Load on Axle Group is Changed, (After Southgate et al., 1985)	33
3.12	Basic Fatigue Loading Parameters, (After ASTM E 1049, 1985)	35
3.13	ASTM Level Crossing Counting and Derived Cycles, (After ASTM E 1049, 1985)	36
3.14	ASTM Peak Counting and derived cycles, (After ASTM E 1049, 1985)	37
3.15	ASTM Simple Range Counting Method, (After ASTM E 1049, 1985)	38
3.16	ASTM Range-Pair Counting Method, (After ASTM E 1049, 1985)	39
3.17	ASTM Rainflow Counting Example, (After ASTM E 1049, 1985)	40
3.18	Maximum Benkelman Beam Rebound versus Cumulative ESAL, (After RTAC, 1986)	42
3.19	A Longitudinal Interfacial Tensile Strain Profile under a Tridem Group, (After RTAC, 1986)	44
3.20	Hypothesized Load-Deflection History for Tridem Pass, (After Hutchinson et al., 1987)	50

3.21	Comparative Methods for Deflection Peak Extraction, (After Hutchinson et al., 1987)	51
3.22	Assumed Deflection Profile for an Axle, (After Majidzadeh et al., 1988)	52
3.23	LEF's for Various Axle Spacing Values, (After Majidzadeh et al., 1988)	54
3.24	Peak Method Applied to Multiple Axle Groups Responses, (After Hajek et al., 1989)	55
3.25	Wave Shape of Loading Pulse Produced by a Tandem, (After Tseng et al., 1990)	61
3.26	Wave Shape of Loading Pulse Produced by a Single Axle, (After Tseng et al., 1990)	63
4.1	Strain Pattern Produced by a Tandem	82
4.2	Range Extraction Based on the Simple Range Counting Method	84
4.3	Cycle Identification According to Peak Counting Method	85
4.4	Cycle Construction According to Peak Counting Method	86
4.5	Cycle Identification According to Rainflow Counting Method	88
4.6	Cycle Counting According to Range-Pair Counting Method	89
4.7	Cycle Extraction Depending on the Slope of the First Range	90
4.8	Cycle Counting According to Restricted Range-Pair Counting Method	91
5.1	Instrumentation Layout	94
5.2	The Strain Gauge Carrier and its Location	96
5.3	Flexible Pavement Cross Section	97
5.4	Dimensions of Test Vehicles	98
5.5	Tire Dimensions of the Experimental Trucks	99
5.6	Layout of Video Logging Camera System, (After Taylor, 1989)	105
6.1	Pooled Strain Peaks versus Lateral Placement at Three Levels of Speed	118
7.1	LEF's for 3-Axle Truck, Steering Axle, Calculated by ASTM Range-Pair Counting Method	126
7.2	LEF's for 3-Axle Truck, Tandem, Calculated by ASTM Range-Pair Counting Method	128
7.3	LEF's for 5-Axle Truck, Steering Axle, Calculated by ASTM Range-Pair Counting Method	130
7.4	LEF's for 5-Axle Truck, 1st Tandem, Calculated by ASTM Range-Pair Counting Method	131
7.5	LEF's for 5-Axle Truck, 2nd Tandem, Calculated by ASTM Range-Pair Counting Method	131

7.6	Two Approaches for Strain Cycles Identification	133
7.7	LEF's for 3-Axle Truck, Entire Vehicle, Calculated by ASTM Range-Pair Counting Method	134
7.8	LEF's for 5-Axle Truck, Calculated by ASTM Range-Pair Counting Method	135
7.9	Comparison of ASTM LEF's to RTAC LEF's for 3-Axle Truck, Steering Axle, Speed 20 km/h	137
7.10	Comparison of ASTM LEF's to RTAC LEF's for 3-Axle Truck, Steering Axle, Speed 40 km/h	138
7.11	Comparison of ASTM LEF's to RTAC LEF's for 3-Axle Truck, Steering Axle, Speed 50 km/h	138
7.12	Comparison of ASTM LEF's to RTAC LEF's for 3-Axle Truck, Tandem, Speed 20 km/h	139
7.13	Comparison of ASTM LEF's to RTAC LEF's for 3-Axle Truck, Tandem, Speed 40 km/h	140
7.14	Comparison of ASTM LEF's to RTAC LEF's for 3-Axle Truck, Tandem, Speed 50 km/h	140
7.15	Comparison of ASTM LEF's to RTAC LEF's for 5-Axle Truck, Steering Axle, Speed 20 km/h	141
7.16	Comparison of ASTM LEF's to RTAC LEF's for 5-Axle Truck, Steering Axle, Speed 40 km/h	142
7.17	Comparison of ASTM LEF's to RTAC LEF's for 5-Axle Truck, Steering Axle, Speed 50 km/h	142
7.18	Comparison of ASTM LEF's to RTAC LEF's for 5-Axle Truck, Tandems , Speed 20 km/h	143
7.19	Comparison of ASTM LEF's to RTAC LEF's for 5-Axle Truck, Tandems, Speed 40 km/h	144
7.20	Comparison of ASTM LEF's to RTAC LEF's for 5-Axle Truck, Tandems, Speed 50 km/h	144
7.21	Comparison of ASTM LEF's to AASHO LEF's for 3-Axle Truck, Steering Axle, Speed 20 km/h	146
7.22	Comparison of ASTM LEF's to AASHO LEF's for 3-Axle Truck, Steering Axle, Speed 40 km/h	147
7.23	Comparison of ASTM LEF's to AASHO LEF's for 3-Axle Truck, Steering Axle, Speed 50 km/h	147
7.24	Comparison of ASTM LEF's to AASHO LEF's for 3-Axle Truck, Tandem, Speed 20 km/h	148
7.25	Comparison of ASTM LEF's to AASHO LEF's for 3-Axle Truck, Tandem, Speed 40 km/h	149
7.26	Comparison of ASTM LEF's to AASHO LEF's for 3-Axle Truck, Tandem, Speed 50 km/h	149
7.27	Comparison of ASTM LEF's to AASHO LEF's for 5-Axle Truck, Steering Axle, Speed 20 km/h	150
7.28	Comparison of ASTM LEF's to AASHO LEF's for 5-Axle Truck, Steering Axle, Speed 40 km/h	150
7.29	Comparison of ASTM LEF's to AASHO LEF's for 5-Axle Truck, Steering Axle, Speed 50 km/h	151

7.30	Comparison of ASTM LEF's to AASHO LEF's for 5-Axle Truck, Tandems , Speed 20 km/h	152
7.31	Comparison of ASTM LEF's to AASHO LEF's for 5-Axle Truck, Tandems, Speed 40 km/h	152
7.32	Comparison of ASTM LEF's to AASHO LEF's for 5-Axle Truck, Tandems, Speed 50 km/h	153
7.33	Strain versus Time History Presenting a Composite Steering-Interaxle Strain Cycle	157
7.34	LEF's for 3-Axle Truck, Steering Axle, Calculated using Trough-Peak-Trough Integrals	158
7.35	LEF's for 3-Axle Truck, Tandem, Calculated using Trough-Peak-Trough Integrals	159
7.36	LEF's for 3-Axle Truck, Entire Vehicle, Calculated using Trough-Peak-Trough Integrals	160
7.37	LEF's for 5-Axle Truck, Steering Axle, Calculated using Trough-Peak-Trough Integrals	161
7.38	LEF's for 5-Axle Truck, 1st Tandem, Calculated using Trough-Peak-Trough Integrals	162
7.39	LEF's for 5-Axle Truck, 2nd Tandem, Calculated using Trough-Peak-Trough Integrals	162
7.40	LEF's for 5-Axle Truck, Entire Vehicl , Calculated using Trough-Peak-Trough Integrals	163
B.1	Strain versus Time History for Run 2, Gauge 3	186
B.2	Identification of the First Strain Cycle	188
B.3	Processing of the First Strain Cycle	189
B.4	Identification of the Second Strain Cycle	190
B.5	Processing of the Second Strain Cycle	190
B.6	Identification of the Third Strain Cycle	191
B.7	Processing of the Third Strain Cycle	191
B.8	Identification of the Fourth Strain Cycle	192
B.9	Processing of the Fourth Strain Cycle	192
B.10	Compressive Cycle Obtained after the Processing of the Strain versus Time History	193

Table of Tables

Nr.	Title	Page
3.1	Average Pavement Ratios and Load Equivalency Factors at one Experimental Site, (After RTAC, 1986)	45
3.2	Summary of Methods for LEF's Calculation	66
5.1	Static Loads of Test Vehicles	100
5.2	Run Characteristics	102
6.1	Relative Lateral Placement (3-axle truck)	110
6.2	Relative Lateral Placement (5-axle truck)	111
6.3	Selected Runs (3-axle truck)	113
6.4	Selected Runs (5-axle truck)	114
6.5	Runs and Gauges Selected for LEF's Calculation (3-axle truck)	120
6.6	Runs and Gauges Selected for LEF's Calculation (5-axle truck)	120
7.1	Discrete LEF's for 3-axle Truck	124
7.2	Discrete LEF's for 5-axle Truck	124
7.3	Integral LEF's for 3-axle Truck	155
7.4	Integral LEF's for 5-axle Truck	156
C.1	LEF's for the 3-Axle Truck, Steering Axle, (ASTM Range-Pair Counting)	194
C.2	LEF's for the 3-Axle Truck, Steering Axle, (RTAC Method)	194
C.3	LEF's for the 3-Axle Truck, Tandem, (ASTM Range-Pair Counting)	195
C.4	LEF's for the 3-Axle Truck, Tandem, (RTAC Method)	195
C.5	LEF's for the 3-Axle Truck, Complete Configuration, (ASTM Range-Pair Counting)	195
C.6	LEF's for the 3-Axle Truck, Complete Configuration, (RTAC Method)	196
C.7	LEF's for the 5-Axle Truck, Steering Axle, (ASTM Range-Pair Counting)	196
C.8	LEF's for the 5-Axle Truck, Steering Axle, (RTAC Method)	196
C.9	LEF's for the 5-Axle Truck, 1st Tandem, (ASTM Range-Pair Counting)	197
C.10	LEF's for the 5-Axle Truck, 1st Tandem, (RTAC Method)	197
C.11	LEF's for the 5-Axle Truck, 2nd Tandem, (ASTM Range-Pair Counting)	197
C.12	LEF's for the 5-Axle Truck, 2nd Tandem, (RTAC Method)	198
C.13	LEF's for the 5-Axle Truck, Complete Configuration, (ASTM Range-Pair Counting)	198

C.14 LEF's for the 5-Axle Truck, Complete Configuration, (RTAC Method) 198
C.15 LEF's for the 3-Axle Truck, Steering Axle, Speed 20 km/h 199
C.16 LEF's for the 3-Axle Truck, Steering Axle, Speed 40 km/h 199
C.17 LEF's for the 3-Axle Truck, Steering Axle, Speed 50 km/h 200
C.18 LEF's for the 3-Axle Truck, Tandem Axle, Speed 20 km/h 200
C.19 LEF's for the 3-Axle Truck, Tandem Axle, Speed 40 km/h 201
C.20 LEF's for the 3-Axle Truck, Tandem Axle, Speed 50 km/h 201
C.21 LEF's for the 3-Axle Truck, Complete Configuration, Speed 20 km/h 202
C.22 LEF's for the 3-Axle Truck, Complete Configuration, Speed 40 km/h 202
C.23 LEF's for the 3-Axle Truck, Complete Configuration, Speed 50 km/h 202
C.24 LEF's for the 5-Axle Truck, Steering Axle, Speed 20 km/h 203
C.25 LEF's for the 5-Axle Truck, Steering Axle, Speed 40 km/h 203
C.26 LEF's for the 5-Axle Truck, Steering Axle, Speed 50 km/h 204
C.27 LEF's for the 5-Axle Truck, Tandem Axles, Speed 20 km/h 204
C.28 LEF's for the 5-Axle Truck, Tandem Axles, Speed 40 km/h 205
C.29 LEF's for the 5-Axle Truck, Tandem Axles, Speed 50 km/h 205
C.30 LEF's for the 5-Axle Truck, Complete Configuration, Speed 20 km/h 206
C.31 LEF's for the 5-Axle Truck, Complete Configuration, Speed 40 km/h 206
C.32 LEF's for the 5-Axle Truck, Complete Configuration, Speed 50 km/h 206
C.33 LEF's for the 3-Axle Truck, Steering Axle (Trough-Peak-Trough Cycle Integral) 207
C.34 LEF's for the 3-Axle Truck, Steering Axle, (Zero Strain-Peak-Zero Strain Cycle Integral) 207
C.35 LEF's for the 3-Axle Truck, Tandem (Trough-Peak-Trough Cycle Integral) 208
C.36 LEF's for the 3-Axle Truck, Tandem, (Zero Strain-Peak-Zero Strain Cycle Integral) 208
C.37 LEF's for the 3-Axle Truck, Complete Configuration, (Trough-Peak-Trough Cycle Integral) 208

C.38 LEF's for the 3-Axle Truck, Complete Configuration, (Zero Strain-Peak-Zero Strain Cycle Integral) 209
C.39 LEF's for the 5-Axle Truck, Steering Axle, (Trough-Peak-Trough Cycle Integral) 209
C.40 LEF's for the 5-Axle Truck, Steering Axle, (Zero Strain-Peak-Zero Strain Cycle Integral) 209
C.41 LEF's for the 5-Axle Truck, 1st Tandem, (Trough-Peak-Trough Cycle Integral) 210
C.42 LEF's for the 5-Axle Truck, 1st Tandem, (Zero Strain-Peak-Zero Strain Cycle Integral) 210
C.43 LEF's for the 5-Axle Truck, 2nd Tandem, (Trough-Peak-Trough Cycle Integral) 210
C.44 LEF's for the 5-Axle Truck, 2nd Tandem, (Zero Strain-Peak-Zero Strain Cycle Integral) 211
C.45 LEF's for the 5-Axle Truck, Complete Configuration, (Trough-Peak-Trough Cycle Integral) 211
C.46 LEF's for the 5-Axle Truck, Complete Configuration, (Zero Strain-Peak-Zero Strain Cycle Integral) 211

Chapter 1

INTRODUCTION AND BACKGROUND

The load equivalence concept appeared as a design tool, intended to transform pavement damage from mixed traffic into damage from a standard axle. The Load Equivalency Factors (LEF's) emerged from the concept of equivalence as ratios of pavement life. They index the pavement damage caused by a candidate axle i to the damage caused by a standard single axle s (Equation 1.2).

$$LEF_i = \frac{N_s}{N_i} \qquad (1.1)$$

The concept of damage can be considered as fundamental, because it affects activities such as: allocation of pavement construction and maintenance costs to pavement users, pavement performance predictions and pavement design. For this reason, it is important to define equivalency in term of damage by evaluating the reduction in pavement performance. The indicator of the reduction in pavement performance is the serviceability, defined as the ability of the pavement to conveniently accommodate traffic. The serviceability is influenced by a combination of different types of surface distress, namely roughness, cracking, patching, and wheelpath rutting. Failure is reached when the combination of these distress types equals a maximum acceptable value, defined as terminal serviceability.

This approach was adopted by the AASHO Road Test, the most important experiment to date leading to empirical LEF's. Although the results of this study are still in use, with few modifications (AASHTO, 1986), changes in axle weights and configurations create the need to look at alternative methodologies for LEF's determination.

Quantifying damage in terms of pavement distress yields LEF's related to a particular type of distress, such as fatigue cracking or permanent deformation of the pavement. Each type of distress is associated to a pavement response parameter and a corresponding fatigue relationship. For example, the response parameter associated with fatigue cracking is the tensile strain at the bottom of the asphalt concrete layer, while the response parameter associated with permanent deformation of the pavement is the compressive strain at the top of the subgrade. Pavement distress-related LEF's are defined as mechanistic. According to the procedure used to obtain the pavement response parameters, these LEF's can be theoretical, when the response parameter is calculated, or measured when the response parameters are based on experimental measurements.

This study considered one distress type, namely fatigue cracking of flexible pavements.

The form of the fatigue relationship which represents this distress mechanism is shown in Equation 1.3:

$$N_i = k_1\left(\frac{1}{\epsilon_i}\right)^{k_2} \qquad (1.2)$$

where:

N_i = fatigue life corresponding to the ϵ_i level of strain.

ϵ_i = tensile strain at the bottom of the asphalt concrete layer.

k_1, k_2 = material constants.

Similar to other studies (RTAC, 1986; Hutchinson, 1987) the exponent k_2 was considered to be 3.8.

Because the strain versus time histories were experimentally obtained by monitoring pavement instrumentation (strain gauges) under load, the LEF's derived are mechanistic and based on measured pavement response. The standard axle load used as a reference was the trailing axle of the Benkelman Beam truck (18,000 lbs).

Chapter 2

OBJECTIVES

The objectives set forward by the study can be grouped into two main categories. First, to perform a theoretical investigation of cycle identification and counting methodologies used for mechanistic LEF's calculation, focusing on the ASTM E 1049-85 standard approach. Second, to calculate and compare LEF's based on measured tensile strain versus time histories. These suggest the following tasks:

1. Review the literature on mechanistic LEF calculation methods and summarize the findings for effective reference and use.

2. Introduce the concept of fatigue cycle as defined by the ASTM standard E 1049-85 and compare all the fatigue cycle counting methods proposed by the standard in order to find the most suitable one for pavement analysis.

3. Validate numerically the selected method for cycle counting, by comparing its output to that of other mechanistic methods and by relating it to empirical LEF's values.

4. Investigate the suitability of integral methods for LEF's calculation, based on the cycle definition established earlier.

Chapter 3

LITERATURE REVIEW

The load equivalency concept relates two different axle loads, the candidate axle and the standard axle by means of a specified amount of pavement damage. It was introduced in order to facilitate the analysis of pavements under a complex spectrum of traffic loading. Although the concept was formalized in the 40's by Grumm, its widespread use started after the AASHO Road Test. Except for the empirical findings of the AASHO Road Test, there has been a strong tendency to define Load Equivalency Factors (LEF's) based on pavement primary responses. Both calculated and measured deflections, stresses, and strains were extensively used, and various methods of LEF's calculation devised. The objective of this chapter is to summarize chronologically the main methods for LEF's calculation available to date.

3.1 AASHO Road Test (1962)

The AASHO Road Test was the most extensive road experiment undertaken to date being the basis for the first empirical LEF's. The test was conducted by using six traffic loops, five of which carried traffic while the sixth carried no traffic, and played a control role. The loops were divided in sections of different structural designs of roughly 100 ft

long each. The flexible pavement sections included an asphalt concrete layer, crushed limestone base and an uniformly graded sand-gravel subbase. The experiment considered various combinations of each layer.

The main objective of the AASHO Road Test was to relate pavement performance to axle load applications and to the structural design of pavements. A fundamental concept employed at the AASHO Road Test was the serviceability of a pavement, defined as its capacity to conveniently accommodate traffic. Performance is the serviceability history of the pavement. A subjective appraisal of serviceability was initially described by the Present Serviceability Rating in a scale of 0 to 5. The concept of the Load Equivalency Factor was introduced in order to index the pavement damage caused by various axle configurations and weights. A reference value, caused by a single axle on dual tires carrying 18,000 lbs was selected as standard. This can be mathematically expressed as:

$$Load \quad Equivalence_x = \frac{W_t(18)}{W_t(x)} \tag{3.1}$$

where:

$W_t(x)$ = the number of repetition of the candidate axle producing a given amount of damage, and

$W_t(18)$ = the number of repetitions of the standard axle of 18,000 lbs producing the same amount of damage.

Typically, the number of repetitions to failure is considered for both the candidate axle and the standard axle. Failure was defined as the serviceability level at which rehabilitation must be undertaken.

The Road Test adopted an objective evaluation of serviceability, based on measurements of significant pavement distress types related to performance. Equation 3.2 introduced the Present Serviceability Index (PSI or p) as a function of longitudinal pavement profile, and the extent of cracking, patching and rutting.

$$p = 5.03 - 1.91 \log(1 + \overline{SV}) - 0.01\sqrt{C + P} - 1.38\overline{RD}^2 \qquad (3.2)$$

where:

p = present serviceability index

$\overline{SV}$ = average slope variance for the wheelpaths

$C + P$ = cracking and patching of the pavement surface ($ft^2/1{,}000\,ft^2$), and

$\overline{RD}$ = rutting in the wheelpaths (in).

For each section, the serviceability index was calculated based on measurements made at intervals of two weeks. Each interval was called "index period" and the last day of each index period was termed an "index day". Between November 3,

1958 and November 30, 1960 there were 55 index periods. The total number of axle applications accumulated through the t^{th} index period (N_t) was calculated with the Equation 3.3.

$$N_t = n_1 + n_2 + \ldots + n_t \qquad (3.3)$$

where n_t is the number of axles applied during the t^{th} index period.

In order to account for the seasonal changes affecting the rate of damage accumulation, "seasonal weighting functions" q_t, were defined. These were determined on the basis of the mean deflections measured in the unloaded loop (Loop 1) during the various index periods. The total number of weighted applications would be given by Equation 3.4

$$W_t = q_1 n_1 + q_2 n_2 + \ldots + q_t n_t \qquad (3.4)$$

The use of weighted load application was found to increase the correlation and to reduce the mean residuals of the regression equations described next.

For sections that did not survive the test, five pairs of simultaneous values of p and W were taken at p= 3.5, 3.0, 2.5, 2.0 and 1.5. For sections that survived the test period, serviceability versus accumulated number of axle applications was chosen at 11, 22, 33, 44 and 55 index days. For modeling serviceability, various mathematical models were proposed. The one chosen is given by Equation 3.5.

$$p = c_0 - (c_0 - c_1)\left(\frac{W}{\rho}\right)^{\beta} \qquad (3.5)$$

where:

p = the serviceability value after W load applications

c_0 = the initial serviceability value, (i.e., taken equal to 4.2), and

c_1 = the terminal value of the serviceability (i.e., taken equal to 1.5).

The function β determines the shape of the serviceability curve with increasing axle load applications, while ρ represents the number of axle load applications that cause pavement failure (i.e, terminal p).

After rewriting Equation 3.5 in a logarithmic form and introducing G to be a function of the serviceability loss, (Equation 3.6), a new expression relating serviceability, loading and design parameters was obtained, (Equation 3.7).

$$G = \log\frac{(c_0 - p)}{(c_0 - c_1)} \qquad (3.6)$$

$$G = \beta(\log W - \log\rho) \qquad (3.7)$$

Using the five pair values for p, W, the corresponding values of G were calculated and a straight line was fitted to the five pairs of G, W. The slope of the line, β and the intercept

on the $\log W$ axis, $\log\rho$ were determined. An estimate of the relationship between β, the load and design variables was also produced, as shown below:

$$\beta = \beta_0 + \frac{B_0(L_1+L_2)^{B_2}}{(a_1D_1+a_2D_2+a_3D_3+a_4)^{B_1}L_2^{B_3}} \qquad (3.8)$$

where:

β_0 = minimum value of β

L_1 = nominal weight of the axle in kips

L_2 = type of vehicle (1 for single axle and 2 for tandem axle vehicles), and

D_1, D_2, D_3 = are the thicknesses of the pavement layers.

The remaining values are regression constants. Assuming that β estimates obtained from Equation 3.8 are better than β estimates based on individual section performance, a feedback process was employed in order to recalculate $\log\rho$ values from Equation 3.7. A relationship between ρ, the load and design variables was also assumed:

$$\rho = \frac{A_0(a_1D_1+a_2D_2+a_3D_3+a_4)^{A_1}L_2^{A_3}}{(L_1+L_2)^{A_2}} \qquad (3.9)$$

In Equations 3.8 and 3.9, the expression $a_1D_1+a_2D_2+a_3D_3$ was defined as the Structural Number (SN) or D and the a_i coefficients were described through regression.

$$D = 0.44D_1 + 0.14D_2 + 0.11D_3 \qquad (3.10)$$

The regression analysis performed gave the following regression relationships for β and ρ:

$$\beta = 0.4 + \frac{0.081(L_1 + L_2)^{3.23}}{(D+1)^{5.19}L_2^{3.23}} \qquad (3.11)$$

$$\rho = \frac{10^{5.93}(D+1)^{9.36}L_2^{4.33}}{(L_1 + L_2)^{4.79}} \qquad (3.12)$$

The above relationships permit the calculation of β and ρ as functions of the pavement structure and loading. However, both equations reflect preset levels of initial and terminal serviceability, particular subgrade and environmental characteristics.

As it will pointed out later, (Section 3.8) findings of the AASHO Road Test are part of current design practices in use today.

3.2 Study by Deacon (1969)

This study describes a mechanistic method for obtaining LEF's. The methodology was based on theoretically obtained strains at the bottom of the asphalt concrete layer which were considered to relate to pavement fatigue failure. Calculations were made using a program developed by Chevron Research Company (Michelow, 1963). The fatigue law is given by Equation 3.13:

$$N_i = K\left(\frac{1}{e_i}\right)^C \qquad (3.13)$$

where:

N_i = the number of repetitions to failure at the strain level e_i, and

K, C = material constants.

Replacing the fatigue law (Equation 3.13) in the expression defining the Load Equivalency (Equation 3.1), LEF's with reference to the standard axle load of 18,000-pound, single-axle, dual-tire can be easily calculated from known maximum principal tensile strains using the following equation:

$$F_i = \left[\frac{e_i}{e_b}\right]^C \qquad (3.14)$$

where:

F_i = load equivalency factor for configuration i

e_i = principal tensile strain under configuration i

e_b = principal tensile strain under standard axle, and

C = constant, assumed equal to 5.5 throughout the study.

Three load configurations were modeled, namely, single tires on single axles, dual tires on single axles and dual tires on tandem axles. Single axles with single tires were loaded with 1 to 17 kips in increments of 1 kip. Loads on

tandem axles with dual tires were four times those of single axles with single tires while loads on single axles with dual tires were twice those of single axles with single tires. Figure 3.1 presents the load positioning used for stress determination. The single axle with single tire was modeled locating the load at the origin (A) of the cartesian coordinate system.

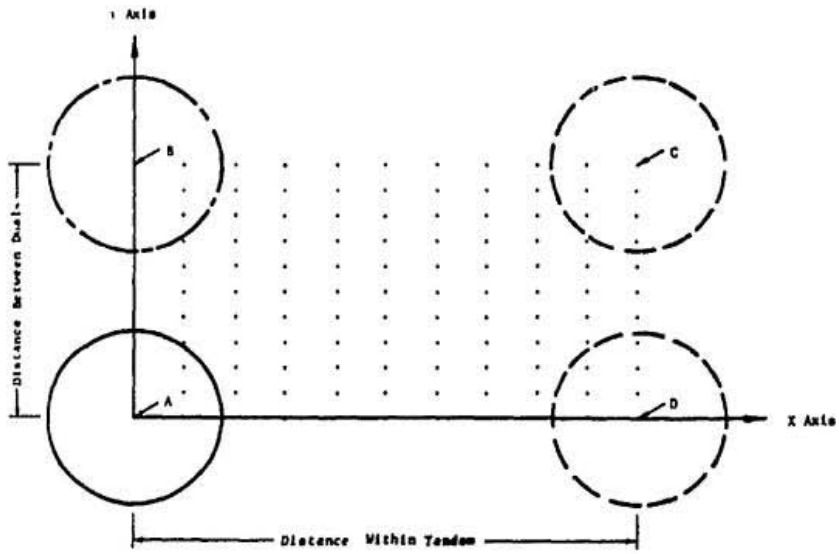

Figure 3.1 : Plane view of load arrangement for stress computations, (After Deacon, 1969).

For the single axle with dual tires the points A and B were simultaneously loaded, while for tandem axles with dual tires the loads were positioned at points A, B, C and D. Dividing the distance between duals and the distance within tandem axles

in ten intervals, 121 evaluation points were identified in the first quadrant. For each load configuration and each evaluation point, the maximum principal tensile stress and strain were computed.

The study recognizes that tensile strains generated by tandem axles are more complex than those generated by single axles. Figure 3.2 presents three strain patterns under a tandem axle.

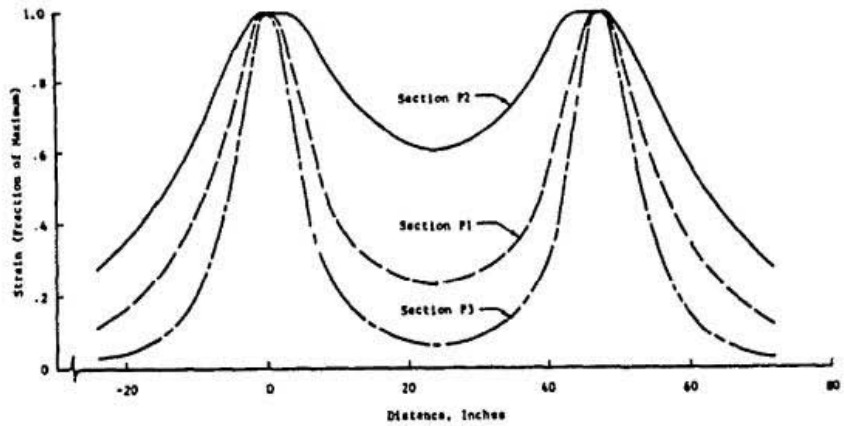

Figure 3.2 : Strain distribution for 36-kip tandem axle, (After Deacon, 1969).

After identifying the curves for sections P2 and P3 as extreme limits for the strain pattern of the tandem axles, a procedure for processing intermediate strain curves, such as those obtained from section P1, was devised. This was done by theoretically approximating the effects of a tandem axle by two passages of a single axle which produces the same maximum

principal tensile strain. In other words, the LEF of a tandem axle is twice the LEF of a single axle whose maximum principal tensile strain is equal to the maximum principal tensile strain of the tandem.

3.3 Study by Ramsamooj et al. (1972)

This study focused on theoretical development and experimental verification of fatigue cracking and failure mechanisms, based on fracture mechanics concepts.

The fatigue life was described by the Paris' crack propagation law (Equation 3.15), as a function of the dominant parameter controlling crack growth (C). This was the stress intensity factor, which measures the magnitude of the stress field in the vicinity of the crack.

$$\frac{dC}{dN} = AK^4 \qquad (3.15)$$

where:

$\frac{dC}{dN}$ = rate of crack propagation

K = stress intensity factor, and

A = constant of the material.

Based on the experimentally obtained average crack growth curves, the rate of crack propagation was given by Equation 3.16

$$\frac{dC}{dN} = 5.00 * 10^{-12} K^4 \qquad (3.16)$$

The stress intensity factor is a function of the bending stress σ^*, (which cannot account by itself for the cracking and the subsequent stress redistribution), the crack length, the relative stiffness of the pavement (Equation 3.17), and the geometrical and boundary conditions.

λ' is the relative stiffness of the pavement expressed as,

$$\lambda' = \sqrt[4]{\frac{k}{D}}\ c \qquad (3.17)$$

where:

$D = \frac{Eh^3}{12(1-\nu^2)}$ flexural rigidity

k = modulus of subgrade reaction

E = Young's modulus

ν = Poisson's ratio

h = thickness of the slab

The stress intensity factors were determined from Equation 3.18 using the measured change in compliance with increasing crack length.

$$K_1^2 = \frac{E}{2(1-\nu)} P^2 \frac{1}{h} \frac{\delta L}{\delta (2c)} \qquad (3.18)$$

where:

K_1 = stress intensity factor

L = compliance

P = load, and

$2c$ = crack length

From equation 3.15, and the fact that K is proportional to the load P, it was concluded that the LEF's for single axle loads are proportional to the fourth power of the load.

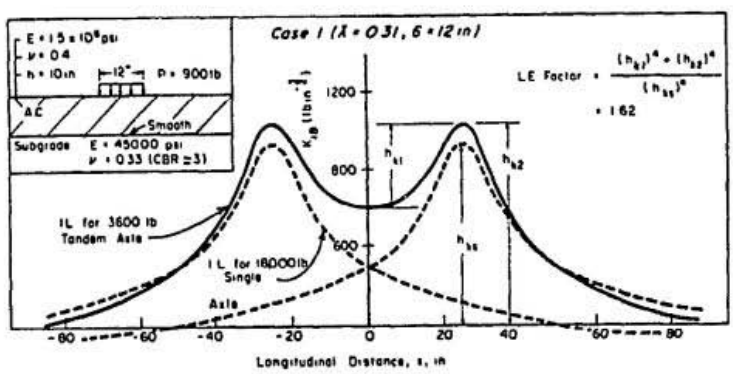

Figure 3.3 : LEF calculation for tandem axle, (after Ramsamooj et al., 1972).

The stress intensity factor versus distance from the crack tip distribution for tandem axles (Figure 3.3) was constructed using the influence line of the stress intensity factor at the tip of the crack. According to Figure 3.3, the equation for LEF's calculation is:

$$LEF = \frac{(h_{k1})^4 + (h_{k2})^4}{(h_{ks})^4} \qquad (3.19)$$

where:

h_{k1} = maximum value of the stress intensity factor produced by the tandem,

h_{k2} = minimum peak-to-trough value of the stress intensity factor produced by the tandem, and

h_{ks} = maximum value of the stress intensity factor produced by the 18-kip standard axle.

Using this approach, the LEF is defined as the destructive ratio, or crack ratio produced by one passage of the candidate axle load as compared to an 18-kip single axle load.

3.4 Study by Christison et al. (1978)

This study used measurements of pavement response to calculate mechanistic equivalence factors of various axle configurations. The experimental site was built in 1973 in

Alberta consisting of two full depth asphalt concrete pavements. The instrumentation consisted of transducers measuring deflection, stress, strain and pavement temperature. The loading configuration included single axles on single tires, single axles on dual tires and tandems on dual tires. All the response parameters obtained for the above configurations were compared to the effects of the Benkelman Beam truck axle of 80-kN (18,000-lb), adopted as standard axle. The tests were performed when the subgrade was unfrozen and the pavement temperature ranged from 2° C to 30° C (36° F to 86° F). Vehicle velocities ranged from 3 to 56 km per hour (2 to 35 mph).

The definition of the Load Equivalency Factors given by Equation 3.1 was employed throughout the study.

Failure was defined with respect to two criteria, namely, the tensile strain at the bottom of the asphalt concrete layer and the surface deflection.

In the first case, the procedure adopted by Deacon (1969) was employed, describing fatigue life using Equation 3.13 and obtaining the equivalency factors for single axles from Equation 3.14. Compressive strain peaks of the strain pattern were ignored, the load equivalency factor determination making use of tensile strain only (Figure 3.4).

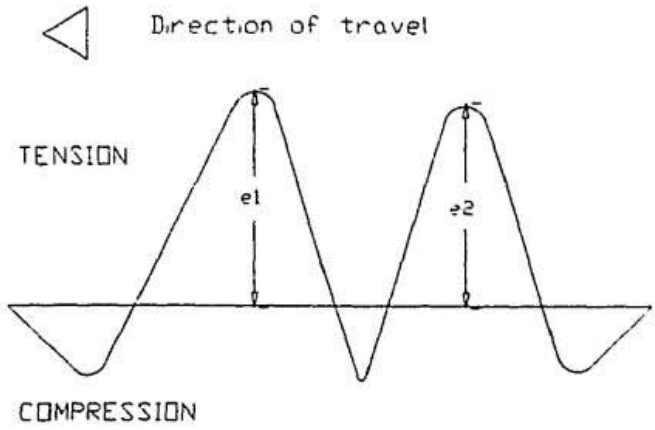

Figure 3.4 : Strain peaks extraction from response curve

For tandem axle loading, the maximum strain obtained under the second axle was correlated to that obtained under the leading axle, by introducing the constant K as shown in Equation 3.20:

$$K = \overline{K}_i = \frac{\sum_{i=1}^{n} K_i}{n} \qquad (3.20)$$

where:

K_i = ratio of the strain recorded under the second axle to the strain recorded under the leading axle of the tandem i, and

n = the number of tandem strain patterns considered.

Equation 3.14 becomes:

$$F_i = \left(\frac{\epsilon_i}{\epsilon_b}\right)^c + \left(K\frac{\epsilon_i}{\epsilon_b}\right)^c \qquad (3.21)$$

where:

F_i = load equivalency factor

K = the average ratio of strains, as shown in Equation 3.20

ϵ_i = maximum tensile strain caused by the leading axle load, and

ϵ_b = maximum tensile strain caused by the standard axle.

In the second case, failure is defined with respect to the maximum tolerable deflection using the following relation:

$$N = K\left(\frac{1}{\delta}\right)^C \qquad (3.22)$$

where:

N = the accumulated axle load expressed as equivalent axle load applications

δ = tolerable rebound deflection under the standard axle, (as per RTAC Pavement Management Guide), and

K, C = experimentally determined constants.

Load Equivalency Factors (F_i) for single axles, based on pavement surface deflection, were predicted using the following equation:

$$F_i = \left(\frac{\delta_i}{\delta_b}\right)^c \qquad (3.23)$$

where:

δ_i = surface deflection under candidate single axle, and

δ_b = surface deflection under standard axle.

For tandem axles (Figure 3.5), an extension of the above formula was proposed, based on suggested procedures for calculating load equivalency factors from longitudinal stress intensity factor profiles (Ramsamooj, 1972).

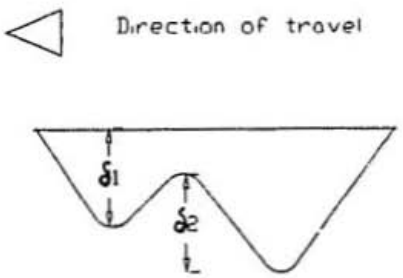

Figure 3.5 : Deflection peaks extraction from response curve

The prediction equation was as follows:

$$F_i = \left(\frac{\delta_i}{\delta_b}\right)^c + \left(\frac{\Delta\delta}{\delta_b}\right)^c \qquad (3.24)$$

where:

The total strain was subsequently correlated to vehicle velocity and pavement temperature, concluding that the maximum rate of change in the total strain values occurred at low vehicle velocities and high asphaltic concrete temperatures.

3.5 Study by Treybig (1983)

The objective of this study was to calculate mechanistic LEF's for different loading configurations, based on theoretical pavement response parameters, and to compare the results to AASHO Road Test LEF's. The study was based on the premise that relationships can be developed between predicted pavement response and the AASHO empirical equivalency factors.

In order to make the comparison possible, the pavement cross section and material properties modeled were selected to represent AASHO Road Test conditions. The maximum tensile strain at the bottom of the asphalt concrete layer and the compressive strain at the top of the subgrade were calculated by the elastic-layered analysis using the computer program ELSYM5 (FHWA, 1985). The following equation formed the basis of the proposed "curvature method", for calculating LEF's, which is exemplified in Figure 3.7.

$$F(x_n) = \left[\frac{\epsilon_1(x_n)}{\epsilon(18_s)}\right]^B + \sum_{i=1}^{n}\left[\frac{\epsilon_{i+1}(X_n) - \epsilon_{i-i+1}(X_n)}{\epsilon(18_s)}\right]^B \qquad (3.25)$$

δ_1 = surface deflection under the leading axle, and

$\Delta\delta$ = maximum deflection under the second axle minus minimum deflection between axles.

For both fatigue and deflection criteria, the exponent C was assumed as being equal to 3.

Exploring a new idea, without applying it to the LEF calculation, the study introduced the concept of "total strain", defined as the sum of the absolute values of the maximum compressive strain preceding the tensile peak and the maximum recorded tensile strain, marked in Figure 3.6 as S_1 and S_2, respectively.

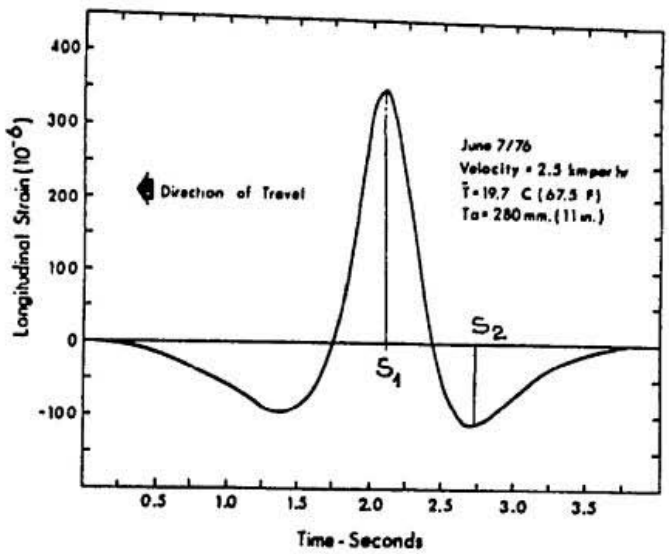

Figure 3.6 : Typical strain profile under 80 kN single axle dual tire load, (After Christison et al., 1978)

where:

$F_i(x_n)$ = predicted equivalency factor for axle configuration n of load x.

$\epsilon(18_s)$ = maximum asphalt tensile strain or subgrade vertical strain for the 18-kip (80kN) equivalent single axle load (ESAL), in./in.

$\epsilon_1(x_n)$ = maximum asphalt tensile strain or subgrade vertical strain under the leading axle for axle configuration n of load x, in./in.

$\epsilon_{i+1}(x_n)$ = maximum asphalt tensile strain or subgrade vertical strain under the axle i+1 for axle configuration n of load x, in./in.

$\epsilon_{i-i+1}(x_n)$ = maximum asphalt tensile strain or subgrade vertical strain, in critical direction, between axles i and i+1 for axle configuration n of load x, in./in.

Figure 3.7 applies the curvature method for calculating strain extraction for the vertical strain at the top of the subgrade pattern under a tridem configuration.

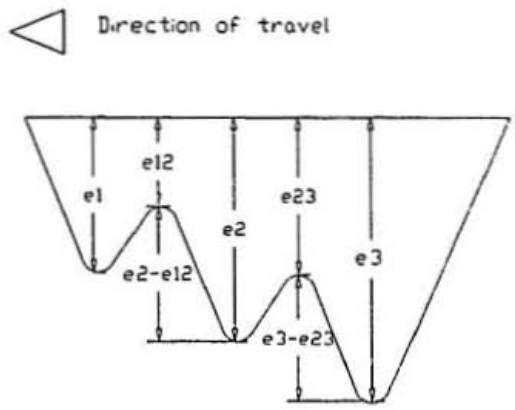

Figure 3.7 : Strain extraction based on the Curvature Method for a subgrade vertical strain pattern.

The exponent B, given by Equation 3.26, is primarily dependent on asphaltic mix composition. For a structural number of 3.75 and a terminal serviceability of 2.0, the computed B value was 5.06.

$$B = \frac{\text{Log}\, F(x_s)}{\text{Log}\, \frac{\epsilon(x_s)}{\epsilon(18_s)}} \qquad (3.26)$$

where:

$F(x_s)$ = empirical equivalency factor for an x-kip single axle load, and

$\epsilon(x_s)$ = maximum asphalt tensile strain or subgrade vertical strain for an 18-kip single axle load, (in/in).

It is specified that in Equation 3.25, zero strain should be used when the asphalt tensile strain between the axles is compressive, or if the subgrade vertical strain between the axles is tensile. Figure 3.8 presents LEF's computed for a section with a SN of 5.51.

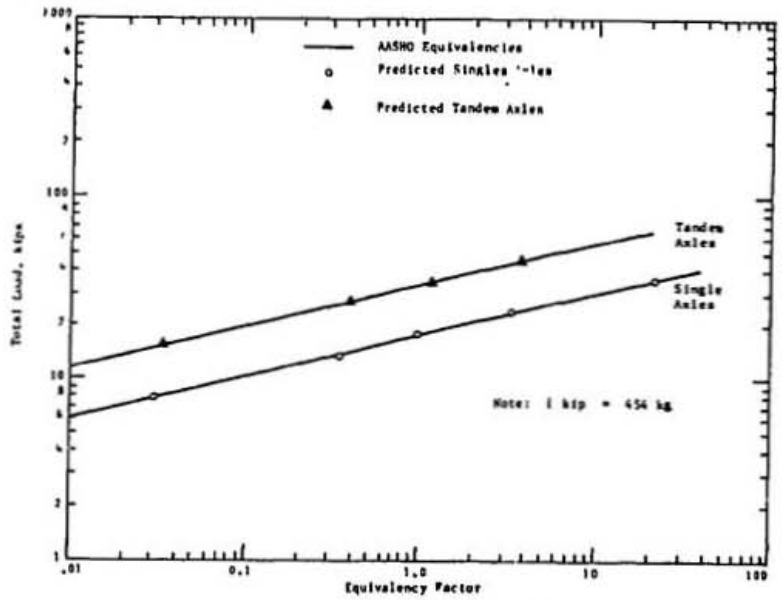

Figure 3.8 : Development of equivalency factors based on tensile strain using Curvature Method, for SN=5.51, (After Treybig, 1983).

Compressive strain was also calculated for different structural numbers as a function of axle load. For this condition, considering a structural number of 3.75 and a terminal serviceability of 2.0, B had a value of 4.49. Figure 3.9 shows AASHO LEF's and predicted LEF's based on compressive strain at the bottom of the subgrade.

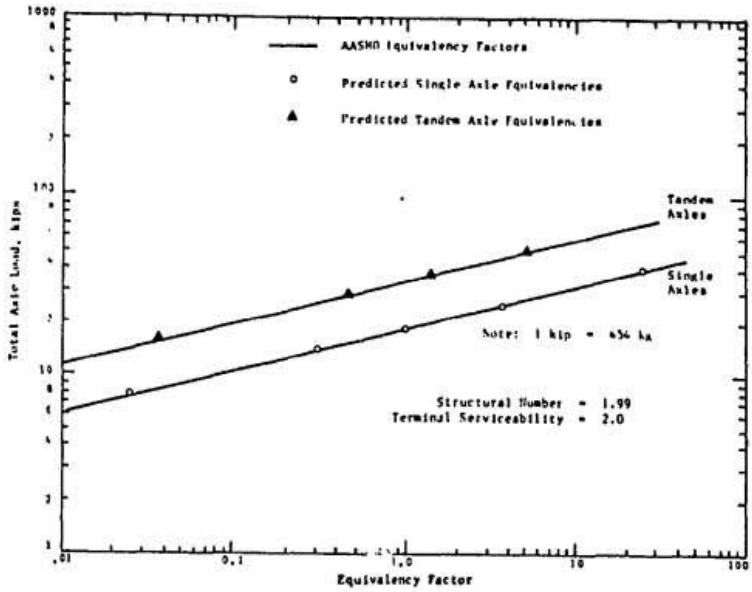

Figure 3.9 : Comparison of LEF based on compressive strain, Curvature Method versus AASHO, (After Treybig, 1983).

The author suggested the use of asphalt tensile strain for equivalency calculation only for pavements with asphalt thicknesses greater than 3 in. (7.6 cm). It is explained that the elastic layer theory (ELSYM5) computes for certain conditions compressive strains in thin asphalt concrete layers. When the above condition is not satisfied, the subgrade vertical strain should be used.

3.6 Study by Southgate et al. (1985)

This study focused on obtaining Load Equivalency Factors (referred to as Damage Factors) using a mechanistic approach.

The method followed consists of relating the repetitions to failure in fatigue to the strain energy density derived from strains calculated by the Chevron N-layer computer program.

The strain energy is defined as the energy stored by a solid when a force is applied to it. The strain energy per unit volume at a specific point in the solid is the strain energy density at that point. Strain energy density is a function of material characteristics and nine strain (or stress) components. The equation for strain energy density derived by Sokolnikoff (1956) can be expressed as:

$$W = \frac{\lambda \psi^2}{2} + G(e_{11}^2 + e_{22}^2 + e_{33}^2 + 2e_{12}^2 + 2e_{23}^2 + 2e_{31}^2) \qquad (3.27)$$

where:

e_{ii} = the strain component in the ii direction

$$\psi = e_{11} + e_{22} + e_{33}$$

$$\lambda = \frac{E_y \mu}{(1+\mu)(1-2\mu)}$$

E_y = Young's modulus of elasticity of the material

μ = Poisson's ratio, and

$G = \frac{E_y}{2(1+\mu)}$ = the modulus of rigidity, or the shear modulus.

The work strain e_w may be obtained from the strain energy density as:

$$e_w = \sqrt{\frac{2W}{E_y}} \qquad (3.28)$$

The work strain has the same units as the strain components e_{ii}. However, because the strain energy includes all components of strain, it is stated that the work strain indicates better the internal behavior of the pavement under load.

The Chevron N-layer computer program was modified to calculate strain energy density at the bottom of the asphalt concrete layer and the top of the subgrade. All the possible AASHO Road Test layer thicknesses were considered, obtaining 100 possible pavement cross sections. The standard 18-kip (80 kN) four- tired single axle was applied as reference condition to all 100 structures.

A relationship was established between computer calculated values of work strain and tensile strain at the bottom of the asphalt concrete layer, as f llows:

$$\log(e_a) = 1.1483 \log(e_w) - 0.1638 \qquad (3.29)$$

where:

e_a = tensile strain at the bottom of the asphalt concrete layer.

Figure 3.10 presents graphically these relationships. The work strain replaced the tensile strain in the number of repetitions to failure relationship, resulting in Equation 3.30:

$$\log(N) = \frac{\log(e_w) + 2.6777807}{-0.15471249} \qquad (3.30)$$

where N represents the number to repetitions to failure in fatigue.

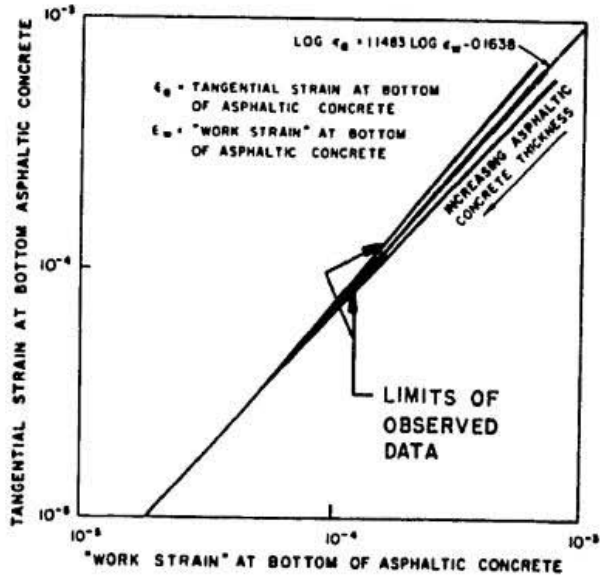

Figure 3.10 : Tensile strain versus work strain, (after Southgate et al., 1985).

The following step is to define the Damage Factor, based on Equation 3.1, and to express the load-damage factor relationship (Equation 3.26). Figure 3.11 shows the variation of the damage factors for different axle group weights.

$$\log(DF) = a + b\log(Load) + c(\log(Load))^2 \qquad (3.31)$$

where:

DF = damage factor of total load on axle configuration relative to standard axle load

$Load$ = axle load in kips, and

a, b, c = regression coefficients.

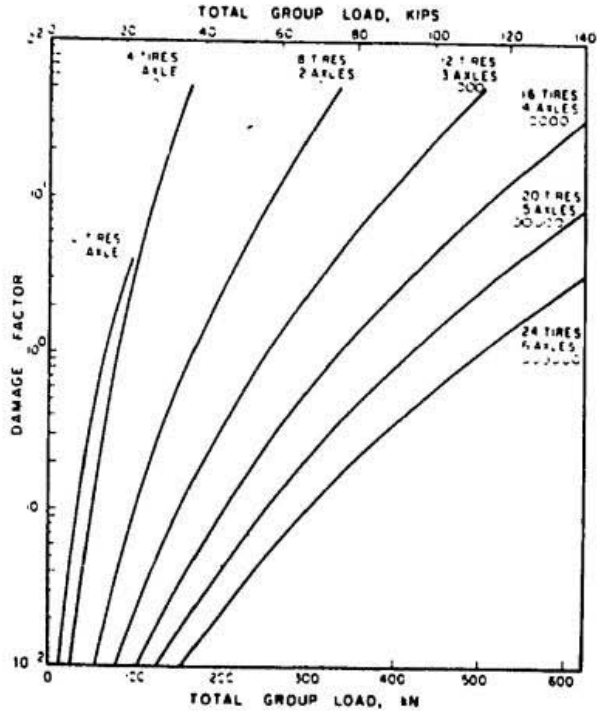

Figure 3.11 : Variation of damage factor for selected axle groups as load on axle group is changed, (after Southgate et al., 1985).

In order to account for the effect of the uneven axle load distribution on tandems and tridems, a multiplicative factor was developed. This factor adjusts the damage factors obtained for even loaded axle groups. The effect of uneven load

distribution on the axles of a 36-kip (160 kN) tandem and a 54-kip (240 kN) tridem was investigated. Analysis revealed a 40% increase in the damage factor for tandems with unevenly distributed load, and the proposed multiplicative factor was:

$$\log(MF) = 0.0018635439 + 0.0242188935\,p - 0.0000906996\,p^2 \quad (3.32)$$

where:

MF = factor to multiply the damage factor for evenly loaded axles

p = 100 * (Axle load 1 - Axle load 2) / (Axle load 1 + Axle load 2)

Various uneven loading patterns were defined for the 54-kips tridem. Comparing the effect of the unevenly loaded tridems with the effect of the evenly loaded tridems an overall damage factor increase of 130% resulted.

3.7 ASTM E 1049-85 Standard Practices for Cycle Counting in Fatigue Analysis (1985)

This standard presents a compilation of procedures employed for counting fatigue cycles. Cycle counting summarizes random load versus time histories by means of quantifying the size and number of component cycles.

The standard defines particular points of a load-time history, such as the mean crossings, reversals, peaks, valleys,

and ranges. These basic fatigue loading parameters are shown in Figure 3.12. The mean crossing represents a point at which the load-time history crosses the mean-load level, but the definition extends also to the crossing of a load level considered as reference. Reversals are defined as points of change of sign for the first derivative of the load-time history. They can be peaks or valleys, depending on the sign of the adjacent ranges. The range is the algebraic difference between successive valley and peak loads (positive range) or between successive peak and valley loads (negative range).

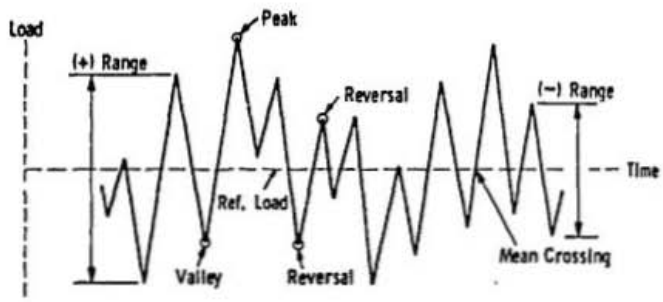

Figure 3.12 : Basic fatigue loading parameters, (After ASTM E 1049, 1985).

The four main methods of cycle counting are: Level-Crossing counting, Peak counting, Simple-Range counting and Rainflow counting. The last method comprises three variations, namely, Range-Pair counting, Rainflow counting and Simplified Rainflow counting for repeating histories.

3.7.1 Level-Crossing Counting

This method considers equidistant load levels above and below the reference load. One count is recorded each time the positive sloped portion of the load-time history exceeds a level above the reference load, or the negative sloped portion exceeds a level below the reference load. Often, other restrictions are applied to the level-crossing counts in order to eliminate small amplitude variations of the load-time history. As Figure 3.13 shows, the largest possible cycle is constructed first, followed by the second largest, etc., until all level crossings are used.

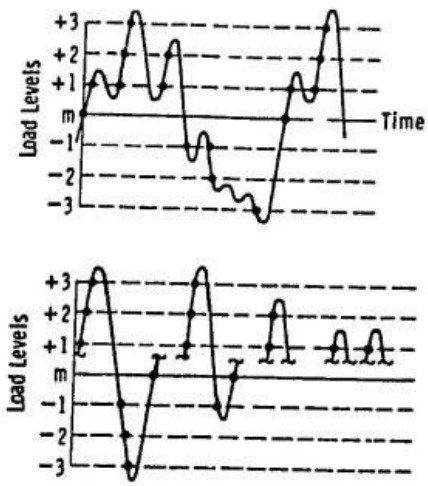

Level	Counts
+3	2
+2	3
+1	5
0	2
-1	2
-2	1
-3	1

Range (levels)	Cycle Counts
7	1
6	0
5	1
4	0
3	0
2	1
1	2

Figure 3.13 : Level Crossing counting and derived cycles, (After ASTM E 1049, 1985).

3.7.2 Peak Counting

Peak counting considers the peaks above the reference load and the valleys below the reference load. In order to eliminate small amplitude loadings, mean-crossing peak counting can be used, which consists of counting only the largest peak or valley between two successive crossings of the mean.

Figure 3.14 presents both the peak counting and the derivation of cycles based on it.

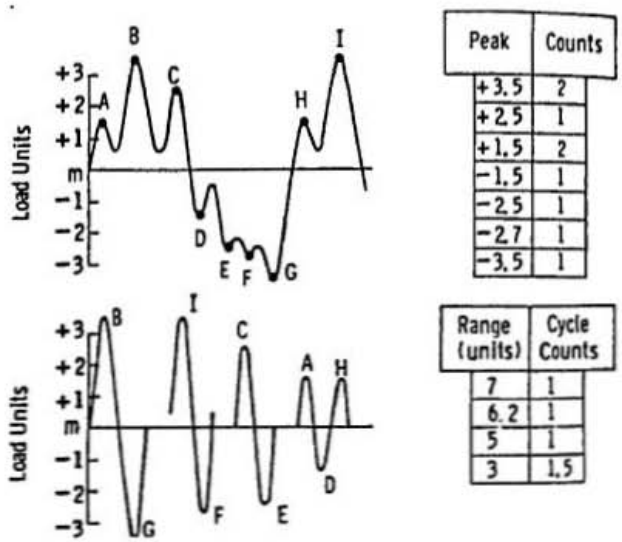

Figure 3.14 : Peak Counting and derived cycles, (After ASTM E 1049, 1985).

The larges cycle is constructed using the highest peak and lowest valley, followed by the second largest cycle, etc., until all the counts are used.

3.7.3 Simple-Range Counting

This method defines a range as the difference between two successive reversals. A positive range consists of a valley followed by a peak while a negative range consists of a peak followed by a valley. If only positive or negative ranges are counted, then each of them is counted as a cycle. If both positive and negative ranges are counted, then each is counted as one-half cycle. Figure 3.15 shows such an example of single-range counting .

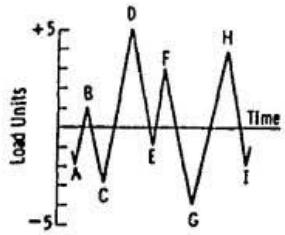

Range (units)	Cycle Counts	Events
10	0	
9	0	
8	1.0	C-D, G-H
7	0.5	F-G
6	1.0	D-E, H-I
5	0	
4	1.0	B-C, E-F
3	0.5	A-B
2	0	
1	0	

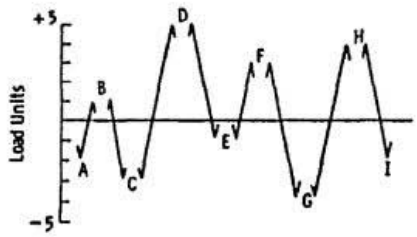

Figure 3.15 : Simple Range Counting method, (After ASTM E 1049, 1985).

3.7.4 Range-Pair Counting

The Range-Pair method defines a cycle when a range can be paired with a subsequent range of opposite sign. Three reversals are considered at a time, and the ranges between each pair of reversals are compared. When a cycle is counted, the two reversal points corresponding to the shortest range are eliminated. Figure 3.16 presents an example of Range-Pair counting.

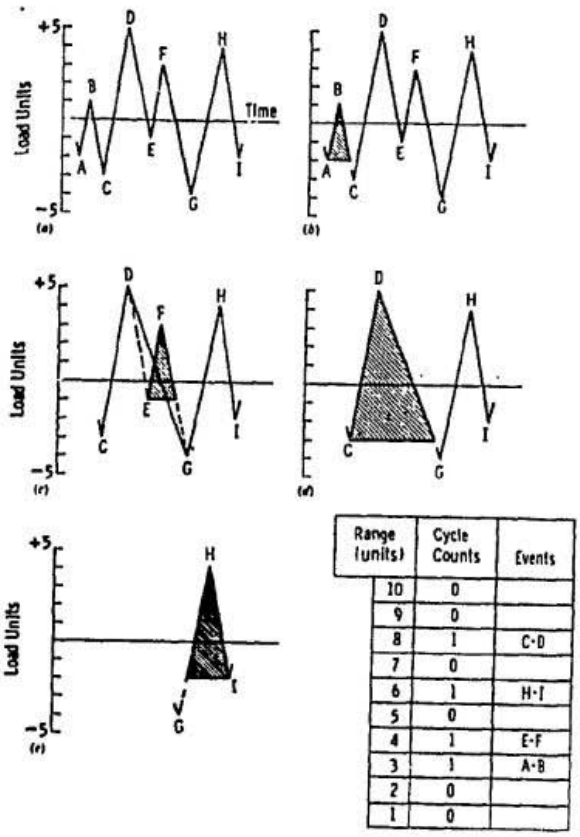

Range (units)	Cycle Counts	Events
10	0	
9	0	
8	1	C-D
7	0	
6	1	H-I
5	0	
4	1	E-F
3	1	A-B
2	0	
1	0	

Figure 3.16 : Range-Pair Counting method, (After ASTM E 1049, 1985).

3.7.5 Rainflow Counting

The rainflow counting compares every two consecutive ranges, also taking into account the starting point of the load-time history. Figure 3.17 presents an example of cycle counting using this method.

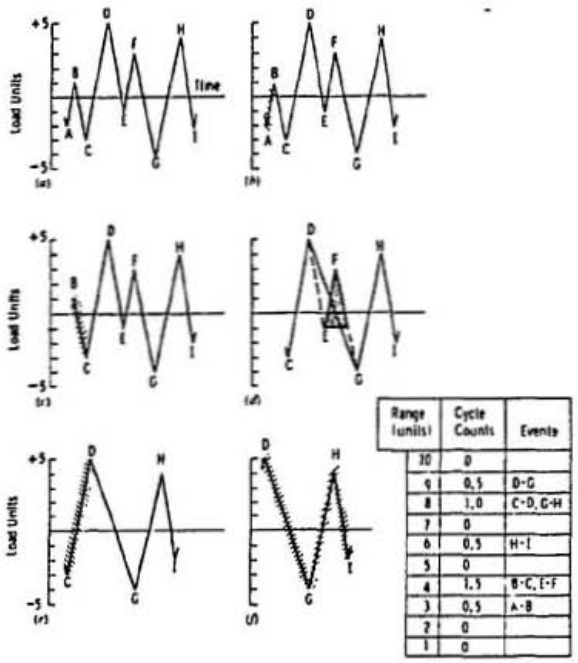

Range (units)	Cycle Counts	Events
10	0	
9	0.5	D-G
8	1.0	C-D, G-H
7	0	
6	0.5	H-I
5	0	
4	1.5	B-C, E-F
3	0.5	A-B
2	0	
1	0	

Figure 3.17 : Rainflow Counting example, (After ASTM E 1049, 1985).

When a range that include the starting point is smaller than the next range, one-half cycle is counted , the first point of the smallest range is eliminated, and the starting point moves to its second point. When a range that does not include the starting point is smaller than the next range, a

cycle is counted and the smallest range is eliminated. The cycles counted are summarized according to their range value.

The Simplified Rainflow Counting for Repeating Histories method assumes that a typical segment of a load history is repeatedly applied. Because of the nature of the strain pattern due to a single vehicle passing, this last version of the Rainflow method is not directly applicable in this study, and it will not be presented herein.

3.8 RTAC Vehicle Weights and Dimensions Study (1986)

The Load Equivalency Factors study was a component of the Pavement Response to Heavy Vehicle Test Program, developed as a part of the Vehicle Weights and Dimensions Study. Its objective was to determine mechanistic LEF's and to evaluate the influence of pavement structure on the magnitude of calculated LEF.

During the summer of 1985, 14 instrumented pavement test sites located across Canada were used to measure pavement response parameters under diverse loading and environmental conditions, and to allow calculation of mechanistic equivalency factors. Two pavement response parameters were measured, namely pavement surface deflections and asphalt surface-base layer interfacial tensile strains.

The use of deflection data for the determination of LEF was based on an empirical relationship between the surface deflection and the anticipated traffic loading, (Figure 3.18).

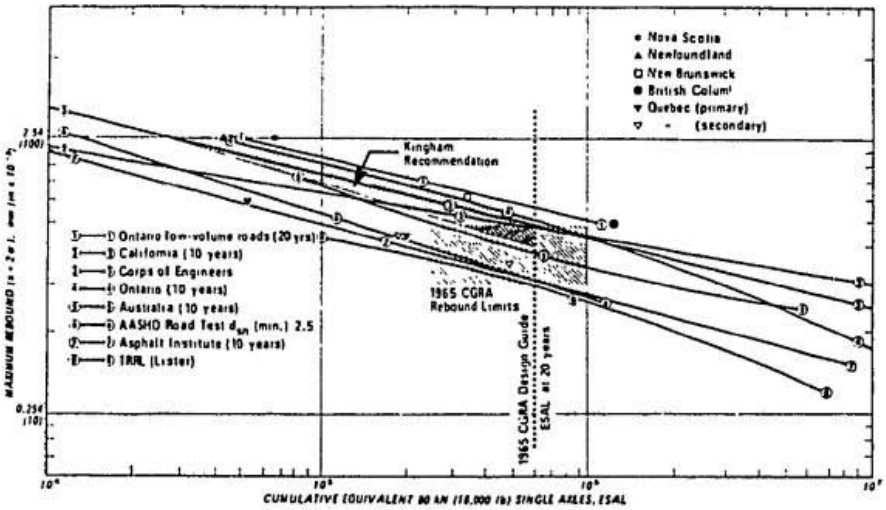

Figure 3.18 : Maximum Benkelman Beam Rebound versus Cumulative Equivalent Single Axle Load, (After RTAC, 1977).

The methodology for LEF's calculation from surface deflection is identical to that presented by Christison in 1978 (Section 3.4).

Because the pavement response associated with the fatigue cracking distress mechanism is the tensile strain at the bottom of the asphalt concrete layer, the use of strain response data for the determination of LEF is based on asphalt concrete fatigue life relationships.

According to Equation 3.13 and the LEF definition presented

on Equation 3.1, equivalencies based on the tensile strain at the bottom of the asphalt concrete were predicted for multiple axle loads by the expression:

$$F = \sum_{i=1}^{n} \left(\frac{S_i}{S_b} \right)^C \qquad (3.33)$$

where:

S_b = longitudinal interfacial tensile strain recorded under the standard load

S_i = longitudinal interfacial tensile strain recorded under each axle

n = the number of axles in the axle group, and

C = the slope of the fatigue life versus tensile strain relationship.

According to the above formula and to Figure 3.19, only the tensile part of the strain profile was taken into account, neglecting the compressive strain peaks. LEF based on deflection and tensile strain were calculated for each experimental site, and average pavement response ratios and LEF's were tabulated in the form shown in Table 3.1.

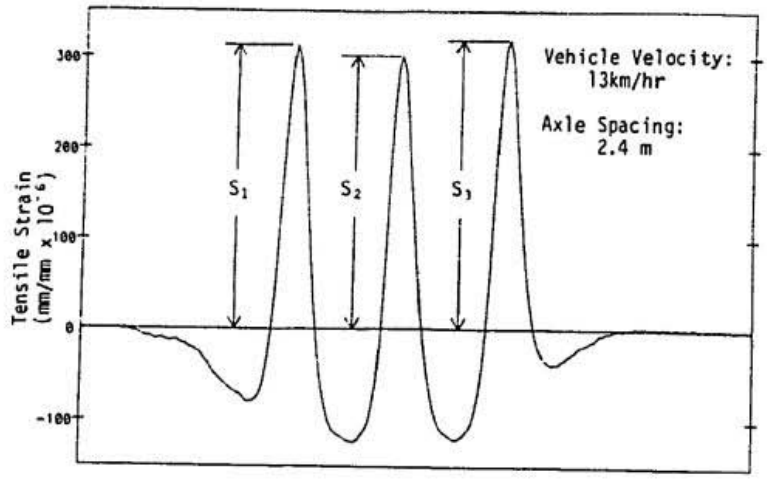

Figure 3.19 : A longitudinal interfacial tensile strain profile under a tridem group, (After RTAC, 1986).

In order to generate overall statistics, data from all sites were combined. It is worth mentioning that for both pavement deflection and interfacial tensile strain analysis, the selected value of the exponent C was 3.8. This value was described as being consistent with results of laboratory fatigue tests on asphalt concrete mixes. Finally, analysis was carried out to assess the influence of pavement structure on the predicted LEF. The deflection based LEF shown no measurable trend with changes in equivalent base thickness while the strain related LEF revealed that for lighter load, LEF decreased as the asphalt concrete thickness increased.

Table 3.1

Average Pavement Response Ratios and Load Equivalency Factors at one Experimental Site, (After RTAC, 1986)

Loading Condition	Average Pavement Response Ratios						Load Equivalency Factors Based on	
	Pavement Surface Deflections			Interfacial Tensile Strains				
	D_1/D_0	Δ_1/D_0	Δ_2/D_0	S_1/S_0	S_2/S_0	S_3/S_0	Deflections	Strains
Single Axle								
9182 KG	1.188			1.045			1.924	1.184
11127 KG	1.314			1.105			2.825	1.463
Tandem Axle (1.2m)								
13582 KG	1.014	0.600		0.935	0.934		1.199	1.548
22327 KG	1.403	0.773		1.082	1.081		3.994	2.695
Tandem Axle (1.5m)								
5445 KG	0.545	0.368		0.641	0.584		0.122	0.315
9555 KG	0.851	0.604		0.861	0.827		0.688	1.052
10645 KG	0.787	0.565		0.939	0.935		0.518	1.564
11718 KG	0.907	0.624		0.985	0.944		0.858	1.748
12500 KG	0.916	0.684		1.049	0.996		0.952	2.184
13136 KG	0.980	0.722		1.085	1.031		1.214	2.489
13236 KG	0.986	0.752		1.020	1.002		1.288	2.085
14582 KG	0.979	0.679		1.039	1.021		1.151	2.237
15336 KG	1.017	0.713		1.079	1.059		1.341	2.580
15582 KG	1.085	0.722		1.086	1.045		1.656	2.552
Tandem Axle (1.8m)								
14064 kg	1.020	0.759		0.991	1.014		1.431	2.020
22127 kg	1.313	0.932		1.111	1.101		3.578	2.937
Triaxle (2.4m)								
20082 kg	1.110	0.646	0.599	0.981	0.918	0.932	1.819	2.416
31645 kg	1.273	0.722	0.642	1.089	1.021	1.069	2.981	3.753
Triaxle (3.7m)								
20509 kg	1.003	0.743	0.742	0.937	0.953	0.985	1.656	2.568
31664 kg	1.131	0.887	0.876	1.114	1.072	1.081	2.839	4.152

3.9 AASHO Interim Guide for the Design of Flexible Pavements (1986)

The AASHO Interim Guide for the Design of Flexible Pavements recommended an empirical design procedure, based on data accumulated during the AASHO Road Test. The Appendix F of this guide details the determination of LEF's. In order to obtain the load equivalencies as the ratio between the number of 18,000 lb. single axle load, W_{t18}, and the number of any other axle load causing the same decrease in serviceability, W_{tx}, Equation 3.7 was written as:

$$\log W_t = \log \rho + \frac{G_t}{\beta} \tag{3.34}$$

Expanding the above equation by introducing the expression for the logarithm of ρ, (Equation 3.12), the logarithm of the number of applications of a specific axle can be expressed as:

$$\log W_t = 5.93 + 9.36 \log(\overline{SN} + 1) - 4.79 \log(L_1 + L_2) + 4.33 \log L_2 + \frac{G_t}{\beta} \tag{3.35}$$

where $\overline{SN}$ is the structural number; L_1 and L_2 were defined earlier. Values of W_t may be obtained for the 18,000 lb. single axle ($L_1 = 18, L_2 = 1$) and a candidate single axle ($L_1 = X, L_2 = 1$). The subtraction of the resulting expressions will result in Equation 3.36 :

$$\log\left(\frac{W_{t18}}{W_{tx}}\right) = 4.79\log(L_x + 1) - 4.79\log(18+1) + \frac{G_t}{\beta_{18}} - \frac{G_t}{\beta_x} \qquad (3.36)$$

For a tandem axle ($L_1 = X, L_2 = 2$), another expression was obtained:

$$\log\left(\frac{W_{t18}}{W_{tx}}\right) = 4.79\log(L_x + 2) - 4.79\log(18+1) - 4.33\log 2 + \frac{G_t}{\beta_{18}} - \frac{G_t}{\beta_x} \qquad (3.37)$$

In Equations 3.36 and 3.37, the ratio of W_{t18} and W_{tx} represents the Equivalency Factor, (Equation 3.1). Analyzing the above equations and the expression of β, (Equation 3.11), it can be concluded that the LEF's depend on the candidate axle weight, its configuration (single axle or tandem), the structural number of the pavement and the selected value of terminal serviceability. Although using the Equations 3.36 and 3.37 a wide range of LEF's can be calculated, the AASHO Interim Guide presents two sets of values, for $p_t = 2$ and $p_t = 2.5$. Those values were determined for a axle weight range of 2,000 - 40,000 lb. (single axle) and 10,000 - 48,000 lb. (tandem axles), given 6 levels of the Structural Number (1 - 6).

3.10 Study by Hutchinson et al. (1987)

The study calculated LEF's using the mechanistic approach, applied to the same data base as the Canadian Vehicle Weights and Dimensions Study.

The method developed by the authors, referred to as

University of Waterloo method, was used for isolating and counting of load deformation cycles, in order to accumulate the induced pavement damage. A parallel to the metal fatigue area was made, and the peak counting methodology introduced by the ASTM Standard Practice for Cycle Counting in Fatigue Analysis was referenced, (ASTM E 1049, 1985).

Although the Canadian Vehicle Weights and Dimensions Study generated both surface deflection and interfacial tensile strain data, this study only focused on surface deflection. Throughout the study, methodology and result comparisons and references to the Load Equivalency Factors section of the Pavements Response to Heavy Vehicle Test Program (Christison, 1986) were made. Regression equations for tandem axle groups as well as the effect of pavement structure, pavement temperature and vehicle speed on the LEF's of the axle groups were also developed.

For the estimation of LEF functions in a mechanistic way, the study recommended the following steps:

i) select the pavement response parameter

i) measure the response parameter under different axle groups

iii) isolate and count damage related response cycles under an axle group accumulating the damage created by cyclic loading

iv) express damage as the equivalent number of passes of a standard axle load.

Analyzing the pavement surface deflection, it was observed that the pavement does not recover fully after the passing of successive axles, and the maximum and residual deflections increase under successive axles in most cases. Considering the deflection signature of a tridem axle group, the counting of cycles is exemplified and the results are compared to those obtained in the Canadian Vehicle Weights and Dimensions Study. The Load Equivalency Factor for an axle group is defined (Equation 3.38) as the sum of the LEF of each axle belonging to the group,

$$LEF(X)=\left[\frac{D1(X)}{D(S)}\right]^{C}+\left[\frac{D2(X)}{D(S)}\right]^{C}+\left[\frac{D3(X)}{D(S)}\right]^{C} \qquad (3.38)$$

where:

$D1(X)$ = the largest deflection cycle under the axle group

$D2(X)$ = the second largest deflection cycle under the axle group

$D3(X)$ = third largest deflection cycle under the axle group

$D(S)$ = deflection under the standard axle, and

C = material constant.

The method for individual LEF calculation used by the authors, (Figure 3.21), was derived from the ASTM Standard mentioned above. It implies the extraction of the deflection under the axle group for the largest load-deflection cycle D1(X), followed by the deflection for the second largest load-deflection cycle D2(X) and the deflection for the third largest load-deflection cycle D3(X), as shown in Figure 3.20.

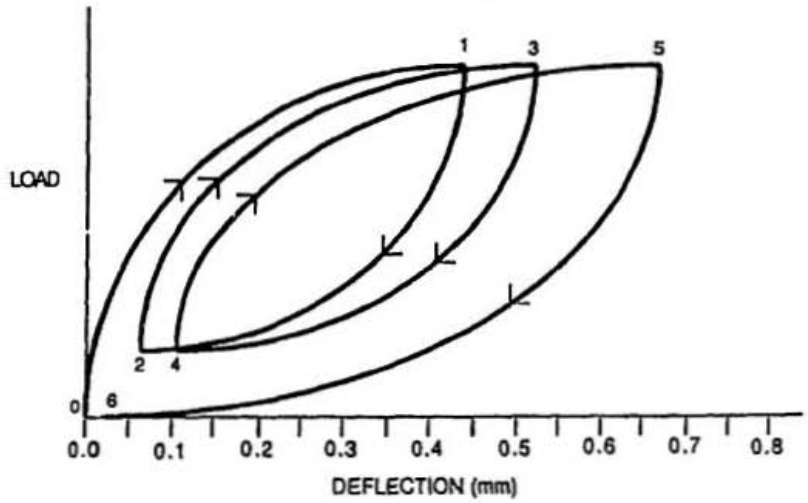

Figure 3.20 : Hypothesized load-deflection history for tridem pass, (After Hutchinson et al., 1987).

The Load Equivalency Factor for each axle results by calculating the ratio of the extracted deflection over the deflection under the standard axle load D(S), and raising the result to the exponent C. Throughout the study, an exponent value of 3.8 was used, considering this value as being representative for the AASHO Road Test and making possible the comparison to the results obtained by RTAC (1986).

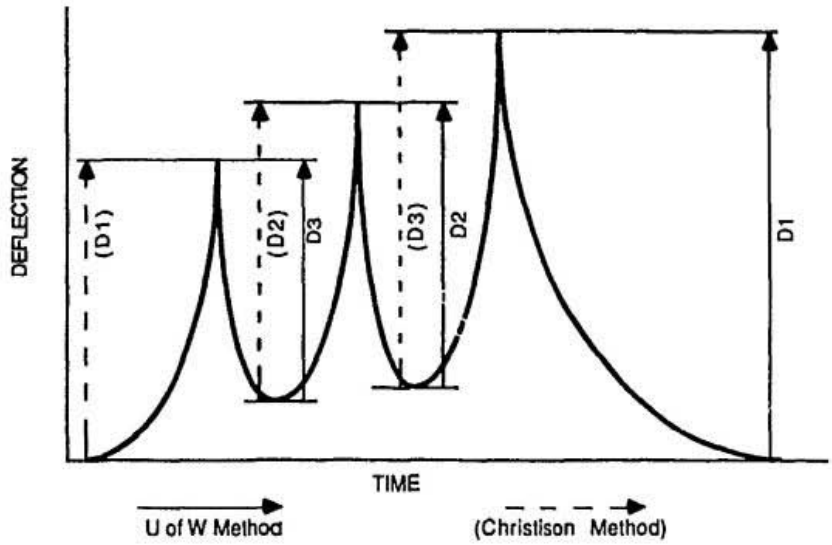

Figure 3.21 : Comparative methods for deflection peak extraction, (After Hutchinson et al., 1987).

The study acknowledged the sensitivity of LEF estimates to the method employed to isolate and count damage cycles, as well as to the value of the cumulative damage function exponent C. The use of the ASTM Standard methodology produced higher LEF values than those obtained by considering the deflection under the lead axle as the primary damage cycle, as used in the Canadian Vehicle Weights and Dimensions Study (Section 3.8). Compared to the RTAC (1986) results, the average increase in LEF values obtained by the Waterloo method was 8% for tandems and 16% for tridems.

side, considering asphalt concrete's plastic behavior.

The use of the area under the deflection curves was examined as an alternative indicator of relative damage. This, however was also rejected because: *"since the area under two superimposed curves is just the sum of areas of the individual curves, the load equivalency is always 2 (assuming equal areas) and is independent of curve shape or axle separation"*.

Using both Equation 3.24 and Equation 3.33, LEF's were calculated for different axle separations. In both cases, when the axle separation equals the length of loading side of the assumed deflection profile, there is a discontinuity in the shape of the LEF curve, as shown in Figure 3.23. Based on this discontinuity and on discrepancies in LEF's obtained by the Canadian Vehicle Weights and Dimensions Study from deflection responses, Equation 3.24 is considered as yielding unrealistic LEF's.

The study concludes that "completely satisfactory" methods for deriving primary response equivalency factors from measured peak deflection or areas under the response curves cannot be obtained. Equation 3.24 should not be used, while Equation 3.33 can be accepted until some better scheme is developed.

3.11 Study by Majidzadeh et al. (1988)

This study analyzed the LEF calculation procedure employed in the Canadian Vehicle Weights and Dimensions Study (RTAC, 1986), based on theoretical considerations.

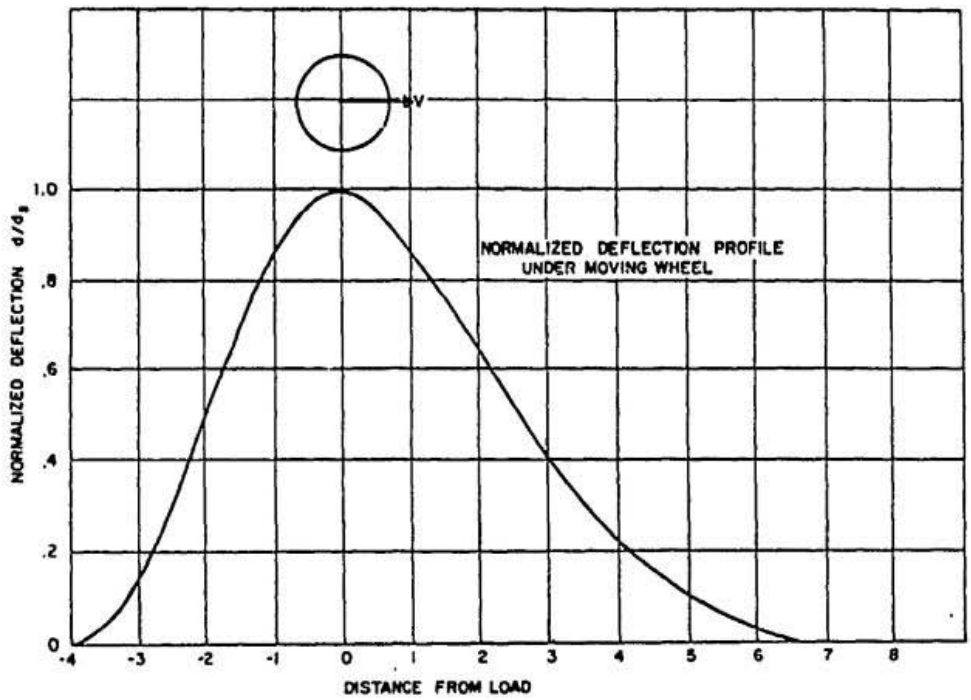

Figure 3.22 : Assumed deflection profile for an axle, (After Majidzadeh et al., 1988).

The deflection profile under a tandem axle with a small axle separation was simulated by superposing the single axle response, (Figure 3.22).

The loading side of the deflection profile was considered sinusoidal and having a shorter duration than the unloading

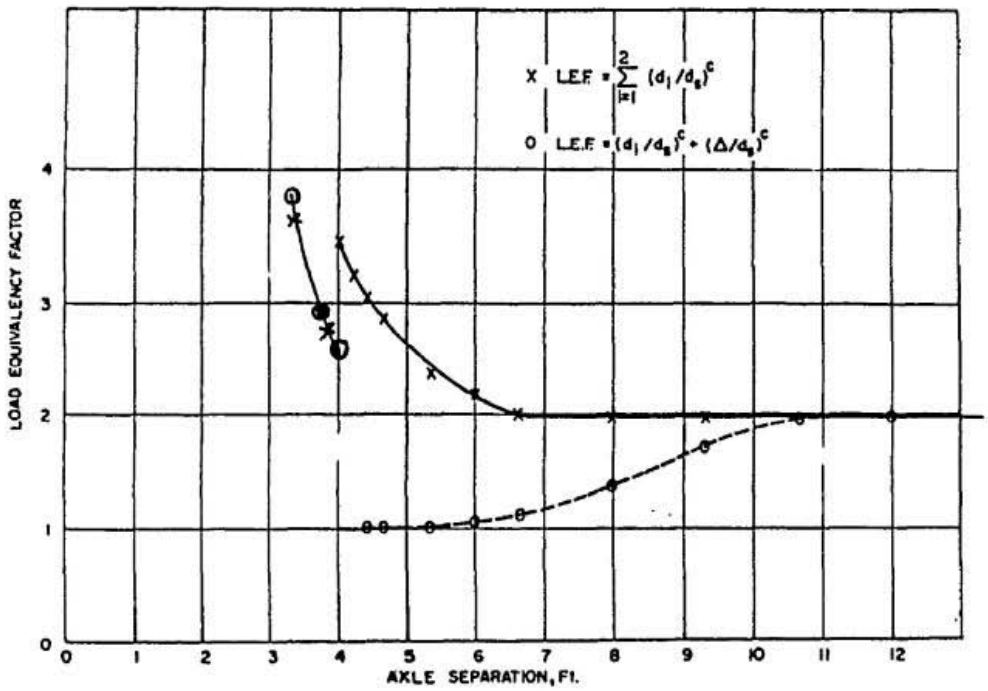

Figure 3.23 : Load equivalency factors for various axle spacing, (After Majidzadeh et al., 1988).

3.12 Study by Hajek et al. (1989)

This is a study based on data accumulated throughout the Vehicle Weights and Dimensions Study (RTAC, 1986) and theoretical pavement response data calculated using the computer program ELSYM5 (FHWA, 1985). The objectives were to evaluate the influence of axle spacing on flexible pavement damage, and to determine the maximum weights of individual tandem and tridem axles which will cause the same damage as

single axles with the maximum legal load.

For the determination of LEF's, peak and valley values were extracted from both strain and deflection response curves according to the ASTM E 1-49-85 Peak Method. For the deflection, this method consists of extracting the whole value of all the peaks of the response curve. For the strain response, the method consists of extracting the response curve peaks taking into account both tension and compression. Figure 3.24 presents peak deflection or strain values involved in LEF calculation for a tridem.

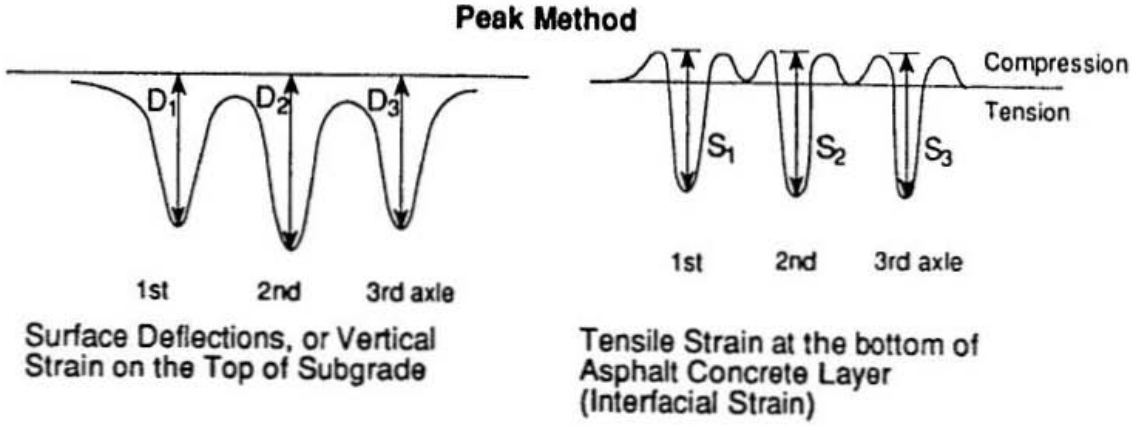

Figure 3.24 : Peak method used to calculate the effect of multiple axle groups. After Hajek et al. (1989).

Three approaches of summation of discrete response values were compared, namely the method used in the Vehicle Weights and Dimensions Study (RTAC, 1986), the method proposed by Hutchinson et al. (1987), and the Peak Method proposed here.

For surface deflections, the assumption of zero deflection between loads is made (rest position) and the total deflection under each axle measured from the rest position was extracted. It was assumed that the inclusion of the total deflection under each axle models best the overall pavement response even though deflection between two subsequent axles does not reach a zero level. The above procedure, discussed also by Prakash et al., is also recommended for subgrade strains summation.

For interfacial strains, the peaks-to-trough rise and fall are extracted as presented in Figure 3.24. This procedure was considered to be identical to that recommended by the ASTM Standard Practice for Cycle Counting in Fatigue Analysis (ASTM, 1985).

The study yielded the following results. First, summation methods influence LEF values; second, the Peak Method produced the highest LEF's, followed by the method proposed by Hutchinson and that used in the RTAC study (1986). It was concluded that based on available information and data, it was not possible to positively recommend any particular summation method.

3.13 Study by Govind et al. (1989)

This study attempts to derive a fatigue failure model adopting a theoretical approach based on calculated pavement responses (stresses, strains and displacements). The model

estimates the dynamic load and determines induced pavement responses for specific load configurations and pavement profiles. Using the rate of change of stress, damage transforms are obtained and related to pavement life according to the load equivalency concept. The model is calibrated employing AASHO Road Test data. The fatigue damage forecasting may be performed for any axle weight and axle group configuration.

The rationale of this study was to develop damage transforms relating the fatigue damage domain to one of the simulated pavement responses, namely stress. According to the observation that fatigue is determined both by load magnitude and its rate of application, the rate of change of force, stress or energy can be considered as representative of damage. Also, because the size of the test specimen influences the rate of energy absorption and dissipation, it is necessary to normalize the power (i.e., rate of change of energy) by the volume of the specimen. Equation 3.39 shows the dimensional representation of power per unit volume:

$$Power\ \ per\ \ unit\ \ volume\ = \frac{M}{LT^3} \qquad (3.39)$$

where:

L = the length dimension

M = the mass dimension, and

T = the time dimension.

The stress history of the pavement is a function of both time and distance because it can be thought as a function of time at a particular point in space, or as a function of distance for a particular point in time. Equation 3.40 presents the differential with respect to time of the stress history for small magnitudes of time increments.

$$\left[\frac{\delta\sigma(t,x)}{\delta t}\right]=\frac{d\sigma}{dt} \tag{3.40}$$

where:

$\sigma(t,x)$ = the stress function

δ = denotes the process of partial differentiation

t = notation for time, and

x = notation for distance.

The dimensional analysis of Equation 3.40 reveals the following dimensional relationship:

$$\frac{d\sigma}{dt}=\frac{M}{LT^3} \tag{3.41}$$

Examining the dimensional equivalency of Equations 3.39 and 3.41 it was concluded that the rate of change of stress can be adopted as the parameter used to derive a damage function.

In deriving the damage transform, three operations are recommended, namely, summation over time duration of the event,

the use of absolute values of the exact differential, and normalization with respect to time. The damage transform presented in Equation 3.42 applies to single-peak events.

$$D^n = \left(\int_{t_0}^{t_1} \frac{1}{t_1 - t_0} \left| \frac{\delta \sigma}{dt} \right| dt \right)^n \tag{3.42}$$

where:

t_0 = initial moment of the event

t_1 = final moment of the event.

An event comprising of more than one peak will be divided into subevents starting at each successive negative to positive change in slope. Equation 3.43 introduces the damage transform for an event comprising m single stress peak subevents D_i.

$$\sum_{i=1}^{m} D_i^n = \sum_{i=1}^{m} \left(\frac{1}{t_{i-1} - t_i} \int_{t_{i-1}}^{t_i} \left| \frac{\delta \sigma}{dt} \right| dt \right)^n \tag{3.43}$$

The damage transforms can be used to compare the effects of different loading events. Considering two single peak events a and b, the law of equivalency can be expressed as:

$$LEF = \left(\frac{D_a}{D_b} \right)^n = \left(\frac{L_b}{L_a} \right) \tag{3.44}$$

where:

D_a = damage by the event a

D_b = damage by the event b

L_a = number of cycles to failure of the specimen undergoing the event a, and

L_b = number of cycles to failure of the specimen undergoing the event b.

The calculation of the exponent n was done using the AASHO Road Test data and the standard 18-kip axle as reference. Given a specific load x, the values L_x and L_{18} were obtained at the AASHO Road Test, while the damage transforms D_x and D_{18} were calculated from the simulated stress patterns. Using the right part of Equation 3.44, the n value can be obtained. Subsequently, a regression analysis was done in order to find the range of value the variable n can take. The range $3 \leq n \leq 7$ was found to be reasonable. Sensitivity analysis of ESAL with respect to n using the methodology described above was performed and the results tabulated. Also, an ESAL table, for PSI=3 and six levels of the Structural Number, was provided.

3.14 Study by Tseng and Lytton (1990)

The objective of this study was to calculate the fatigue damage properties K_1 and K_2 (the ones referred to as K and C, respectively in Equation 3.13) based on the fracture mechanics and compare them to coefficients obtained by regression analysis on experimental fatigue data. The most commonly used fatigue

distress function, presented by Equation 3.13, was employed through the study. From a phenomenological point of view, K_1 and K_2 can be obtained as regression constants based on laboratory fatigue life determination.

The approach adopted for deriving laboratory fatigue damage properties due to multiple axle loads, and for converting them to field values is of interest.

It is known that a multiple axle load generates multiple tensile strain peaks, reducing the fatigue life in terms of number of axle loads to failure.

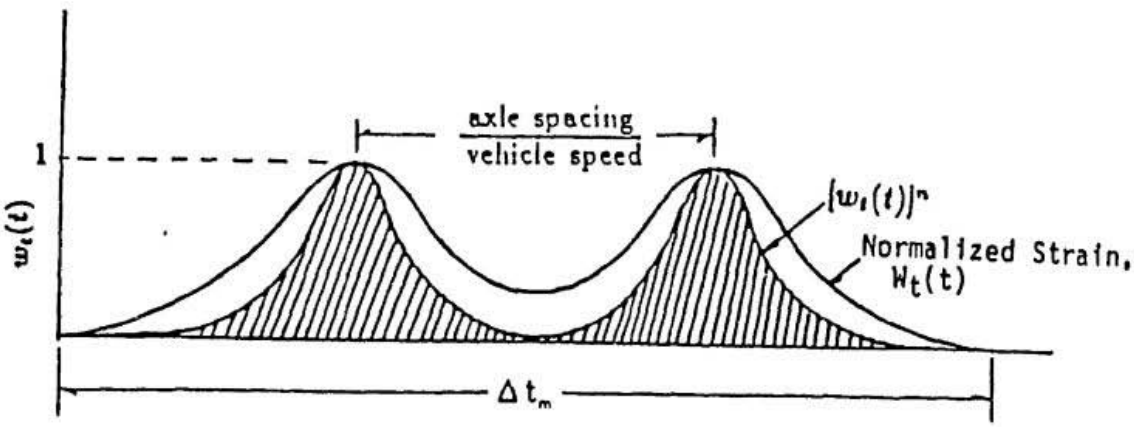

Figure 3.25 : Wave shape of loading pulse produced by a tandem. After Tseng et al. (1990).

The study relates the tensile strain at the bottom of the asphalt concrete layer produced under a multiple axle to that produced under a single axle load by introducing the parameter

ξ according to Equation 3.45. The first integral corresponds to the shaded area in Figure 3.25 while the second integral corresponds to the shaded area presented in Figure 3.26.

$$\xi = \frac{\int_0^{\Delta t_m} w_m(t)^n dt}{\int_0^{\Delta t_s} w_s(t)^n dt} \qquad (3.45)$$

where:

$w_m(t)^n$ = the wave shape of the normalized tensile strain at the bottom of the asphalt concrete layer produced by a multiple axle load

$w_s(t)^n$ = the wave shape of the normalized tensile strain at the bottom of the asphalt concrete layer produced by a single axle load

Δt_m = time required for the strain caused by a multiple axle load to build up and completely decay

Δt_s = time required for the strain caused by a single axle load to build up and completely decay

$n = K_2$ = damage property.

Considering theoretical calculations, the wave shape of the loading due to a tandem axle is obtained by superposing the tensile strain waveform due to each individual axle.

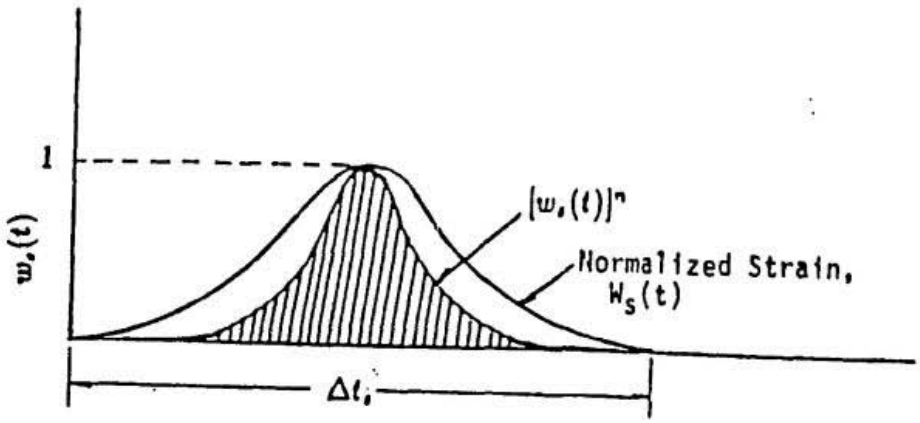

Figure 3.26 : Wave shape of loading pulse produced by a single axle, (after Tseng et al., 1990).

It was suggested that because laboratory loading is applied without rest periods between applications, causing residual stresses in fatigue samples, laboratory fatigue tests underpredict field fatigue life. In order to solve this problem, a shift factor between laboratory and field fatigue life was proposed, as shown in Equation 3.46.

$$SF = (SF_x)(SF_h) \qquad (3.46)$$

where:

SF_x = the shift factor due to residual stresses, and

SF_h = the shift factor due to healing during the rest period.

The shift factor due to residual stress considers the behavior of the residual stress during a rest period and can be estimated by Equation 3.47.

$$SF_x = \frac{N_{fc}}{N_{fa}} = \left(\frac{1}{1 \pm p_0 t^{-m}} \right)^{k_{2l}} \qquad (3.47)$$

where:

N_{fc} = the number of load cycles to failure for the tensile strain altered by the residual stress

N_{fa} = the number of load cycles to failure for the total tensile strain

K_{2l} = the value of K_2 determined from the laboratory

p_0 = the percent of total strain remaining in the pavement as residual strain immediately after the passage of the load, and

m = the exponential relaxation rate.

The shift factor due to rest periods is related to the healing of the material after the rest period, and can be estimated by Equation 3.48.

$$SF_h = \frac{N_f}{N_0} = 1 + \frac{n_r m_0}{N_0} \left(\frac{t_i}{t_0} \right)^h \qquad (3.48)$$

where:

N_f = number of cycles to failure with a rest period

N_0 = number of cycles to failure without a rest period

n_r = number of rest periods of length t_1

t_0 = the time length of a load pulse without rest periods, and

t_1 = the time length of a load pulse with rest periods, and

m_0, h = regression constants.

The shift factor is used to adjust laboratory-obtained K_1 and K_2 to field loading conditions. For validation, the methodology presented above was applied to field sections of the AASHO Road Test and to Florida pavement sections. It was concluded that good fatigue life predictions may be obtained by using it.

3.15 Summary of Methods for LEF's Calculation

Table 3.2

Summary of Methods for LEF's Calculation

Deacon (1969)

$$F = 2^{*}\left(\frac{SMAX}{S18}\right)^{C}$$

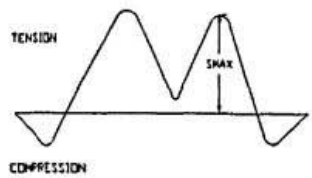

AC strain

*

Calculated

Ramsamooj (1972)

$$F = \left(\frac{H1}{H18}\right)^{4} + \left(\frac{H2}{H18}\right)^{4}$$

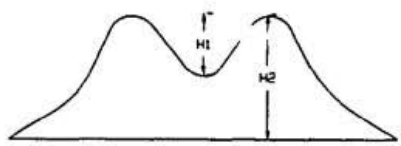

Stress intensity

factors

Measured

Christison

(1978)

$$F = \left(\frac{D1}{D18}\right)^{C} + \left(\frac{D2}{D18}\right)^{C}$$

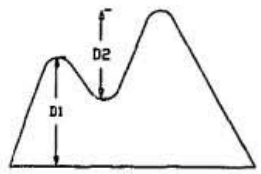

Deflection

Measured

$$F = \left(\frac{S1}{S18}\right)^{C} + \left(K\frac{S1}{S18}\right)^{C}$$

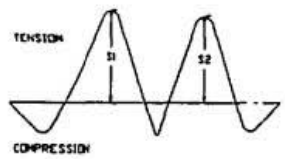

AC strain

Measured

---

* AC - Asphalt Concrete

Table 3.2

Summary of Methods for LEF's Calculation (Continued)

Treybig (1983)

$$F = \left(\frac{S1}{S18}\right)^c + \left(\frac{S2}{S18}\right)^c + \left(\frac{S3}{S18}\right)^c$$

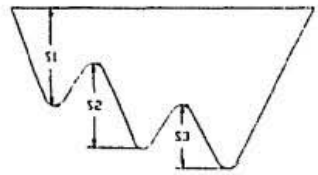

Subgrade strain

Calculated

AC strain

Calculated

$$F = \left(\frac{S1}{S18}\right)^c + \left(\frac{S2}{S18}\right)^c + \left(\frac{S3}{S18}\right)^c$$

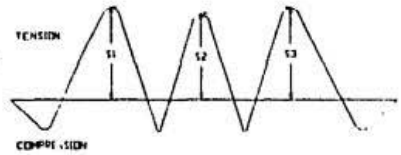

Southgate (1985)

Strain energy density

Calculated

$$F = \frac{N18}{N} \qquad \log(N) = \frac{\log(\epsilon_w) + 2.6777807}{-0.15471249}$$

RTAC (1986)

Deflection — as Christison (1978)

Measured

AC strain — as Treybig (1983)

Measured

Table 3.2

Summary of Methods for LEF's Calculation (Continued)

Hutchinson (1987) Deflection Measured	$F = \left(\frac{D1}{D18}\right)^C + \left(\frac{D2}{D18}\right)^C + \left(\frac{D3}{D18}\right)^C$	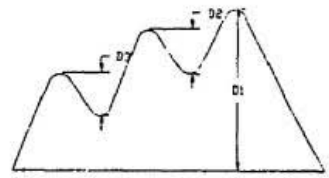
Hajek (1989) Deflection Calculated & measured	$F = \left(\frac{D1}{D18}\right)^C + \left(\frac{D2}{D18}\right)^C + \left(\frac{D3}{D18}\right)^C$	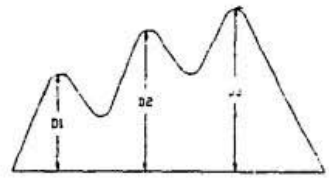
AC strain Calculated & measured	$F = \left(\frac{S1}{S18}\right)^C + \left(\frac{S2}{S18}\right)^C + \left(\frac{S3}{S18}\right)^C$	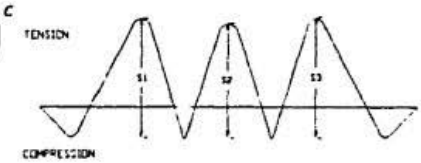
Govind (1989) AC stress Calculated	Damage Factors (LEF's) were calculated based on the rate of change of stress.	

Table 3.2

Summary of Methods for LEF's Calculation (Continued)

Tseng (1990)	
AC strain Calculated	The AC strain pattern was used to modify the value of the exponent C.

Chapter 4

CRITICAL OVERVIEW OF LITERATURE

The following chapter discusses the methods for LEF's calculation reviewed in Chapter 3. It is structured in three sections, starting with the AASHO Road Test and its influence on the more recent research. The second section analyzes the mechanistic methods for LEF's calculation, and the third section is dedicated entirely to the cycle counting methods introduced by the ASTM E 1049-85 standard.

4.1 The AASHO Road Test

The AASHO Road Test produced LEF's related to pavement performance, as defined by serviceability. The LEF values produced were based on statistical analysis of empirical data. They were functions of axle load, axle configuration (single or tandem), type of pavement (flexible or rigid), terminal serviceability and Structural Number. Also, they inherently accounted for a number of other factors, such as variable impact of the traffic throughout the seasons, vehicle dynamics, tire contact pressure as well as axle spacing and tire type. With few modifications the AASHO Road Test LEF's are still a part of current pavement design practices (AASHTO Design Guide, 1985).

Subsequent efforts to obtain LEF's have adopted a mechanistic approach, being based on either measured or

calculated response parameters. However, AASHO LEF's were extensively used by researchers in order to verify proposed LEF calculation methodologies.

The studies mentioned bellow used AASHO Road Test data as a basis for LEF's calculation. Deacon (1969) computed asphalt concrete strain responses for AASHO Road Test sections, concluding that theoretically obtained LEF's offer evidence of the validity of the AASHO Road Test LEF's in design situations. Christison (1978) obtained a close agreement between LEF's based on measured asphalt concrete strain/deflection and AASHO LEF's. The same LEF's served as verification basis for Treybig (1983). Extensive use of the AASHO Road Test pavement cross-section data and loading configurations was made by Southgate (1985) in order to verify the proposed strain energy density method. Govind (1990) calculated normal and longitudinal stress profiles and normal displacements produced at the AASHO Road Test, and used them as input to a fatigue failure model.

There is no doubt that the intent to validate a LEF's calculation methodology by comparing empirical LEF's to mechanistic LEF's cannot be conclusive. This is because the empirical LEF's are based on performance, which represents an overall assessment of pavement serviceability, while the

mechanistic LEF's reflect one particular type of distress, such as fatigue cracking or rutting, usually described by a simple fatigue relationship (Equation 3.13).

4.2 Mechanistic methods for LEF's determination

Advanced analytical and experimental techniques combined with an improved knowledge of fatigue behavior of bituminous mixes, led to the development of mechanistic methodologies for LEF's calculation based on calculated or measured pavement response parameters. These methodologies can be classified into two categories. The first category comprises most of the work done in this area, and includes methods based on strain magnitude. Considering a method belonging in this class, there are four main aspects which must be pointed out; the first is related to the type of response parameter the method is based on, (eg., deflection, tensile strain at the bottom of the asphalt concrete layer, or compressive strain at the top of the subgrade). The second considers how the response parameter is obtained (calculated or measured). The third explains the way the method treats the part in compression of the trough-peak-trough cycles, when analyzing tensile strain at the bottom of the AC layer. The fourth aspect clarifies the relationships with earlier methods.

Deacon (1969) considered the tensile strain at the bottom of the asphalt concrete layer as the response parameter. The computed strain patterns were symmetric curves in tension. The recommended methodology was to identify single axles producing the same tensile peak as the tandem. As a result, the LEF of the tandem axles would be twice the LEF of a single axle carrying the same load.

Ramsamooj (1972) used the stress intensity factor, a function of stress compliance and crack length, as the response parameter for LEF calculation. The influence lines of the stress intensity factors were determined on the basis of experimental measurements. The resulting stress intensity factor curves for tandems had also a symmetrical shape characterized by two equal peaks (Figure 3.3). However Ramsamooj adopted a new approach, extracting one maximum peak and the following peak-to-trough value (Table 3.2).

Experimental techniques allowed the measurement of pavement response parameters, making possible the calculation of LEF's from in-situ pavement response parameters. The curves based on measured response parameters were shown to have unequal peaks as a result of the visco-plastic behavior of the asphalt concrete.

Christison (1978) measured deflection and asphalt concrete strain responses. For deflection peak identification, the method proposed by Ramsamooj (1972) was followed. The only difference was that Christison dealt with deflection patterns with unequal peaks, situation that raised the issue of an identification order for the deflection cycles. Christison proposed the identification of the deflection peak under the leading axle of the tandem as a first cycle, followed by the peak-to-trough value of deflection as a second cycle. However, the deflection peak under the trailing axle of a tandem axle is bigger than the peak under the leading axle because of residual deflections. This would suggest a cycle identification method based on the highest deflection peak. Dealing with asphalt concrete strain, Christison faced both tension and compression. It was decided to ignore the part in compression, considering only the tension part of the strair response. Also, a constant K was introduced, as an average ratio of the strain recorded under the second axle divided by the strain recorded under the leading axle of a tandem axle, for all the experimental runs. This constant was employed in the LEF's expression (Equation 3.31).

Treybig (1983), used calculated subgrade strain and asphalt concrete strain for calculating LEF's. The mathematical formulation of the proposed Curvature Method included a

comprehensive formula for LEF calculation, which could be applied for any response parameter (Equation 3.25). The subgrade strain response versus time was similar in shape to that of deflection. In this case, Treybig used the method proposed by Christison (1978). However, for the AC strain, Treybig explicitly commented that the compressive values of the AC strain between axles should be neglected. That is, the LEF calculation was based only on the tensile peaks of the AC strain curve.

The RTAC study (1986), used Christison's (1978) method for calculating LEF's on the basis of deflection, and the method proposed by Treybig (1983) for asphalt concrete strain.

Hutchinson et al. (1987) was the first to use of the ASTM E 1049-85 Standard for calculating LEF's from measurements of pavement deflection. Although the Peak Counting method (which constructs the largest cycle first, followed by the second largest, etc.) was described, the Range-Pair method (which adopts a sequential left-to-right cycle determination approach) was used for the calculations. The applied method considered the highest deflection peak and the subsequent peak-to-trough deflection values.

Majidzadeh (1988) calculated strain response patterns under tandem axles on the basis of a simulated single-axle strain

pattern. The governing assumption was that "the response of multiple axle can be obtained from the superposition of the single axle response". Also, it was considered that the load received by the tandem was equally distributed to the component axles. The analysis was directed at pavement responses in general, without differentiating between strain and deflection. Varying the distance between the axles of the tandem and plotting LEF's versus axle separation, a discontinuity in the curve was observed (Figure 3.23). This discontinuity was the base for questioning the LEF's calculation methodologies employed at the time.

Hajek (1989) applied another method of the ASTM E 1049-85 Standard, namely the Peak Counting Method. Both calculated and measured deflections and asphalt concrete strains were used. For these response parameters, the method recommended the consideration of all peaks of the curve. In the case of asphalt concrete strains, a peak included both the part in tension and the part in compression of a single cycle.

From the above discussion a number of conclusions is drawn. First, there have been a tendency to devise more elaborate methods of peak identification and counting. Another trend is the development of methodologies applicable to any type of response parameter. The introduction (Hutchinson et al., 1987)

of the cycle concept, including both tension and compression in the case of the asphalt concrete strain can be considered as an innovation.

It is worth observing that one of the main differences between methods employing calculated and measured response parameters is the treatment of the dynamic/viscous component of pavement loading. The computer programs used to calculate pavement response, (eg., ELSYM5, BISAR, etc.) model only static load under ideal (i.e., elastic, isotropic) material conditions. Therefore, measured response parameters reflecting real material properties and loading characteristics are more credible than calculated response parameters.

The second category of methods for LEF's determination, utilized the pavement response curves in a different manner, devising methods that are based on the actual shape of the pavement response versus time (Govind, 1989; Tseng, 1990). Also, other methods employed new concepts, such as the strain energy density, which is indirectly related to the pavement response curves (Southgate, 1985).

Govind (1989) developed a model which simulated response parameters (stress, strain and deflection) and derived Damage Transforms based on the rate of change of stress. The Damage Transforms were subsequently used for LEF's calculation

(Equation 3.44).

Tseng (1990) integrated the processed response curves, aiming at the development of "fatigue damage properties", and developed shift factors for converting them to field values.

Southgate (1985) related fatigue life to calculated strain energy density, considering that the latter indicates better the internal behavior of the pavement under load. Because the proposed Damage Factors accounted only for evenly loaded axle groups, a multiplicative factor was statistically derived, for the case of unevenly axle loading in multiple axles (Equation 3.32).

4.3 Methods for cycle counting by the ASTM E 1049-85 Standard

The following section will analyze comparatively the methods proposed by the ASTM Standard Practices for Cycle Counting in Fatigue Analysis (ASTM E 1049-85). Each method will be described in terms of its basic elements and the recommended procedure for cycle counting. The purpose of this analysis is to evaluate the suitability of each method proposed by the ASTM in calculating pavement LEF's. Although the standard presents the processing of load versus time cycles, in its Section 4 it is stated that "cycle counts can be made

for time histories of force, stress, strain, torque, acceleration, deflection, or other loading parameters of interest". In accordance with the topic of this study, the discussion that follows deals exclusively with strain versus time loading histories.

A few definitions follow:

A reversal is defined as the point at which the first derivative of the strain versus time history changes sign. If the sign changes from positive to negative, the reversal is a peak. On the contrary, the reversal is defined as a valley (alternatively referred to as trough).

A range is defined as the algebraic difference of strain values belonging to two successive reversals. If a valley precedes a peak, the range is called positive range or increasing strain range. If a peak precedes a valley, the range is called negative range or decreasing strain range.

An overall range is defined by the algebraic difference between the largest peak and the smallest valley of the strain versus time history, which are not necessarily successive events.

Each method for cycle counting should be evaluated from two points of view, namely the basic element processed (range or reversal), and the cycle construction procedure. Considering

axle of the group is subsequently related to the cycle produced by the standard axle load (Equation 3.14). According to this requirement dictated by the LEF's calculation methodology, the method used for cycle counting should be able to identify and yield the value of the strain cycle produced by each individual axle. Consequently, methods making use of non successive ranges or methods constructing overall ranges do not seem to be suitable for LEF calculation.

Also, the fatigue behavior of asphaltic pavements, and the dependence of distress types on specific pavement response parameters suggests the use of methods able to differentiate between trough-peak-trough and peak-trough-peak cycles. Considering fatigue cracking and the associated response parameter, namely tensile strain at the bottom of the asphalt concrete layer, the cycles of interest will be of trough-peak-trough type. For compressive strain at the top of the subgrade, related to rutting, only peak-trough-peak cycles will be counted. Methods employing non sequential ranges or construct overall ranges do not comply with the above requirement and do not seem to be suitable for LEF's calculation.

All the methods discussed below will be exemplified using the strain versus time history for a tandem axle, supported by the corresponding σ versus ϵ diagram, both presented in Figure 4.1.

the basic element processed, the cycle counting methods can be classified in two categories. The first category includes methods dealing with ranges, such as the Simple Range Counting, the Range-Pair Counting, and the Rainflow Counting. The second category, represented by the Peak Counting method, considers response reversals as the basic element.

A further differentiation of cycle counting methods, which yields three categories, is on the basis of the cycle construction procedure. First, methods making use of ranges construct cycles based on successive ranges (Range-Pair Counting). Second, methods based on non successive ranges (Simple Range Counting), and third, a combination of the precedents (Rainflow Counting). These methods construct a cycle by pairing two ranges defined as half-cycle each. If there are leftover ranges after the pairing is completed, they are recorded as half-cycles. In the case of the Peak Counting method, a cycle is constructed by pairing two reversals, namely one peak and one valley. Half cycles start and end at zero strain and include only one reversal (Figure 4.3).

The subsequent use of cycle values produced by the methods discussed above, dictates another group of basic requirements. For example, based on the premise that damage is additive, the calculation of LEF for a multiple axle load is based on fatigue cycles caused by individual axles. The cycle produced by each

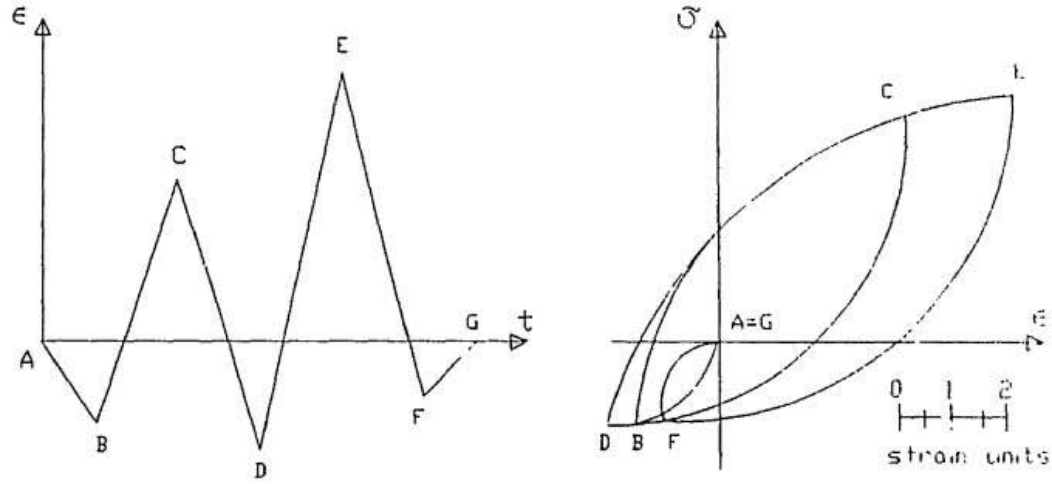

Figure 4.1 : Strain pattern produced by a tandem.

Throughout the text, the same sign convention will be employed, namely positive ordinate for tensile strain and negative ordinate for compressive strain. In quantitative terms, the strain versus time history consists of five reversals, three in compression and two in tension. For the sake of simplicity, each reversal was assigned a conventional numeric value, namely 1.5 strain units for B, 3 for C, 2 for D, 5 for E, and 1 for F. Where appropriate, those values will be employed explaining numerical procedures characterizing the analyzed methods.

4.3.1 The Simple Range Counting Method

The first method to be considered is the Simple Range Counting. It defines each range of the strain history as a

half cycle. Two ranges, not necessarily successive, having the same numerical value, are paired and form a cycle without differentiating between their signs.

Figure 4.2 presents each extracted range, both in terms of ϵ versus t and σ versus ϵ. The ranges obtained (A-B 1.5 strain units, B-C 4.5 strain units, and so on) represent half cycles. Because in this particular example there are no equal half cycles, their pairing and the construction of full cycles is not possible. In this case, the method yields six half cycles.

It becomes evident that the Simple Range Counting is not differentiating between trough-peak-trough and peak-trough-peak cycles, being concerned only with the absolute value of each range. Also, the method is not isolating cycles produced by a specific axle, allowing the construction of cycles based on ranges that are not necessarily successive. As a result of the two observations presented above, the Simple Range Counting method was found to be unsuitable for strain cycles identification and counting for calculating LEF's in flexible pavements.

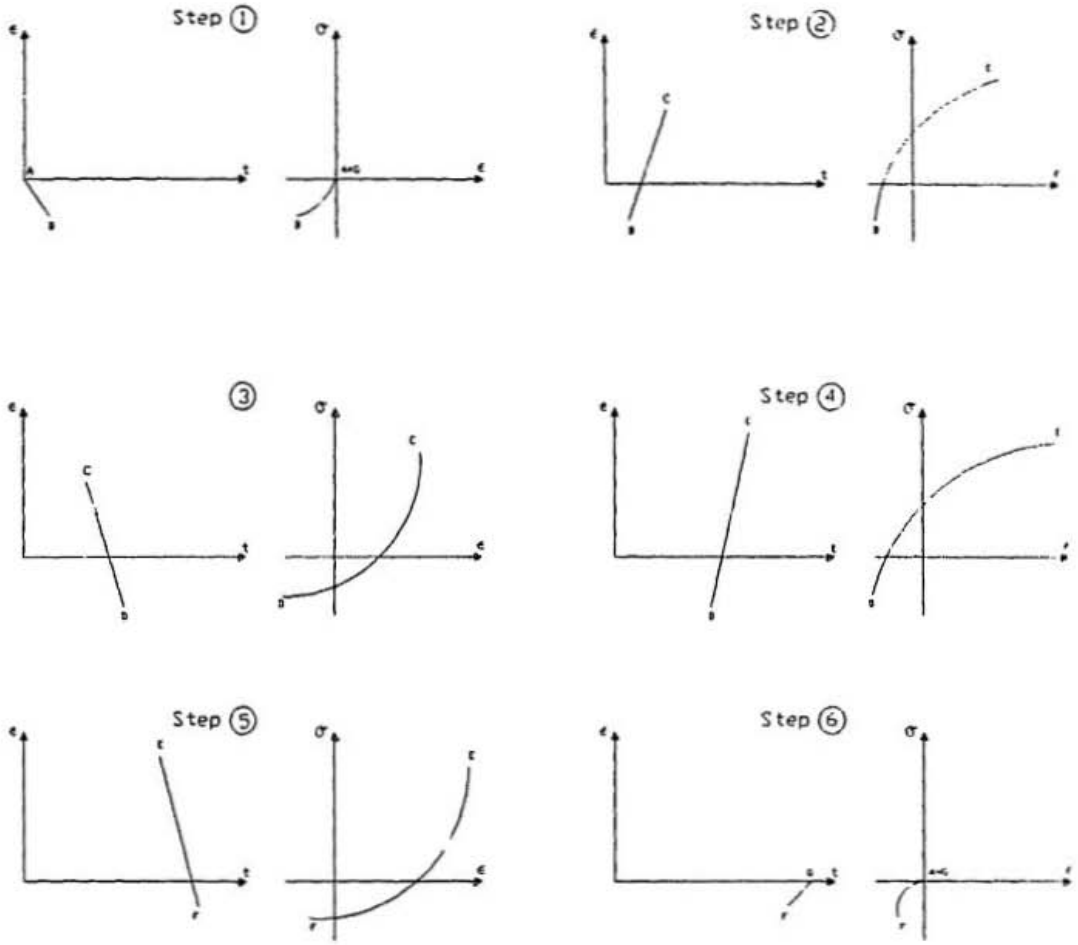

Figure 4.2 : Range extraction based on the Simple Range Counting method.

4.3.2 The Peak Counting Method

The Peak Counting method considers each reversal, in tension or compression, as half a cycle.

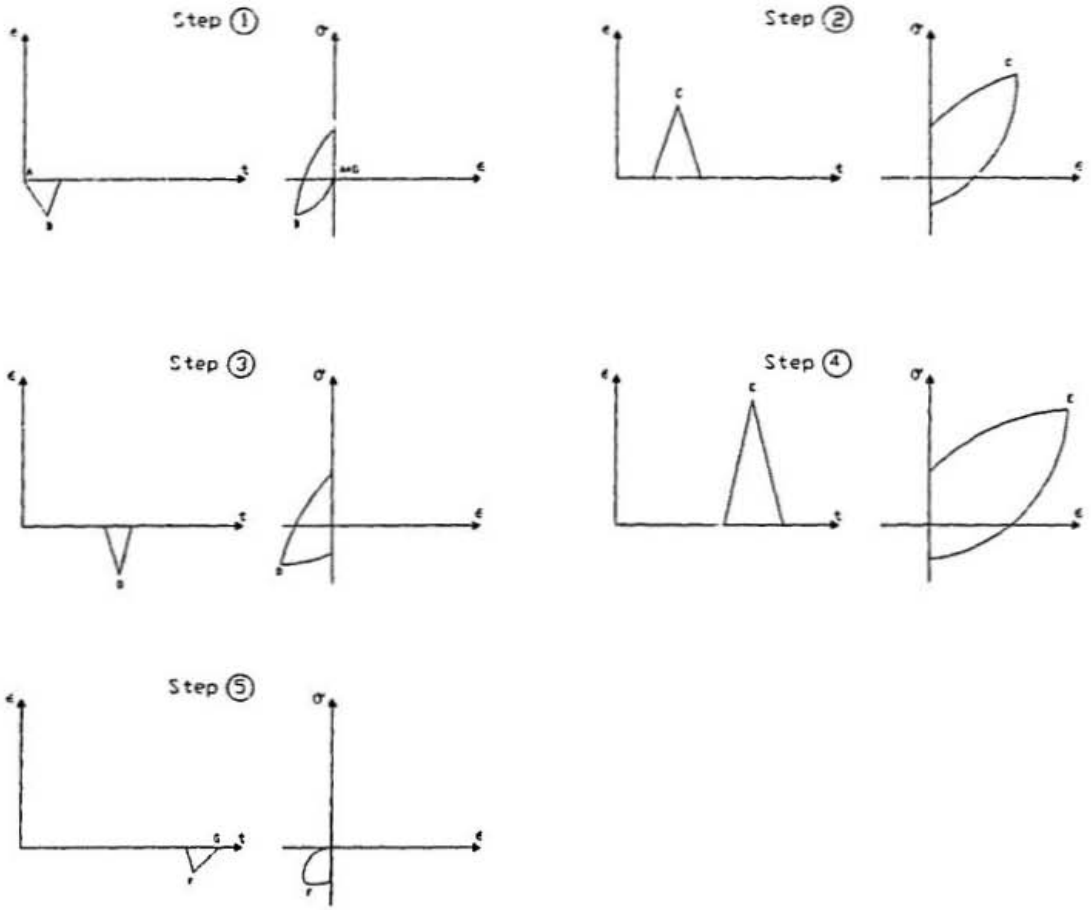

Figure 4.3 : Cycle identification according to Peak Counting method.

Each half cycle starts and ends at zero strain, and its numerical value is the absolute value of the reversal point's strain level. Figure 4.3 presents the half cycles corresponding to each reversal of the strain pattern.

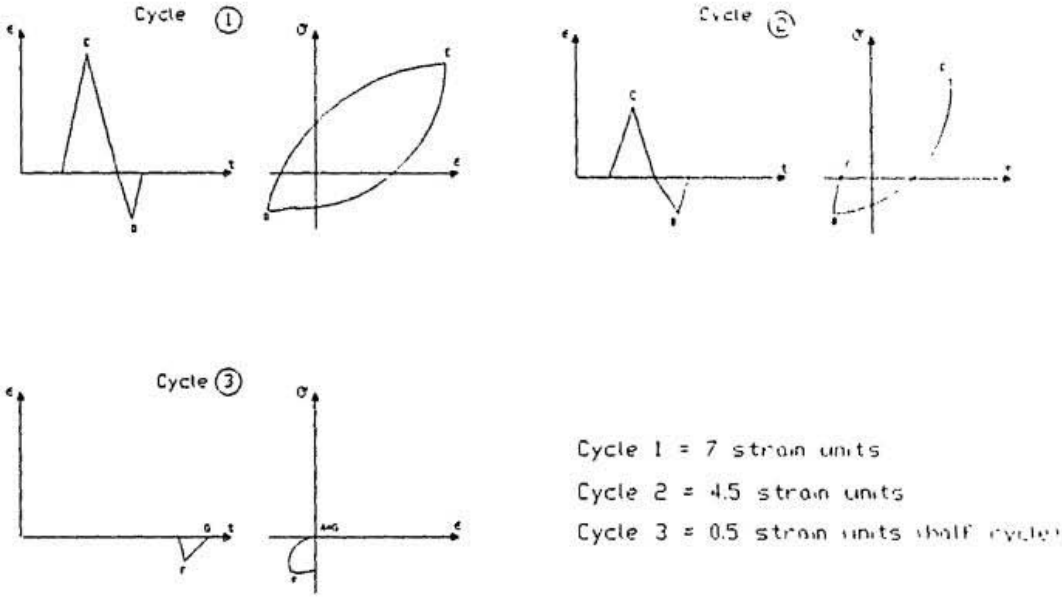

Figure 4.4 : Cycle construction according to Peak Counting method.

The cycle construction, depicted in Figure 4.4, is based on the following procedure. The first cycle is to be formed by composing the largest tensile and compressive half cycles. The second cycle is composed by the second largest tensile and compressive half cycles. If there is a remaining half cycle, it will be counted separately. Cycles based on eventually non successive reversals may be composed. Also, because tensile and compressive reversals are composed, the constructed cycles cannot represent a specific type of distress. As a result of

these features, this method has to be rejected as unsuitable.

4.3.3 The Rainflow Counting method

The Rainflow Counting considers three parameters at the same time, namely the starting point of the strain history and two consecutive strain ranges. According to the method, if the first range is smaller than the second range, and the starting point of the history belongs to the first range, the method will yield half cycles. If the starting point does not belong to the analyzed ranges, full cycles will be yielded. Figure 4.5 shows the application of the Rainflow Counting method for the strain pattern under a tandem axle. The Rainflow Counting procedure is not including backward counting when reaching the ending point of the loading history, while uncounted ranges are still available. The remaining sequence of ranges will generate a number of half cycles equal to the number of ranges in the sequence (see Step 4 in Figure 4.5). Any two half cycles having the same absolute value can be paired as a full cycle. According to this procedure, the Rainflow Counting may yield both full cycles and half cycles. The possibility to obtain half cycles is the feature that makes this method unsuitable for flexible pavement strain cycle counting.

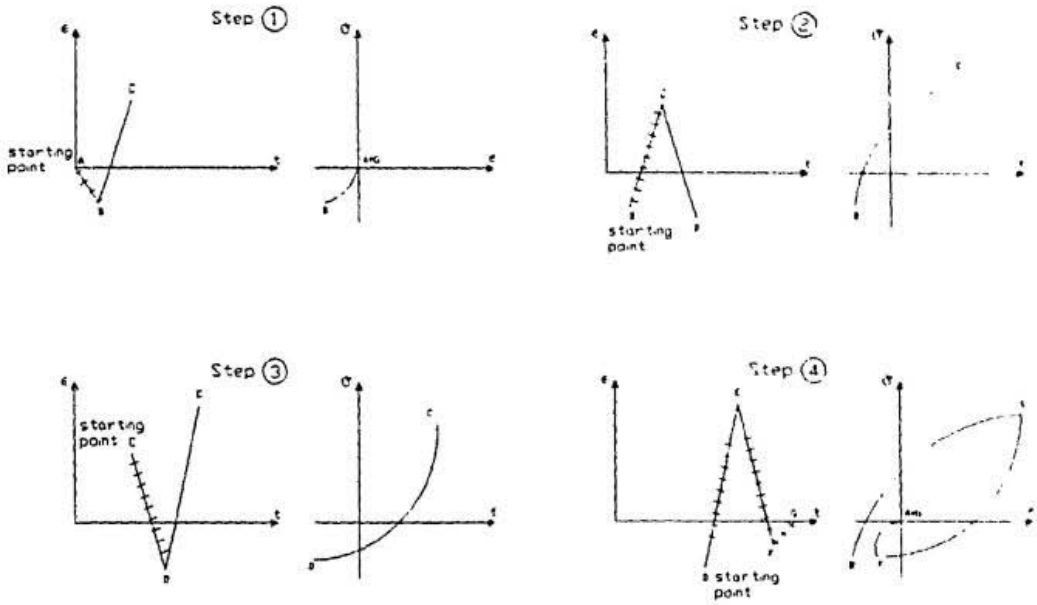

Figure 4.5 : Cycle identification according to the Rainflow Counting method.

4.3.4 The Range-Pair Counting Method

The Range-Pair Counting method compares each pair of successive ranges and extracts a cycle when the first range of the pair has a lower value than the second one. The cycle has the same value as the lowest range. If the final point of the history is reached without using all the ranges, the final point of the history becomes the starting point, and the pairing procedure is repeated backwards. Figure 4.6 demonstrates the Range-Pair Counting method applied as

recommended by the standard. It yields full cycles, each composed by subsequent ranges, and all the cycles are of the same type, in this case peak-trough-peak.

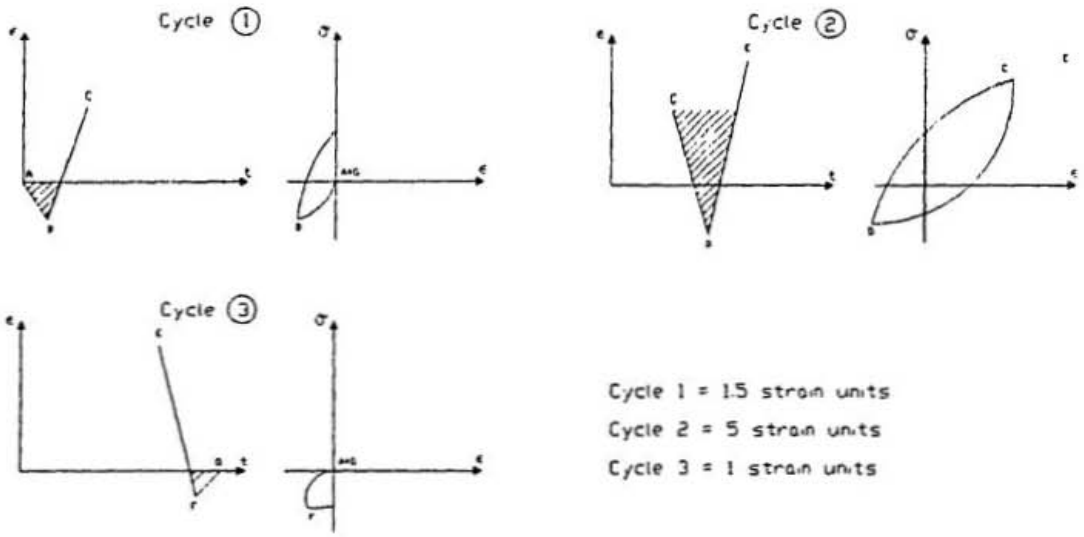

Figure 4.6 : Cycle counting according to Range Pair Counting method.

This method is suitable for flexible pavement strain cycle counting, because is compatible with the requirements presented at the beginning of the section. However, the type of failure, either compressive or tensile should determine the type of cycle to be counted. For fatigue cracking, with the pavement

failing in tension, only trough-peak-trough cycles should be extracted. According to Figure 4.7, the type of cycles counted depends also on the slope of the first range.

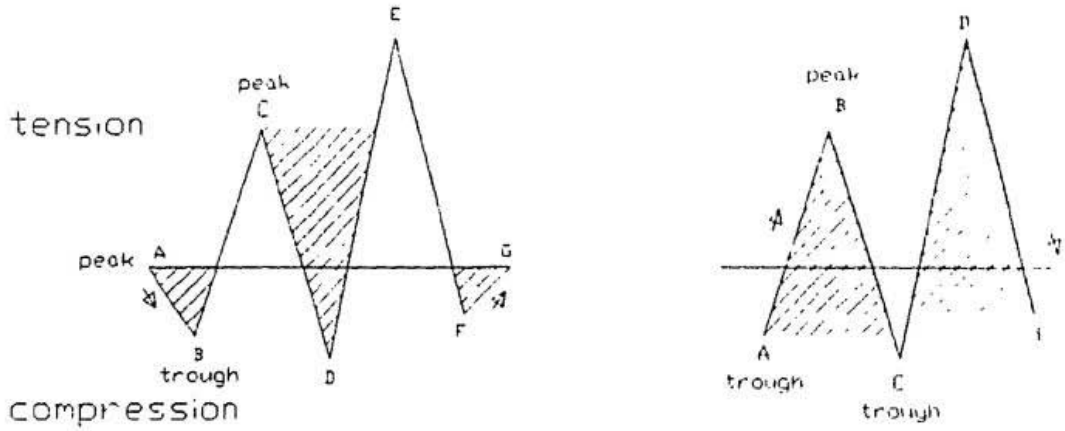

Figure 4.7 : Cycle extraction depending on the slope of the first range.

If the starting range is negative (or decreasing strain), the method will extract peak-trough-peak cycles. For a positive (or increasing strain) starting range, the method will extract trough-peak-trough cycles. Because an approaching axle or axle group will generate always an initial compressive reversal, starting with a negative range, the method recommended by the standard will yield always peak-trough-peak cycles.

In order to obtain trough-peak-trough cycles, compatible with the type of distress considered, a restriction should be added to the cycle counting methodology proposed by the Standard ASTM E 1049-85. Either trough-peak-trough or peak-trough-peak cycles should be counted in relation to the failure type studied, but not both. Figure 4.8 presents the results of the Range-Pair Counting method considering the fatigue cracking type of distress.

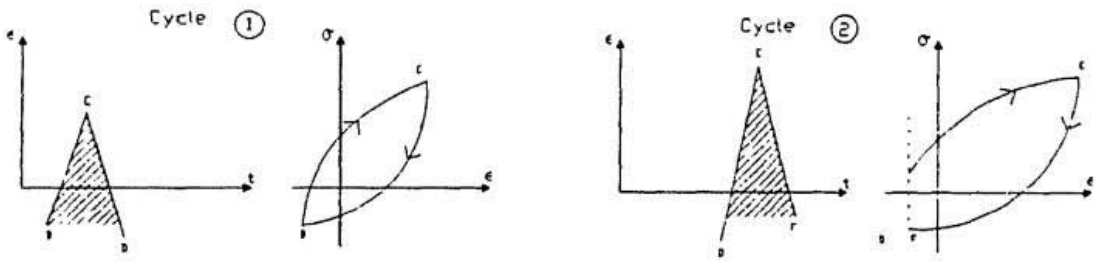

Figure 4.8 : Cycle counting according to restricted Range Pair Counting method.

For strain versus time histories made of an odd number of ranges, another point has to be considered. The leftover (unpaired) range obtained when reaching the end point of the history will change the sign of the cycles to be counted. In that case, the backward counting will yield cycles having an opposite sign than the forward counting, fact which disagrees with a specific type of failure (either compressive or tensile).

In conclusion, the Range-Pair Counting method seems to be the only method suited for cycle counting of the strain histories generated by axle or axle group on flexible pavements. An addition could supplement the ASTM Standard, namely only the cycles whose direction agree with the type of failure should be counted.

Chapter 5

THE EXPERIMENTAL PROGRAM

This chapter offers the description and characteristics of the experimental site, using information provided by Taylor (1989). Also, it includes the description of the experiment undertaken in order to obtain the strain measurements used in the study at-hand.

5.1 The experimental site

The pavement instrumentation used for this study was built in the fall of 1988 on the Saskatchewan Provincial Highway 16, about 16 km North East of Saskatoon. During the summer of 1988, this highway, which was originally a two-lane structure, was widened to four lanes.

Figure 5.1 presents the instrumentation layout. The measuring system was instaled on the outer wheel path of the outside lane. It consists of 7 deflection transducer assemblies and 21 strain transducer assemblies. Transversely, the transducers are organized in three blocks of three rows each. The first row of each block consists of longitudinal strain transducers, the intermediate row consists of deflection transducers while the last row consists of longitudinal and transverse strain transducers. The distance between consecutive rows is 1 meter.

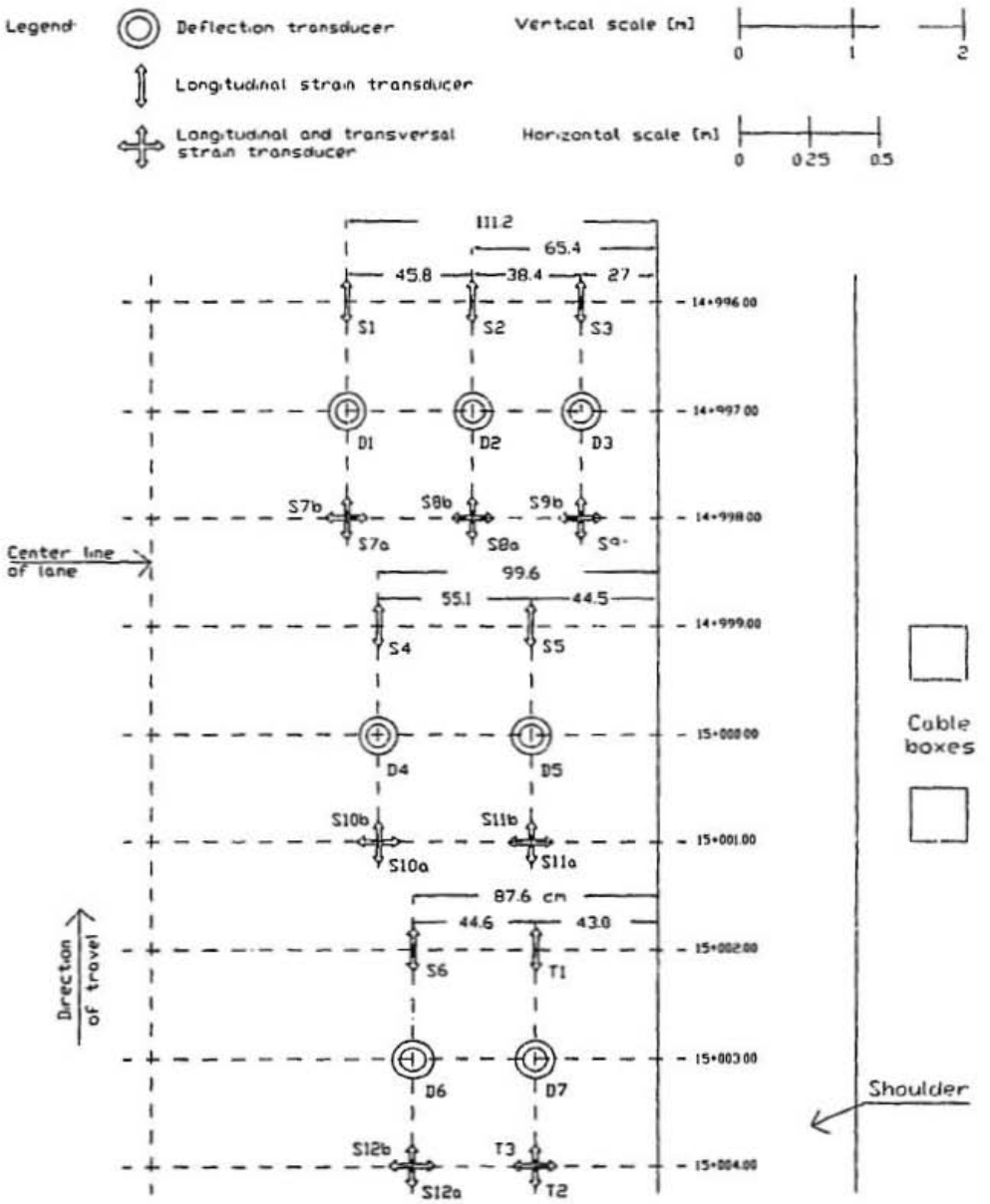

Figure 5.1 : Instrumentation layout

The downstream block consist of three transducers of the same type in each row, while the middle and the upstream block consists of two transducers of the same type in each row. The initial design proposed the transducers to be arranged in seven columns along the wheel path, equally spaced apart by 150 mm. Each row included one deflection and two strain transducers. However, during the construction the distances between the seven columns were modified, arriving at the layout presented in Figure 5.1. The temperature of the asphalt concrete is provided by thermocouples.

The strain assemblies consists of two foil strain gauges (Alberta Research Council type), one of which is active. They are embedded in an asphaltic mastic carrier which is placed at the interface between the base and the surface course before the placement of the asphaltic mix (Figure 5.2).

The deflection transducers (linear variable displacement type), were installed in a steel housing and anchored deep into the subgrade. Because of their sensitivity to humidity and dust, they are removed from the steel housing when not used.

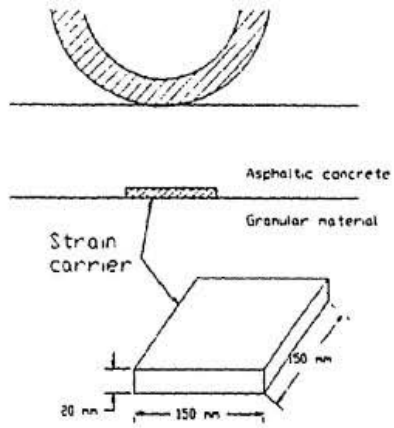

Figure 5.2 : The strain gauge carrier and its location

The thickness of the surface layer ensures that the strain gauge carrier is not damaged during the paving process. Due to the temperature of the paving material, at the time of construction, the asphaltic mastic had softened and was firmly embedded into the surrounding layer.

The thickness of the asphaltic concrete layer, initially planed to be 110 mm, was increased to 175 mm (see Figure 5.3) in order to increase the life of the measuring devices.

5.2 The experiment

The experiment was conducted during the summer of 1990. It monitored two pavement response parameters, namely

longitudinal tensile strain at the bottom of the asphalt concrete layer and deflection.

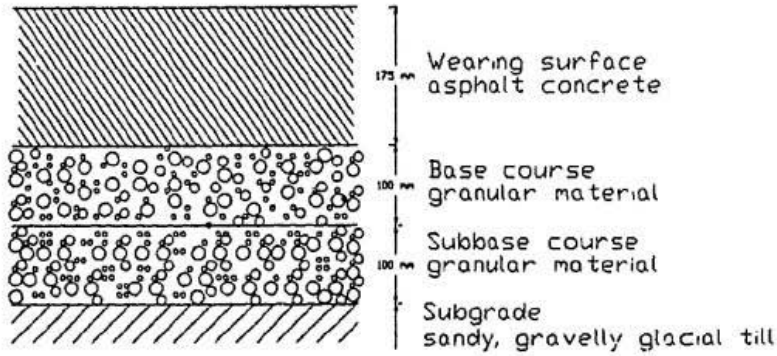

Figure 5.3 : Cross section of flexible pavement structure

However, only the longitudinal tensile strain provided by 12 strain gauges was analyzed in this study. Based on the notation used in Figure 5.1, the strain gauges monitored were S1 to S5 and S7a to S12a. The remaining strain gauges measuring longitudinal tensile strain (T1 and T2) were not monitored. It was stated above that strain gauges are located in 7 alignments along the wheel path, each of them having a specific placement relative to the outside edge of the pavement. This experiment made use of strain gauges placed along 6 such columns.

Besides the Benkelman Beam truck, whose trailing axle is used as reference, another two configurations were tested, namely a 3-axle truck and a 5-axle truck. The Benkelman Beam truck and 3-axle truck belonged to the Saskatchewan D.O.T., while the 5-axle vehicle was rented. Figure 5.4 presents the vehicle data pertinent to experiment, namely distances between axles, distances between tires, tire widths and tire pressures.

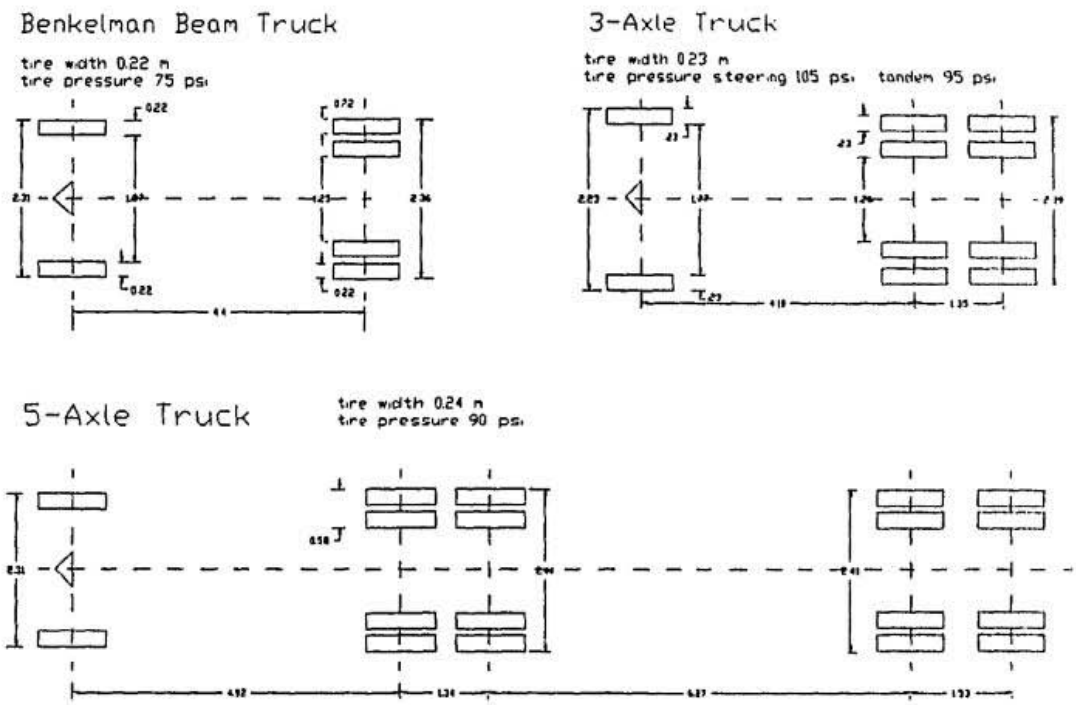

Figure 5.4 : Dimensions of the test vehicles

The two test vehicles were considered at three levels of static load. As presented in Table 5.1, the first level of load, listed as Load Code 1, was the heaviest, while the third level of load (Load Code 3) was the lightest.

Figure 5.5 shows the dimensions of the tires and dual tire groups belonging to the BB truck, the 3-axle truck, and the 5-axle truck.

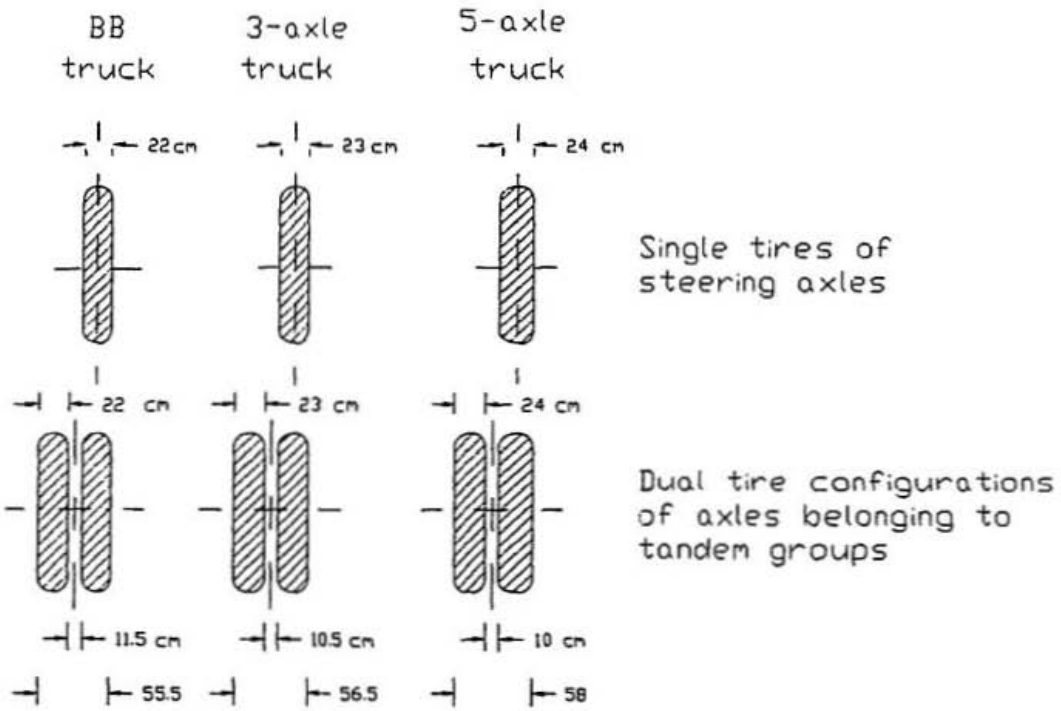

Figure 5.5 : Dimensions of the tires of the experimental trucks

These dimension were used in order to determine the best lateral placement with respect to the strain gauges (Section 6.1)

The experiment started with the heaviest load, subsequently varying the load by unloading part of the cargo.

Table 5.1: Static Loads of Test Vehicles [kg]

Load code	3-Axle truck		5-Axle truck		
	Steering	Tandem*	Steering	Tandem 1	Tandem 2
1	4200	16300	4790	16890	17550
2	4160	13450	4500	10950	9250
3	4020	11240	4320	5020	2940

* Load values are suspect due to improper weighing procedure.

The static load values were obtained using bathroom type scales. The tandem of the 3-axle vehicle was improperly weighted, positioning the scales under only one axle of the group each time, instead of weighing both axles at the same time. This caused the redistribution of the loads, overloading the axle on the scale and reducing the load on the other axle of the tandem. The standardized weight of the trailing axle of the B.B. truck is 8150 kg, while the measured value was

8280 kg.

Besides the three levels of static load of each vehicle, three levels of speed, namely 20, 40 and 50 km/h were included. At each level of static load and speed, a number of 2 replicate runs of the 3-axle and 5-axle vehicles was performed, followed by only one run of the B.B. truck.

Table 5.2 presents the characteristics of all the runs; the type of the truck, the load code, the nominal speed, the pavement temperature, and the distance from the pavement edge to the outside of the outmost tire.

Abbreviations were used for the truck types, namely BB for the Benkelman Beam truck, 3A for the 3-axle truck, and 5A for the 5-axle truck.

It is worth mentioning that each of the runs presented next generated longitudinal strain response from all the 12 strain gauges monitored. The experiment produced a total of 648 strain versus time histories, 216 for each vehicle configuration.

Based on Table 5.2, it was observed that in general the actual speed was different from the proposed nominal speed. For the nominal speed of 20 km/h the average actual speed was 21.94 km/h with a standard deviation of 2.798.

Table 5.2: Run Characteristics

Run nr.	Truck type	Load class	Truck speed [km/h]	Pav. temp. °C	White line - outside of outmost tire distance [cm]				
					Axle 1	Axle 2	Axle 3	Axle 4	Axle 5
1	BB	1	18	27.4	10	5	-	-	-
2	3A	1	22	27.5	30	22	22	-	-
3	3A	1	22	27.4	41	31	31	-	-
4	BB	1	40	27.4	37	30	-	-	-
5	3A	1	40	27.6	21	13	13	-	-
6	3A	1	40	27.6	47	39	39	-	-
7	BB	1	54	27.6	31	25	-	-	-
8	3A	1	53	27.6	33	25	25	-	-
9	3A	1	53	27.6	57	50	50	-	-
10	BB	2	20	29.7	15	12	-	-	-
11	3A	2	26	29.8	25	18	18	-	-
12	3A	2	29	29.8	32	25	25	-	-
13	BB	2	40	29.9	41	37	-	-	-
14	3A	2	40	30.0	31	24	24	-	-
15	3A	2	40	30.0	31	23	23	-	-
16	BB	2	51	30.1	21	18	-	-	-
17	3A	2	53	30.3	30	22	22	-	-
18	3A	2	51	30.3	28	21	21	-	-

Table 5.2: Run Characteristics (continued)

Run nr.	Truck type	Load class	Truck speed [km/h]	Pav. temp. °C	White line - outside of outmost tire distance [cm]				
					Axle 1	Axle 2	Axle 3	Axle 4	Axle 5
19	BB	3	20	30.6	29	25	-	-	-
20	3A	3	26	30.6	38	32	32	-	-
21	3A	3	26	30.6	42	34	34	-	-
22	BB	3	39	30.7	29	25	-	-	-
23	3A	3	40	30.8	45	37	37	-	-
24	3A	3	40	30.9	47	39	39	-	-
25	BB	3	50	30.9	35	31	-	-	-
26	3A	3	51	30.9	27	20	20	-	-
27	3A	3	51	31.0	38	30	30	-	-
28	BB	1	19	26.2	27	24	-	-	-
29	5A	1	21	26.2	24	15	15	12	12
30	5A	1	21	26.3	47	37	37	33	33
31	BB	1	37	26.4	55	52	-	-	-
32	5A	1	38	26.4	65	55	55	51	51
33	5A	1	40	26.5	44	35	35	30	30
34	BB	1	46	26.7	45	41	-	-	-
35	5A	1	50	26.8	45	35	35	32	32
36	5A	1	50	27.0	34	24	24	21	21

Table 5.2: Run characteristics (continued)

Run nr.	Truck type	Load class	Truck speed [km/h]	Pav. temp. °C	White line - outside of outmost tire distance [cm]				
					Axle 1	Axle 2	Axle 3	Axle 4	Axle 5
37	BB	2	21	28.3	29	25	-	-	-
38	5A	2	21	28.6	37	27	27	24	24
39	5A	2	21	28.7	45	37	37	35	35
40	BB	2	40	28.8	55	51	-	-	-
41	5A	2	40	29.0	42	33	33	31	31
42	5A	2	40	29.0	48	39	39	36	36
43	BB	2	48	29.1	55	52	-	-	-
44	5A	2	51	29.0	38	30	30	30	30
45	5A	2	51	29.0	30	22	22	21	21
46	BB	3	20	30.4	46	43	-	-	-
47	5A	3	21	30.4	38	30	30	28	28
48	5A	3	21	30.4	43	34	34	33	33
49	BB	3	40	30.4	43	39	-	-	-
50	5A	3	40	30.5	40	33	33	31	31
51	5A	3	40	30.6	36	28	28	27	27
52	BB	3	46	30.6	27	23	-	-	-
53	5A	3	50	30.6	45	37	37	36	36
54	5A	3	51	30.6	44	36	36	36	36

For the 40 km/h nominal speed, the average actual speed was 39.67 km/h with a standard deviation of 0.81. For the proposed nominal speed of 50 km/h the average actual speed was 50.55 km/h with a standard deviation of 2.11.

The pavement temperature varied from 26.2 °C to 31 °C, the variation range being 4.8 °C.

Figure 5.5 presents the layout of the video logging system.

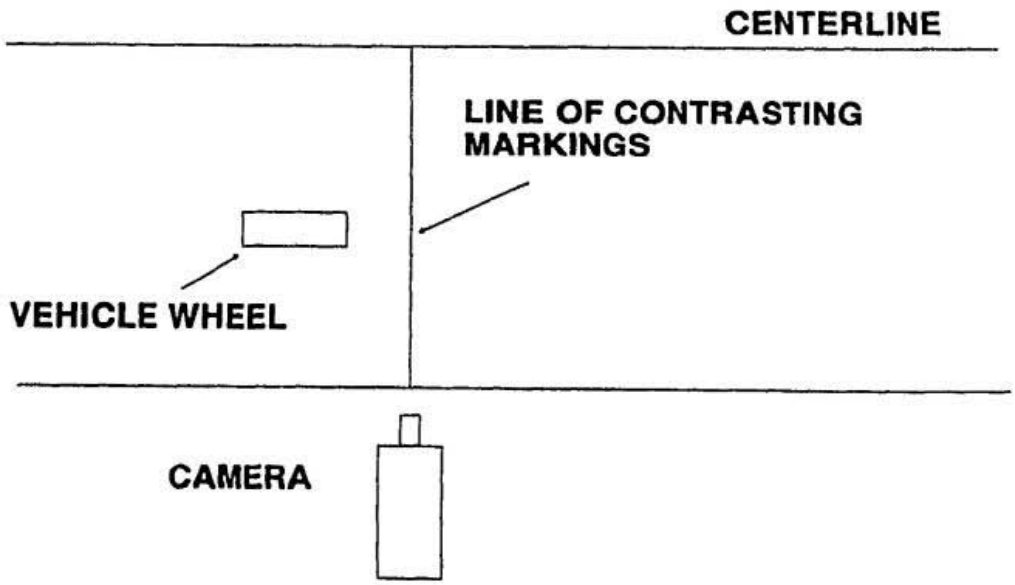

Figure 5.6 : Layout of video logging camera system. After Taylor (1989)

In order to determine the lateral placement of the experimental vehicles during each run, and to calculate their position with respect to the transducers, lines of contrasting color were painted across the lane. The passage of each vehicle was video recorded, and subsequent playback permitted to establish the position of each axle.

Chapter 6

METHODOLOGY

This chapter presents the procedure followed in order to select the runs and the strain gauges whose strain versus time histories were used for LEF's calculations. Also, it delineates the calculations involved and relates each step to the computer software developed as a tool during the study.

6.1 Selection of runs and strain gauge responses to analyze

As stated in section 5.2, the experiment involved two vehicle configurations (a 3-axle and a 5-axle truck) at three levels of speed (20, 40, and 50 km/h) and three levels of load. Two replicate runs were made for each configuration at each level of speed and load. For each run, the 12 strain versus time histories were recorded, corresponding to 12 strain gauges monitored during the experiment. Based on the number of replicate runs (2) and the number of strain gauges monitored (12), it can be concluded that, at a given level of speed and load, each configuration generated 24 strain versus time histories.

At this point, two analysis alternatives were available. First, to calculate the LEF's for all the 24 strain versus time histories corresponding to each vehicle, level of speed

and loading. This alternative involves statistical analysis of the results in order to isolate the effects of many parameters affecting the values of LEF's, such as the lateral placement of the candidate configuration in relation to each strain gauge; lateral placement of the reference axle (the drive axle of the BB truck) and the relative distance between the candidate truck and the BB truck for a specific run.

The second alternative was to select only one of the two replicate runs, and only one of the 12 strain versus time histories related to the run selected. This alternative yields 9 strain versus time histories for each truck configuration, that is one strain versus time history for each level of speed and load considered. The selected load versus time histories reflect the best lateral placement of the candidate truck in relation to a specific strain gauge, and the smallest distance between the candidate truck and the corresponding BB comparison axle.

Given the limited number of runs performed, and the wide range of lateral placement values obtained, it was considered that the second analysis alternative serves better the purpose of this study.

An important requirement in the selection of the best strain versus time histories was the identification of the evaluation criteria involved, namely the lateral placement of a specific

vehicle in relation to a given strain gauge and the distance between the candidate vehicle and the BB truck used for comparison. Both distances introduced above involve measurements from the center of a tire or tire group.

The first step of the selection process delineated above was the elimination of one of the two replicate runs available for each level of speed and loading. The elimination criterion was the distance between the center of the tire or tire group of the candidate truck and the corresponding BB truck. Let us consider a specific position of a certain axle belonging to the candidate truck in relation to a given strain gauge. If the rear axle of the BB truck is closer to the strain gauge than the candidate axle, it will generate higher response, fact that implies lower LEF (Equation 3.14). On the contrary, if the candidate axle is closer to the gauge than the standard BB axle, the induced response will increase due to the better lateral placement of the axle, and the LEF will also increase.

Tables 6.1 and 6.2 show the relative placement data of the 3-axle truck runs, and the 5-axle truck runs respectively. In Table 6.1, D1 represents the absolute value of the distance in centimeters between the center of the right-hand side tire of the steering axle of the 3-axle truck and the center of the right-hand side of the dual tire configuration of the trailing axle of the BB truck.

Table 6.1: Relative lateral placement [cm] (3-axle truck)

Speed	Load cd.	BB Run	Replic	Run	D1	D2
20	1	1	first	2	8.75	17.50
			second	3	19.75	26.50
	2	10	first	11	3.25	6.50
			second	12	3.75	13.50
	3	19	first	20	3.25	7.50
			second	21	0.75	9.50
40	1	4	first	5	25.25	16.50
			second	6	0.75	9.50
	2	13	first	14	22.25	12.50
			second	15	22.25	13.50
	3	22	first	23	3.75	12.50
			second	24	5.75	14.50
50	1	7	first	8	8.25	0.50
			second	9	15.75	25.50
	2	16	first	17	4.25	4.50
			second	18	6.25	3.50
	3	25	first	26	20.25	10.50
			second	27	9.25	0.50

Table 6.2: Relative lateral placement [cm] (5-axle truck)

Speed	Load cd	BB Run	Replic	Run	D1	D2	D3
20	1	28	first	29	15.80	7.80	10.80
			second	30	7.20	14.20	10.20
	2	37	first	38	3.75	3.25	0.25
			second	39	4.25	13.25	11.25
	3	46	first	47	20.75	11.75	13.75
			second	48	15.75	7.75	8.75
40	1	31	first	32	2.75	4.25	0.25
			second	33	23.75	15.75	20.75
	2	40	first	41	24.75	16.75	18.75
			second	42	18.75	10.75	13.75
	3	49	first	50	14.75	4.75	6.75
			second	51	18.75	9.75	10.75
50	1	34	first	35	11.75	4.75	7.75
			second	36	22.75	15.75	18.75
	2	43	first	44	29.75	20.75	20.75
			second	45	37.75	28.75	29.75
	3	52	first	53	6.25	15.25	14.25
			second	54	5.25	14.25	14.25

D2 represents the distance between the center of the right-side dual tire configuration of any axle of the 3-axle tandem group and the same center of the trailing axle of the BB truck.

In Table 6.2, D1, D2, and D3 denote the same distances, corresponding to the steering axle, the first and the second tandem of the 5-axle truck. The above distances are shown for each of the two replicate runs, together with the number of the run.

The selection of one of the two runs was based on the lowest of the D1 and D2 distances, and the lowest of the D1, D2, and D3 distances for 3-axle 5-axle truck runs, respectively. When a specific run had a better lateral placement of the steering axle (D1) than its replicate, but a worst tandem lateral placement (D2 and/or D3), the run was rejected and its replicate was selected. This was because almost always tandems were heavier than steering axles (Table 5.1).

From Table 6.1 can be seen that for the steering axle of the 3-axle truck, the relative lateral placement is between 0.75 cm (run 6) and 22.5 cm (run 14). The tandem distances range from 0.5 cm (run 8) to 17.5 cm (run 1). The 17.5 cm distance is a rather big value, that could affect the quality of the run 1. Table 6.2 reveals the following value ranges for the 5-axle truck runs: from 2.75 cm (run 32) to 29.75 cm (run 44) for the steering axles; from 3.25 cm (run 38) to 20.75

cm (run 44) for the first tandem and from 0.25 cm (runs 32 and 38) to 20.75 cm (run 44). Although run 44 has a better relative lateral placement than its replicate (run 45), its values are high and the impact of this situation on corresponding LEF's has to be considered.

The results of the selection are presented in Table 6.3 for the 3-axle truck runs, and in Table 6.4 for the 5-axle truck runs.

Table 6.3: Selected Runs (3-axle truck)

Speed	Load cd.	BB Run	Run
20	1	1	2
	2	10	11
	3	19	20
40	1	4	6
	2	13	14
	3	22	13
50	1	7	8
	2	16	18
	3	25	27

Because the previous step linked the position of the BB truck to the position of the closest candidate truck, at each level of speed and loading, this step must determine the best BB truck placement in relation to the 12 strain gauges monitored at the experimental site. The selection criterion was the absolute distance between the center of each strain gauge and the center of the right-side dual tire configuration of the rear axle of the BB truck.

Table 6.4: Selected Runs (5-axle truck)

Speed	Load code	BB Run	Run
20	1	28	29
	2	37	38
	3	46	48
40	1	31	32
	2	40	42
	3	49	50
50	1	34	35
	2	43	44
	3	52	54

The second step of the selection process involves the identification of the strain versus time history to be used; one out of 12 available for the already selected run. However, before starting the selection process, there were two problems to be solved. First, it was necessary to check the quality of the sensors involved, based on the available strain responses. Second, it was necessary to define an acceptable strain gauge-tire group distance range, and to approximate the lateral placement producing the highest responses. The qualitative evaluation of the strain gauges was based on the strain response under the trailing axle of the BB truck.

All the strain responses generated by the same strain gauge as a result of the BB truck runs characterized by the same speed, are compatible and can be compared. According to this observation, the experiment comprised 6 runs of the BB truck at each level of speed (20, 40 or 50 km/h). In conclusion, each strain gauge monitored yielded 6 strain versus time histories for BB runs having the same nominal speed. By plotting these six responses for each strain gauge, at each level of speed, the relationship between the gauge response and the lateral placement can be evaluated.

6.2 Selection of the values characterizing the strain cycles

It was decided to process the cycles belonging to the strain versus time histories generated by the experimental vehicles using four methods. First, the peak value of the strain cycle were calculated cf. the Standard ASTM E 1049-1985 (see Section 4.3). Second,the peak values were processed as recommended by the RTAC (Vehicle Weight and Dimensions Study, 1986), based on the tensile part of the strain cycle only. Third, the strain cycle was integrated, and fourth, only the tensile part of the strain cycle was integrated.

The study focused initially on the cycles produced by the trailing axle of the BB truck. Appendix A presents the results of this analysis, the six graphics describing the behavior of each strain gauge being grouped together. For a specific speed, there are two plots, the left one showing the peak values calculated by the methods proposed by ASTM (filled square) and RTAC (cross). The right plot deals with integral values, using the same notations. Above each filled square-cross pair, it is presented the number of the run which generated the original time versus time history.

A general observation concerning the plots was that all the parameters plotted, peaks or integrals, followed the same trend, namely decreased with increasing axle distance from the strain gauge. As expected, considering both tensile and

compressive parts of the cycles yielded higher values than considering only the tensile part. Also, for higher speeds, the values of the strain response was lower.

Based on visual observation of the graphics presented in Appendix A, four of the strain gauges, namely S5, S6, S9a and S10a, were found to behave inconsistently, yielding increased strain values for increased lateral placement, or yielding a wide strain range for the same lateral placement of the BB truck. The strain versus time histories produced by the four strain gauges named above were excluded from subsequent evaluation. The strain response of the remaining 8 strain gauges offered further insight on the behavior of the strain versus lateral placement. It was observed that the maximum strain was obtained when the center of the dual tire group was 20 cm to the left of the center of the strain gauge. Based on the width of each BB tire, and the transverse distance between the two tires (Figure 5.5), maximum strain was obtained when the outside tire of the group is exactly above the strain gauge. In order to verify this observation, all the peak strain values calculated according to the methodology proposed by ASTM were pooled, without differentiating between strain gauges, for each experimental speed. Pooling peak values generated by different strain gauges can be irrelevant because

there are many factors related to the material and experimental site characteristics which may affect the response value of a specific strain gauge.

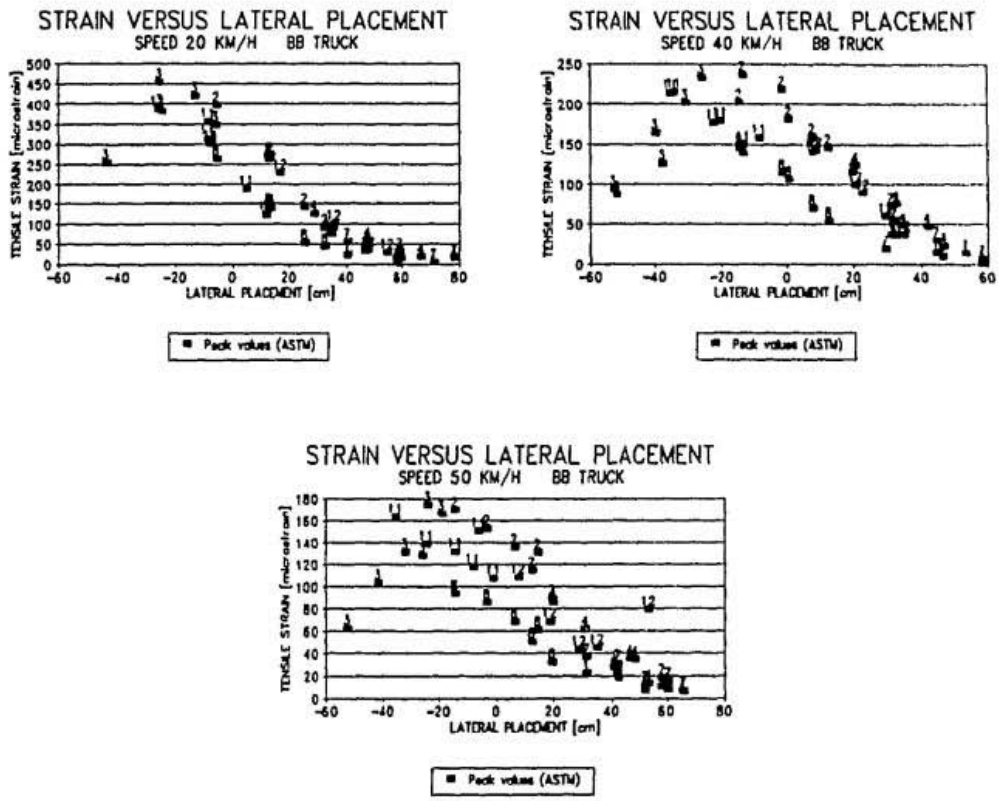

Figure 6.1 Pooled strain peaks versus lateral placement at three levels of speed.

However, despite some range variations, the trend in the strain values versus lateral placement was easy to identify, and

verified the observation that the maximum strain was obtained when the center of the dual tire group was 20 cm to the left of the center of the strain gauge.

Figure 6.1 presents the strain versus lateral placement plots for the gauges S1-S4, S7a, S8a, S11a and S12a, at three levels of speed. The numeric labels inside the plots indicate the number of the gauge which produced the plotted peak. Both the plots presented in Appendix A, and the plots in Figure 6.1 used the following convention related to the lateral placement of an axle: the distance is positive when the center of the axle group is at the right of the center of the strain gauge, and is negative when it is at the left. Considering this convention, and the information provided by Figure 6.1, it was decided to eliminate all the strain versus time histories where the lateral placement was outside the range -40 to 0 cm. From all histories characterized by lateral placements inside this range, the closest to the -20 position was selected.

Table 6.5 presents the results of the above selection for the 3-axle truck runs, while Table 6.6 presents the 5-axle truck runs selected.

The four parameters presented at the beginning of the Section 6.2 were also calculated for the strain versus time histories produced by the selected runs of the 3-axle and the 5-axle truck.

Table 6.5: Runs and Gauges Selected for LEF's Calculation (3-axle truck)

Speed	Load cd.	BB Run	Run	Gauge
20	1	1	2	3
	2	10	11	3
	3	19	20	3
40	1	4	6	3
	2	13	14	2
	3	22	13	3
50	1	7	8	3
	2	16	18	3
	3	25	27	3

Table 6.6 Runs and Gauges Selected for LEF's Calculation (5-axle truck)

Speed	Load cd.	BB Run	Run	Gauge
20	1	28	29	3
	2	37	38	2
	3	46	48	2
40	1	31	32	2
	2	40	42	2
	3	49	50	2
50	1	34	35	2
	2	43	44	2
	3	52	54	3

The peak value of the strain cycle as defined by the Standard ASTM E 1049-1985; the peak values as recommended by the RTAC method; the integral of each strain cycle, and the integral

of the tensile part of the strain cycle were obtained by using a computer program developed during the study. Details about its structure and operation, together with the steps involved in the processing of one of the runs, were provided in Appendix B.

Chapter 7

RESULTS AND DISCUSSION

This chapter presents and discusses the results of the study. Section 7.1 introduces the LEF's calculated by the ASTM Range-Pair Counting Method. First, the LEF's obtained from each axle/axle group are shown for the speed and load combinations tested. The influence of the lateral placement is analyzed and the effects of increasing load and speed on LEF's are described. Second, the concept of the "vehicle" LEF's is introduced and compared to the sum of the LEF's of individual axles/axle groups.

Section 7.2 deals with the comparison of LEF's obtained by two mechanistic methods, namely the proposed ASTM Range-Pair Counting Method and the RTAC Method.

Section 7.3 deals with the comparison of the mechanistic LEF's obtained by the ASTM Range-Pair Counting Method and the empirical LEF's based on the results of the AASHO Road Test.

Section 7.4 discusses the suitability of an integral method for mechanistic LEF's determination. This method retains the cycle definition proposed by the ASTM Range-Pair Counting Method. However, instead of identifying the peak value of the cycle, its integral value is calculated. LEF's values which served as a basis for all the descriptive or comparative plots can be found in Appendix C.

7.1 LEF's obtained by the ASTM Range-Pair Counting Method

As presented in Chapter 4 and 6, discrete methods for LEF's calculation use the peak values of the strain versus time cycles. The following section describes and analyzes mechanistic LEF's obtained by the ASTM Range-Pair Counting Method for individual axles and entire configurations, respectively.

Table 7.1 presents the LEF's for the 3-axle truck, while Table 7.2 presents the LEF's for the 5-axle truck. The LEF's presented in both tables are discussed in Section 7.1.1 (individual axles/axle groups) and Section 7.1.2 (vehicle), respectively.

7.1.1 LEF's for individual axles and axle groups

For flexible pavements, the ASTM Range-Pair Counting Method, uses trough-peak-trough strain cycles (Section 4.3.4), taking into account both the tensile and the compressive part of each cycle. LEF's are calculated using Equation 3.14, based on the peaks generated by the axles of the candidate vehicle and the peak generated by the standard axle of the BB truck.

As a result of the experiment conducted, it was possible to calculate LEF's for each axle/axle group of both truck configurations, at three levels of speed and three levels of loading.

Table 7.1: Discrete LEF's for 3-axle Truck

RUN	LOAD CODE	SPEED km/h	STEERING	TANDEM	VEHICLE
2		20	0.5	3.54	4.04
6	1	40	0.05	3.46	3.52
8		50	0.23	2.38	2.62
11		20	0.37	1.04	1.41
14	2	40	0.004	0.71	0.71
18		50	0.83	1.54	2.38
20		20	0.06	0.75	0.81
23	3	40	0.023	0.06	0.08
27		50	0.37	1.11	1.49

Table 7.2: Discrete LEF's for 5-axle Truck

RUN	LOAD CODE	SPEED km/h	STEERING	TANDEM 1	TANDEM 2	VEHICLE
29		20	0.69	3.00	2.87	6.57
32	1	40	0.22	1.23	1.93	3.40
35		50	0.49	2.24	3.13	5.86
38		20	0.19	1.28	1.06	2.54
42	2	40	0.13	0.95	0.50	1.58
44		50	0.03	0.66	0.34	1.03
48		20	0.05	0.09	0.011	0.15
50	3	40	0.03	0.05	0.004	0.09
54		50	0.045	0.002	0.0005	0.048

The ensuing analysis presents the effect of speed and level of loading on mechanistic LEF's based on the Range-Pair Counting method. Expected trends are described and inconsistencies explained.

Early research done on LEF's (Christison et al., 1978), suggested that "the potential damaging effect of a given load on pavements, as expressed in terms of interfacial strains or surface deflections, is highly dependent on vehicle velocity". Accordingly, it was anticipated to obtain decreasing LEF's for increasing speed. Besides, lower levels of loading will produce lower LEF's. In both cases, the decrease in LEF values is a result of lower levels of tensile strain produced at the bottom of the asphalt concrete layer.

The effects of speed and load on LEF's are easy to distinguish from Tables 7.1 and 7.2. Additionally, bar graphs (Figures 7.1 to 7.40) were used in order to facilitate the analysis of the results. LEF's were grouped by speed, and at each level of speed by level of loading. The height of a given bar is the LEF value corresponding to the speed and load combination represented.

When comparing two different graphs, it is important to remember that usually they have different vertical scales, because each graph was scaled according to the highest strain level it contained.

Figure 7.1 presents the LEF's for the steering axle of the 3-axle truck. Given the small variation between the three levels of load (4200 kg, 4160 kg, and 4020 kg), almost equal LEF's were expected for all three levels of loading at a given speed. However, the LEF's varied across the levels of loading.

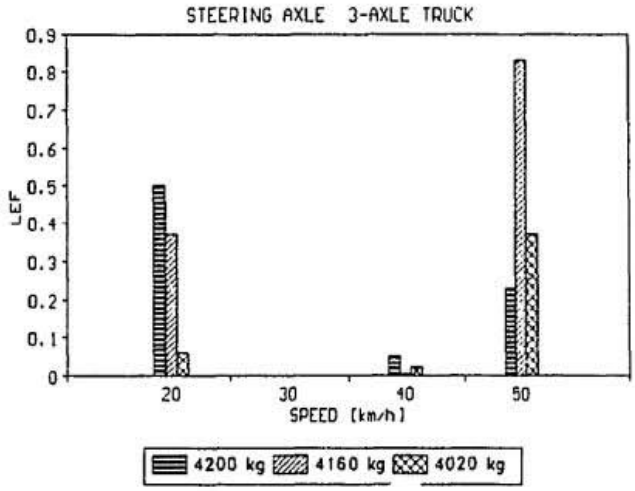

Figure 7.1 : LEF's for 3-Axle Truck, Steering Axle, Calculated by the ASTM Range-Pair Counting Method

For example at 20 km/h, the variation was between 0.06 and 0.5. Inconsistences were found also across the levels of speed. For example, LEF's obtained at 40 km/h are significantly lower than those obtained at 50 km/h. Also, the LEF's obtained at 50 km/h for the lightest load classes exceed those obtained at 20 km/h. It is believed that the inconsistent trend in LEF's values was a result of the relative lateral placement of steering axles versus the BB truck standard axle. Because

the small values of strain peaks produced by those light axles, slight differences in lateral placement could significantly influence the strain ratio of the candidate axle over the BB axle.

For example, let us consider two cases; namely a candidate axle peaking at 300 microstrain and a BB axle peaking at 250 microstrain compared to a candidate axle peaking at 60 microstrain and a BB axle peaking at 50 microstrain. The candidate axle peak over BB peak ratio is 1.2 in both cases, producing an LEF of 2, given an exponent of 3.8. Let us suppose a relative lateral placement of the candidate axle which will produce a peak decrease of 10 microstrain units in both cases. The candidate axle peak over the BB axle ratio becomes 1.16 for the first case, and 1 for the second case. The corresponding LEF's will be 1.75 and 1, respectively. In conclusion, reducing by 10 microstrain units the candidate axle peak, generated a LEF drop of 14% for the first case and a drop of 50% for the second case. Hence, LEF's of light axles are more sensitive to lateral placement than LEF's of heavy axles.

Besides, considering the short duration of strain cycles produced by an axle, vehicle dynamics can be considered as another factor affecting the strain magnitude.

Figure 7.2 presents the LEF's for the tandem axle of the 3-axle truck. The expected trends, namely lower LEF's for increasing speed and decreasing axle load are in general followed.

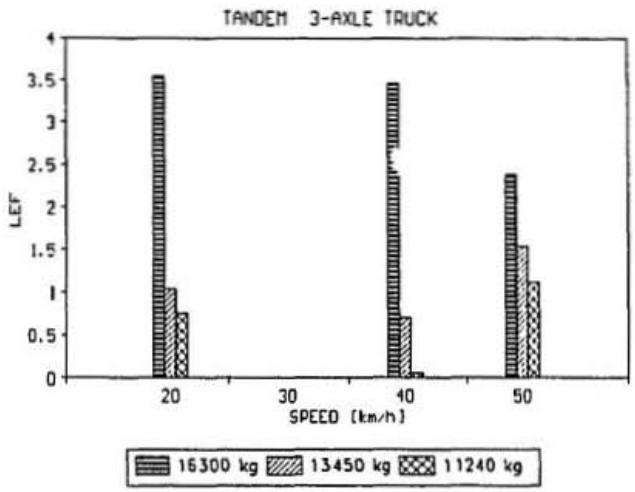

Figure 7.2 : LEF's for 3-Axle Truck, Tandem, Calculated by the ASTM Range-Pair Counting Method

For the same speed, the LEF's are consistently decreasing with decreased load, but across speeds, a certain amount of inconsistency is present at 50 km/h for the lowest levels of loading. As expected, the LEF's obta ed at 40 km/h are lower than those obtained at 20 km/h. However, for load classes 2 and 3, the highest speed (50 km/h) yielded the highest LEF's. In order to determine the cause of this discrepancy, the strain versus time histories for all the runs were examined for the various levels of speed and load tested, considering both the

3-axle and the BB truck. This overall assessment indicated that for the BB truck the level of strain decreased consistently with increased speed and decreased load. However, for the 3-axle truck, it was found that at 50 km/h, load classes 2 and 3, the strain response was very high, exceeding that of the previous level of speed (40 km/h) and loading (1st loading class). Other parameters, namely the lateral placement, the actual speed and the temperature of the pavement were investigated for all the runs, without finding any particular reason for the high levels of strain generated by 3-axle truck runs at 50 km/h. In conclusion, vehicle dynamics remains the only possible explanation of the inconsistencies observed.

For the 5-axle truck, Figure 7.3 shows the LEF's of the steering axle, for three levels of load and speed. Similar to the case of the 3-axle truck, the steering axle varied in weight by less than 10% between load classes (4790 kg, 4500 kg, and 4320 kg, respectively). Still, it was observed that LEF's obtained for the heaviest loading (class 1) were significantly higher that those obtained for the light loading (class 2 and 3).

In general, LEF's followed the expected trends, with the only significant inconsistency observed across speeds, for the heaviest load class. The LEF is lower at 40 km/h than the LEF obtained at 50 km/h.

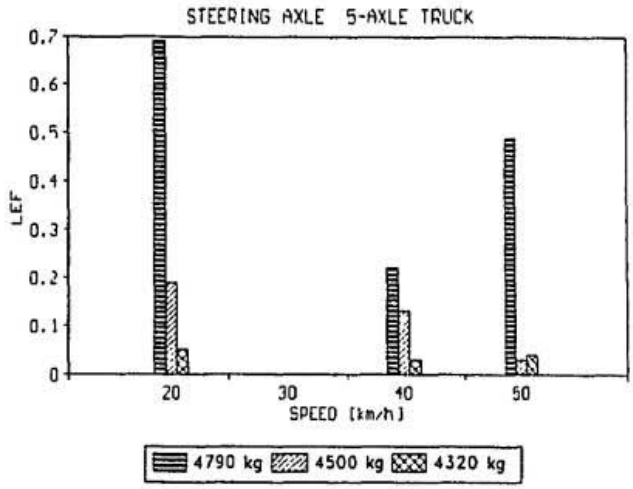

Figure 7.3 : LEF's for 5-Axle Truck, Steering Axle, Calculated by the ASTM Range-Pair Counting Method

This was found to be due to the lateral placement of the 5-axle truck at 40 km/h, load class 1, with respect to the strain gauge selected. The center of the tire group was at around 40 cm to the left of the strain gauge, which was the highest value of lateral placement among all selected runs of the 5-axle truck.

The high value of the lateral placement was also reflected in the LEF's of both the first tandem (Figure 7.4), and the second tandem (Figure 7.5). Excepting this problem, the tandems of the 5-axle truck showed a more consistent trend of LEF's, with speed and level of load. The significant weight variation across loading classes is evidently reflected on the LEF's values. It exceeds in importance the variation of LEF's across

speeds.

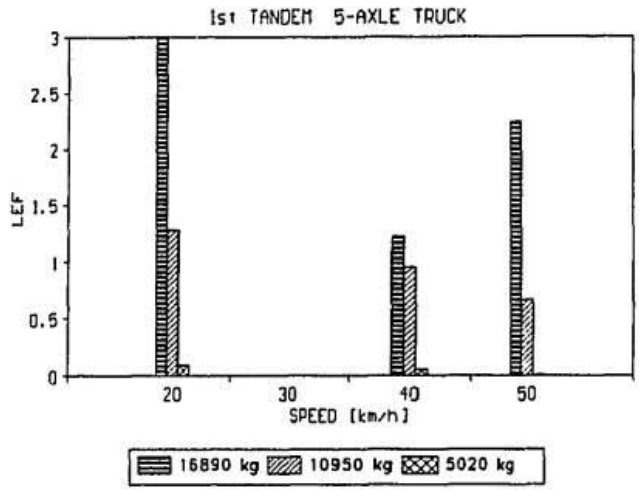

Figure 7.4 : LEF's for 5-Axle Truck, 1st Tandem, Calculated by the ASTM Range-Pair Counting Method

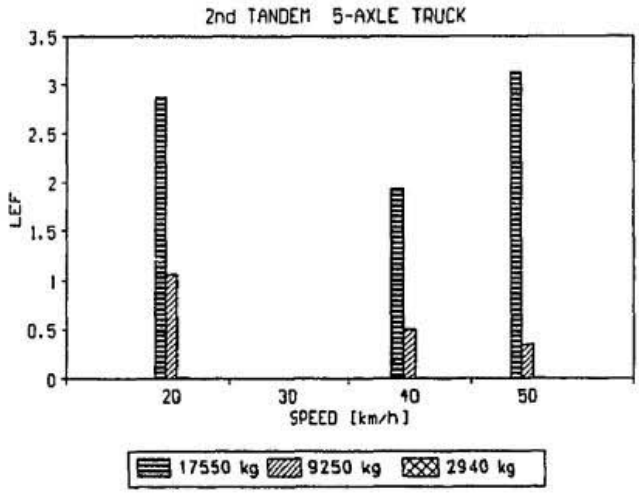

Figure 7.5 : LEF's for 5-Axle Truck, 2nd Tandem, Calculated by the ASTM Range-Pair Counting Method

The reason, as explained and exemplified at the beginning of the section, is that heavier axle and axle groups are less sensitive to small variation of lateral placement (candidate axle to the strain gauge) and/or relative lateral placement (candidate axle to BB axle), than lighter axles.

7.1.2 Vehicle LEF's

Another issue was raised when processing a strain versus time history by using the ASTM Range-Pair Counting method, namely the treatment of the trough-peak-trough cycles existing between the axle groups. These cycles, referred to as inter-axle cycles, are produced by two successive axles which do not belong to the same axle group.

Two analysis approaches are possible, namely to consider the inter-axle cycles, or to neglect them. In the first case, the LEF value of each inter-axle cycle should be calculated. The "vehicle" LEF will include both the LEF's generated by truck axles and the LEF's obtained from the inter-axle cycles. In the second case, the effect of the inter-axle cycles should be neglected, the "axle sum" LEF for an experimental truck being the sum of the LEF's produced by each of its axles.

Figure 7.6 presents the cycle identification for both the 3-axle truck and the 5-axle truck. The left side plots identify all the strain cycles of the history, including the inter-axle cycles.

As stated earlier, the sum of the LEF's produced by all cycles is the "vehicle" LEF. The right side plots identified as cycles only the strain cycles produced by truck axles. The sum of these LEF's is the "axle sum" LEF.

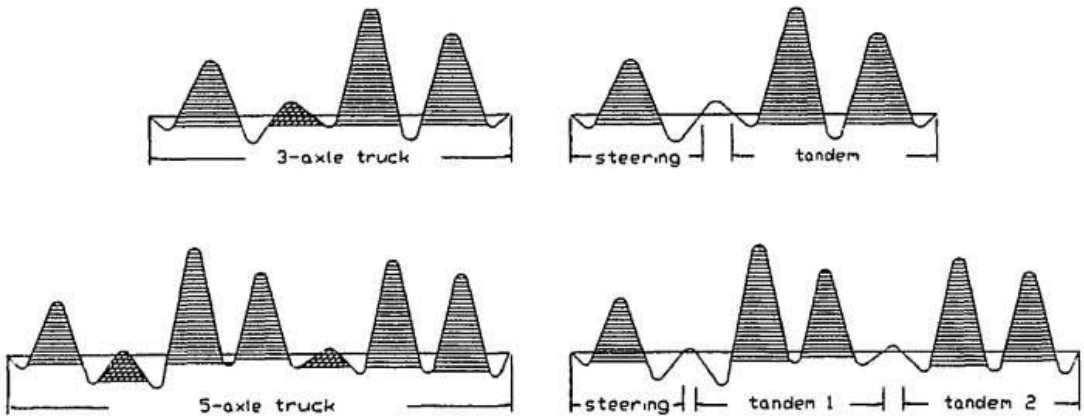

Figure 7.6 : Two Approaches for Strain Cycles Identification

It was found that although the consideration of strain cycles between the axle groups is theoretically sound, the calculations indicated that they do not significantly increase the "axle sum" LEF. For example, the maximum LEF yielded by the inter-axle cycles was 0.00002 for the runs of the 3-axle truck, and 0.00041 for the runs of the 5-axle truck. These quantitatively insignificant LEF's are a result of calculating the ratio of small peaks yielded by an inter-axle cycle over the peak produced by the corresponding BB axle, and raising this ratio at 3.8.

The entire vehicle LEF's for the experimental trucks are presented below. Because the vehicle LEF's are obtained by

summing the LEF's of individual axles, they will also reflect the inconsistencies observed for each individual axle.

The LEF's for the 3-axle truck, calculated by adding the LEF's of the steering axle and tandem axle, are presented in Figure 7.7.

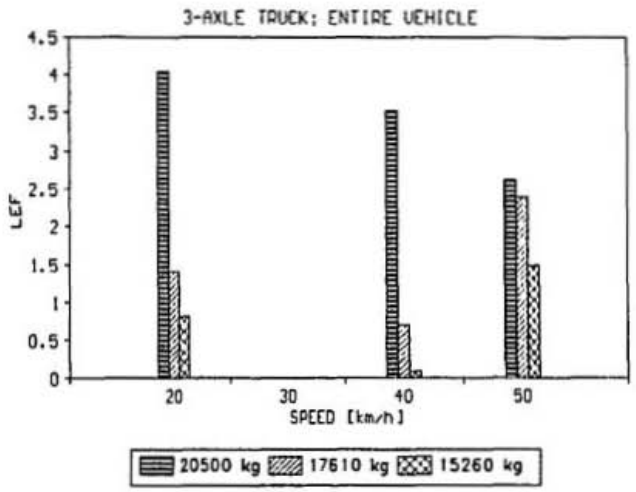

Figure 7.7 : LEF's for 3-Axle Truck, Entire Vehicle, Calculated by the ASTM Range-Pair Counting Method

At each level of speed, lower LEF's are obtained for decreasing loading. Across speeds, and for the heaviest load class, they also follow the expected trend, decreasing with increasing speed. The inconsistencies observed at lower load classes for the highest speed (50 km/h), reflect those of the steering axle and the tandem, explained in Section 7.1.1.

For the 5-axle truck, Figure 7.8 presents the vehicle LEF's.

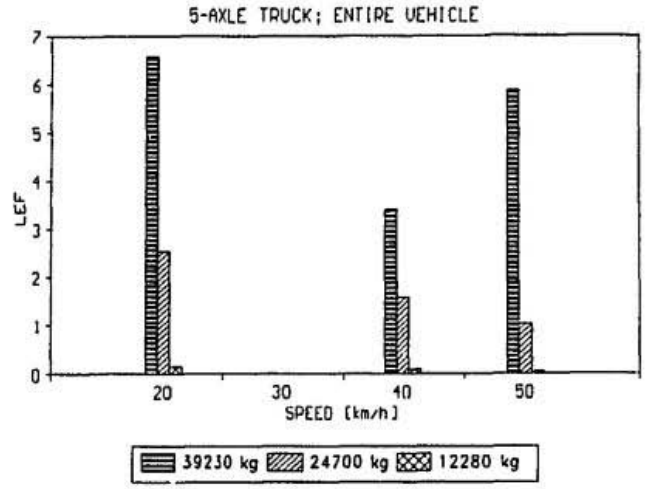

Figure 7.8 : LEF's for 5-Axle Truck, Entire Vehicle, Calculated by the ASTM Range-Pair Counting Method

As explained in Section 7.1.1, the only inconsistency observed at 40 km/h for the highest loading class, is due to the large lateral placement of the candidate vehicle with respect to the strain gauge selected.

In conclusion, it was found that the ASTM Range-Pair Counting Method yielded consistent results for low speeds and high axle loads. For high speeds and lower loads, inconsistent LEF's were sometimes obtained across speed and loading classes. This fact can be explained by the significant influence on strain of the lateral placement of the BB axle versus the candidate axle. These discrepancies, however, are relatively insignificant, considering the small values of the LEF's calculated under these conditions. Another aspect to be

considered is the quality of the candidate axle lateral placement with respect to the strain gauge. For the 5-axle truck at 40 km/h, load class 1, the LEF was significantly altered by the large lateral placement with respect to the strain gauge.

7.2 Comparison of the ASTM LEF's to the RTAC LEF's

The following section presents the comparisons between the LEF's obtained by the ASTM Range-Pair Counting Method and the LEF's obtained by the RTAC Method. The only difference between these two mechanistic methods (considering the interfacial strain as pavement response parameter), is the treatment of the compressive part of trough-peak-trough strain cycles. The comparison is intended to present the effect of the compressive part of trough-peak-trough strain cycles on LEF's values.

Only LEF's produced by individual axles/axle groups were compared. The quantitative inconsistencies of LEF's across the levels of speed and/or load were not discussed again, considering that Section 7.1 already fulfilled that requirement. Instead, this section focuses on identifying general trends characterizing each method. Also, it was intended to compare topics such as sensitivity to speed and load variation. It is worth mentioning that the same type of inconsistencies were observed in both the ASTM and the RTAC method, because both methods are applied to the same strain

versus time histories. Besides, both methods use the tensile part of the Trough-Peak-Trough cycles, the only difference between them being the treatment of the compressive part of the cycles. Each bar graph represents the LEF's generated by a specific axle/axle group at a particular speed. Accordingly, three graphs are needed to present the comparison for the same axle/axle group across speeds. The levels of loading are plotted along the X axis. At each level of load, correspond two LEF's obtained using the ASTM and the RTAC method, respectively.

Figures 7.9 to 7.11 present the LEF's for the steering axle of the 3-axle truck at three levels of speed (20, 40 and 50 km/h).

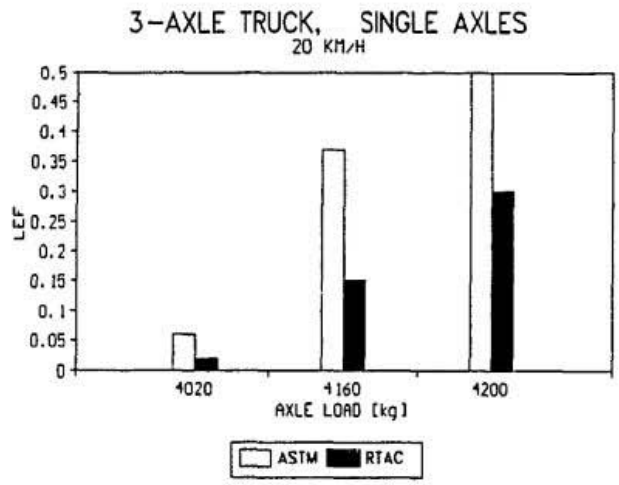

Figure 7.9 : Comparison of ASTM LEF's to RTAC LEF's for 3-Axle Truck, Steering Axle, Speed 20 km/h

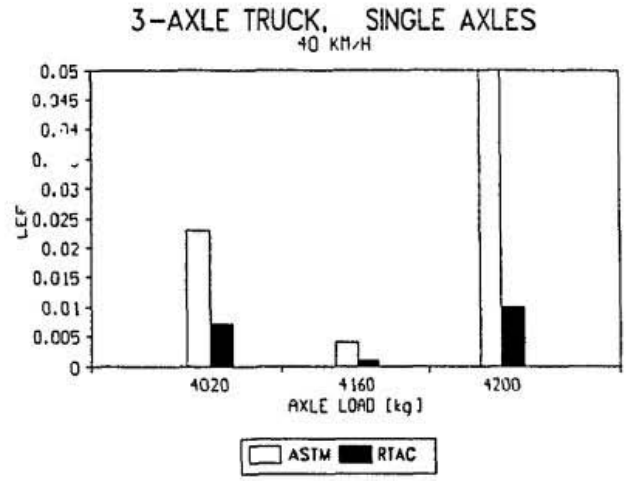

Figure 7.10 : Comparison of ASTM LEF's to RTAC LEF's for 3-Axle Truck, Steering Axle, Speed 40 km/h

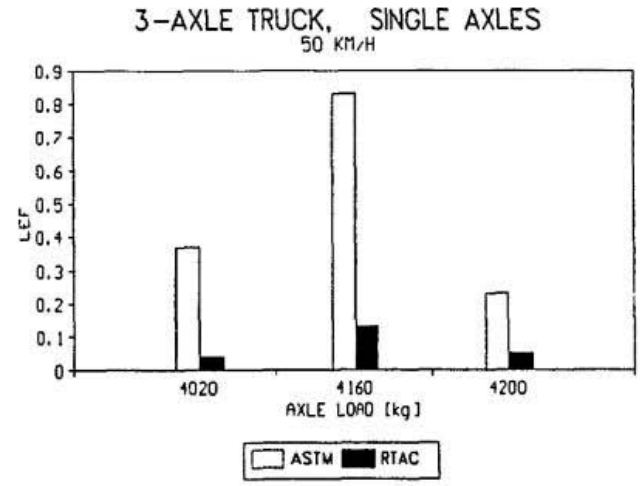

Figure 7.11 : Comparison of ASTM LEF's to RTAC LEF's for 3-Axle Truck, Steering Axle, Speed 50 km/h

As explained in Section 7.1, there are doubts about the quality of the mechanistic LEF's for the steering axle of the 3-axle truck. Nevertheless, it was observed that always the LEF's calculated by the ASTM method were higher than the LEF's calculated by the RTAC method.

Figures 7.12 to 7.14 present the LEF's for the tandem axle of the 3-axle truck at three levels of speed (20, 40 and 50 km/h). The information obtained by studying these plots can be summarized as follows:

- the ASTM method yields the highest LEF's, followed by the RTAC method.

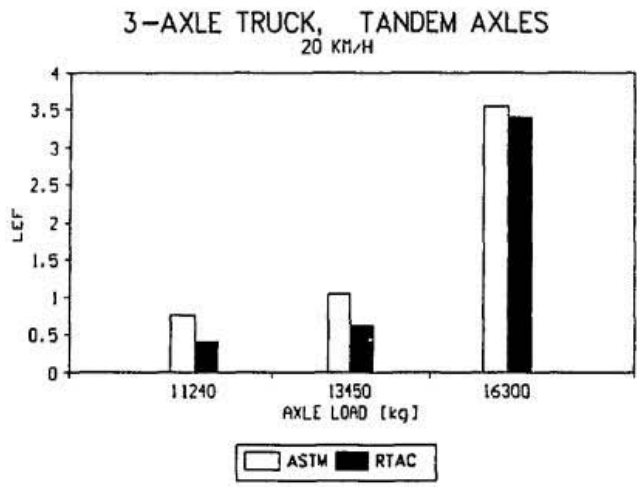

Figure 7.12 : Comparison of ASTM LEF's to RTAC LEF's for 3-Axle Truck, Tandem, Speed 20 km/h

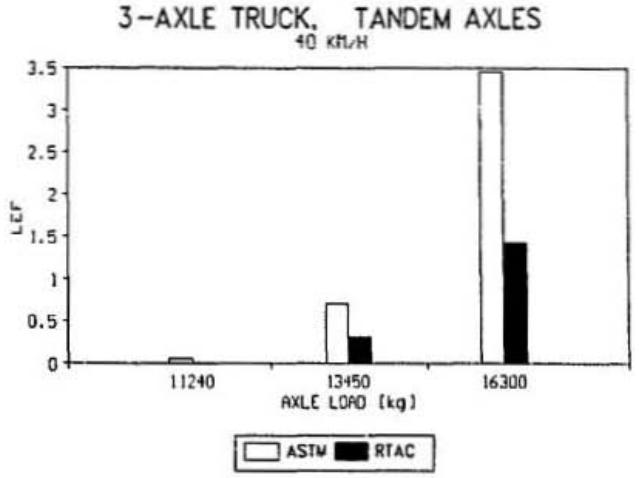

Figure 7.13 : Comparison of ASTM LEF's to RTAC LEF's for 3-Axle Truck, Tandem, Speed 40 km/h

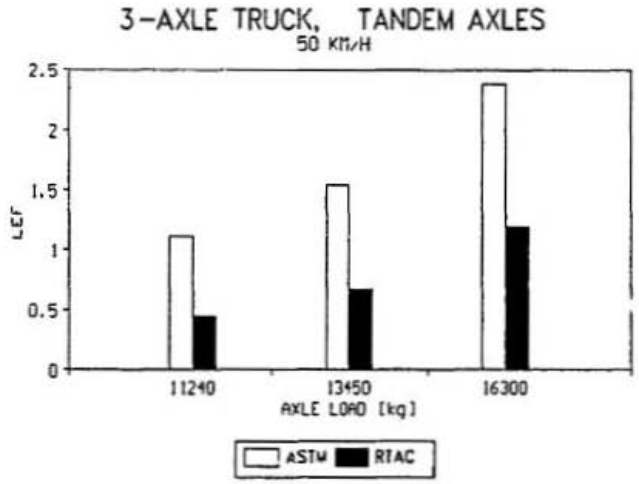

Figure 7.14 : Comparison of ASTM LEF's to RTAC LEF's for 3-Axle Truck, Tandem, Speed 50 km/h

- at 20 km/h, the RTAC LEF's were approximately equal to the ASTM LEF's. However, with increasing speed the differences between them increased. This fact can be interpreted as a higher sensitivity to speed for the ASTM LEF's.
- for the tandem axle of the 3-axle truck, it was observed that the sensitivity to load increase is similar for both mechanistic methods.

The LEF's for the steering axle of the 5-axle truck are presented in Figures 7.15 to 7.17. In agreement with previous observations, the ASTM method produced higher LEF's than the RTAC method. Also, the ASTM method proved to be more sensitive to load than the RTAC method.

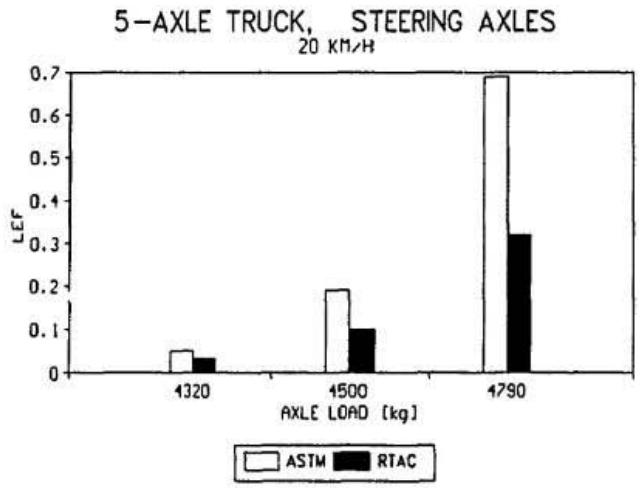

Figure 7.15 : Comparison of ASTM LEF's to RTAC LEF's for 5-Axle Truck, Steering Axle, Speed 20 km/h

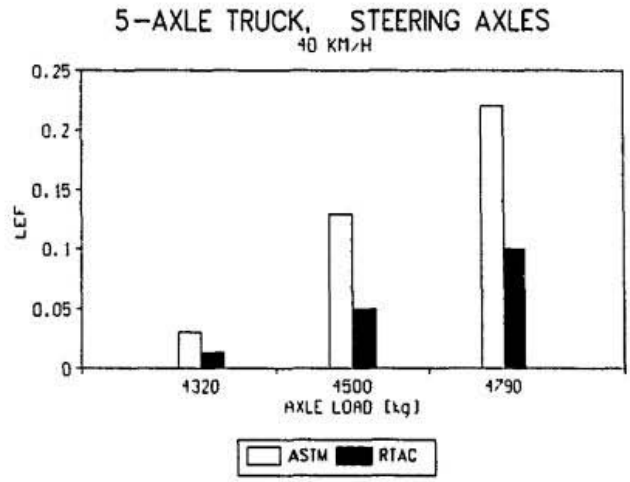

Figure 7.16 : Comparison of ASTM LEF's to RTAC LEF's for 5-Axle Truck, Steering Axle, Speed 40 km/h

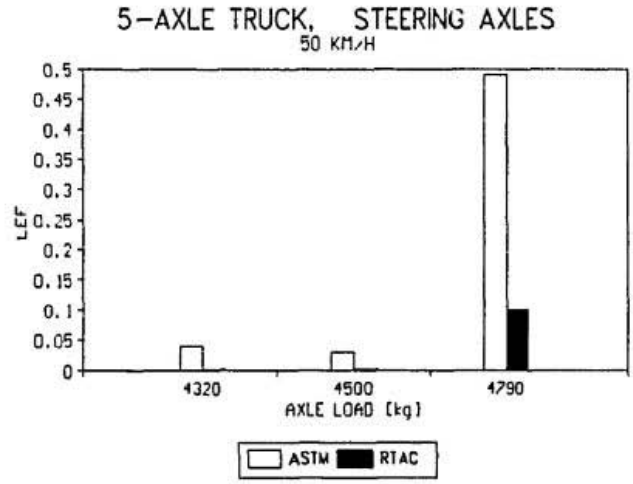

Figure 7.17 : Comparison of ASTM LEF's to RTAC LEF's for 5-Axle Truck, Steering Axle, Speed 50 km/h

The importance of the sensitivity to load is apparent given the non-linear relationship between strain and LEF. Accordingly, a method which exhibited less sensitivity of LEF's to load may underestimate the damage impact of the heaviest axles.

Figures 7.18 to 7.20 show the LEF's for the tandem of the 5-axle truck. The LEF's produced by the tandems of the 5-axle truck were grouped according to speed. At each level of speed both the first and the second tandem were plotted together, according to the total load of the tandem. The information provided by the graphs can be summarized as follows:

- it was observed that the ASTM method yielded the highest LEF values.

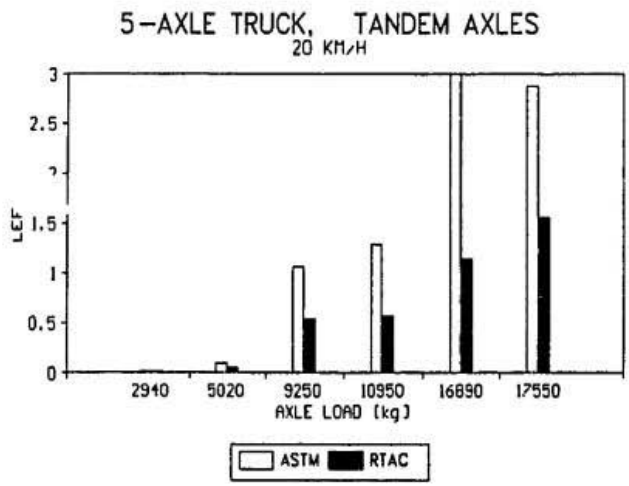

Figure 7.18 : Comparison of ASTM LEF's to RTAC LEF's for 5-Axle Truck, Tandems , Speed 20 km/h

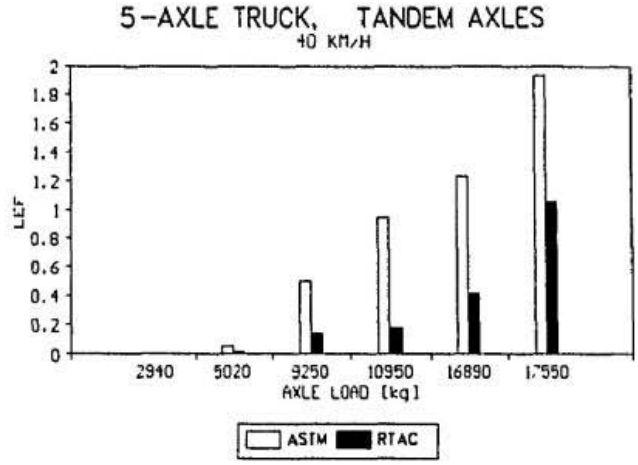

Figure 7.19 : Comparison of ASTM LEF's to RTAC LEF's for 5-Axle Truck, Tandems, Speed 40 km/h

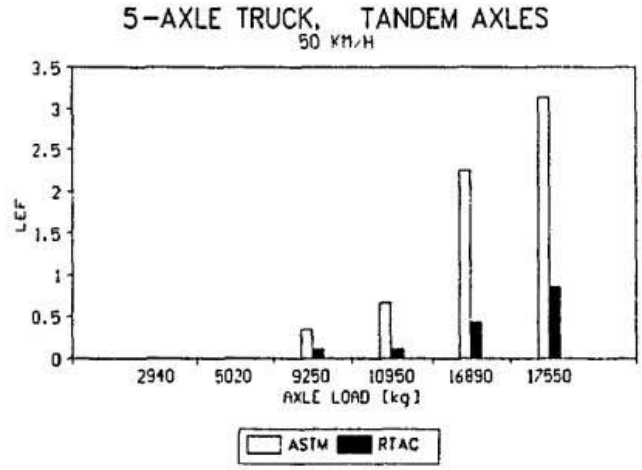

Figure 7.20 : Comparison of ASTM LEF's to RTAC LEF's for 5-Axle Truck, Tandems, Speed 50 km/h

- the ASTM method was the most sensitive to increased tandem load.

- across speeds, the ASTM method presented lower variability than the RTAC method, which yields considerable decreased LEF's at lower speeds.
- at 40 km/h, both 16,890 and 17,550 kg tandem loads yielded low LEF's, again a reflection of the lateral placement of the Run 31.

In conclusion, the comparison between the ASTM Range-Pair Counting Method and the RTAC Method has shown that calculated LEF's are proportional to the load, and decrease with increasing vehicle speed. Also, LEF's obtained by the ASTM Range-Pair Counting Method were higher than those obtained by the RTAC Method. In terms of sensitivity, the ASTM method is the most sensitive to changes in load, but less sensitive to changes in speed than the RTAC method.

Evidence provided by Figures 7.9 to 7.20 does not allow, however, any conclusive statements on the superiority of one method over the other in calculating LEF's. It is believed that this question can be conclusively addressed only by laboratory testing, by experimentally determining the fatigue life of asphalt concrete samples.

7.3 Comparison of the ASTM LEF's to the AASHO LEF's

The comparison between mechanistic ASTM LEF's and empirical AASHO LEF's is included next, keeping in mind that it should be entirely qualitative, given the conceptual differences

between the two approaches. As presented in Sections 3.1 and 3.9, AASHO Road Test LEF's were calculated as ratios of pavement life, being functions of axle configuration, axle load, Structural Number and terminal serviceability. In this comparison, a SN of 4 and a terminal serviceability of 2.5 were used.

Figure 7.21 to 7.23 present the LEF's for the steering axle of the 3-axle truck at three levels of speed (20, 40 and 50 km/h). Considering the quality of the mechanistic LEF's characterizing the steering axle of the 3-axle truck it is difficult to define general trends in LEF's. In general, it appears that LEF's calculated by the ASTM method were higher than the LEF's calculated by the AASHO method.

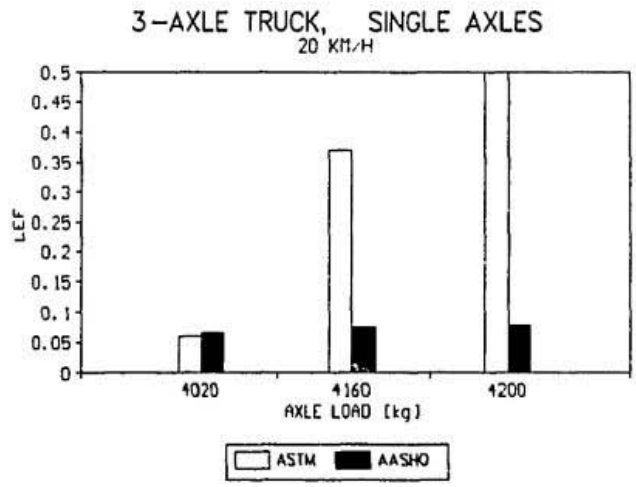

Figure 7.21 : Comparison of ASTM LEF's to AASHO LEF's for 3-Axle Truck, Steering Axle, Speed 20 km/h

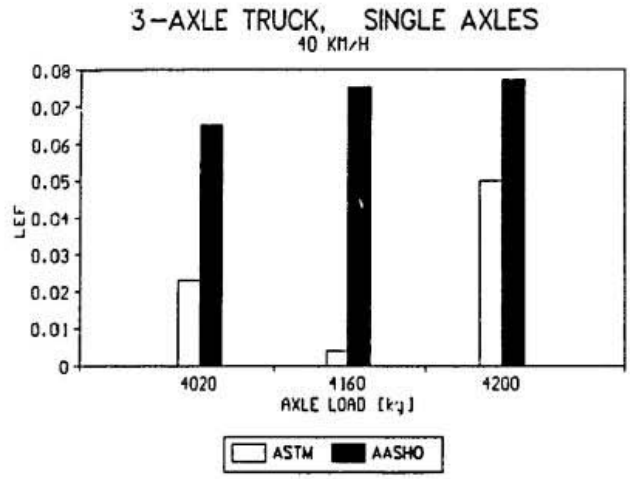

Figure 7.22 : Comparison of ASTM LEF's to AASHO LEF's for 3-Axle Truck, Steering Axle, Speed 40 km/h

Figure 7.23 : Comparison of ASTM LEF's to AASHO LEF's for 3-Axle Truck, Steering Axle, Speed 50 km/h

Figures 7.24 to 7.26 present the LEF's for the tandem axle of the 3-axle truck at three levels of speed (20, 40 and 50 km/h). The information produced by these plots can be summarized as follows:

- the ASTM method yields the highest LEF's.
- the ASTM LEF's are more sensitive at lower speeds to load increase than the AASHO method. The load sensitivity of the ASTM LEF's decreases with increased speed; at 50 km/h, both methods showing similar load sensitivity.
- ASTM LEF's are decreasing with increased speed, while AASHO LEF's are constant across speeds.

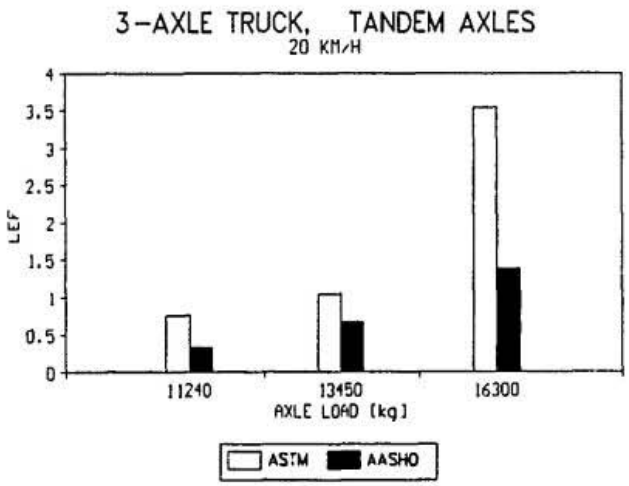

Figure 7.24 : Comparison of ASTM LEF's to AASHO LEF's for 3-Axle Truck, Tandem, Speed 20 km/h

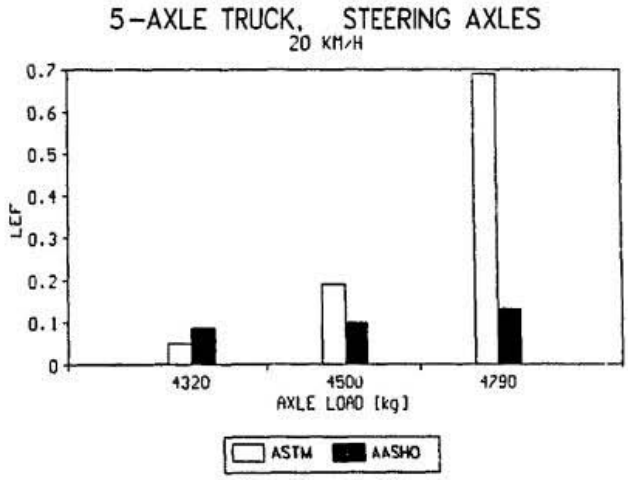

Figure 7.27 : Comparison of ASTM LEF's to AASHO LEF's for 5-Axle Truck, Steering Axle, Speed 20 km/h

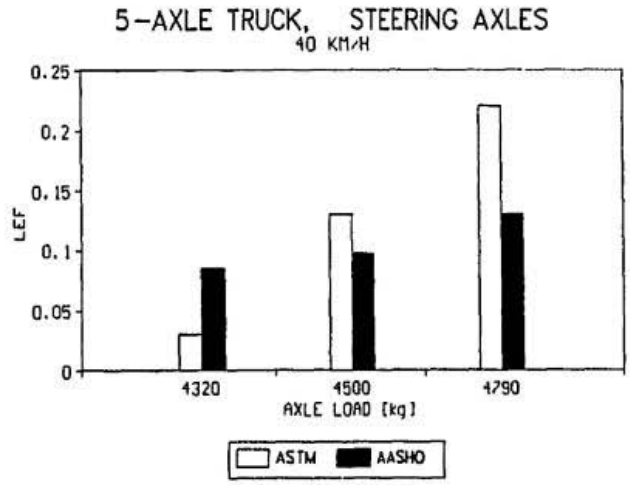

Figure 7.28 : Comparison of ASTM LEF's to AASHO LEF's for 5-Axle Truck, Steering Axle, Speed 40 km/h

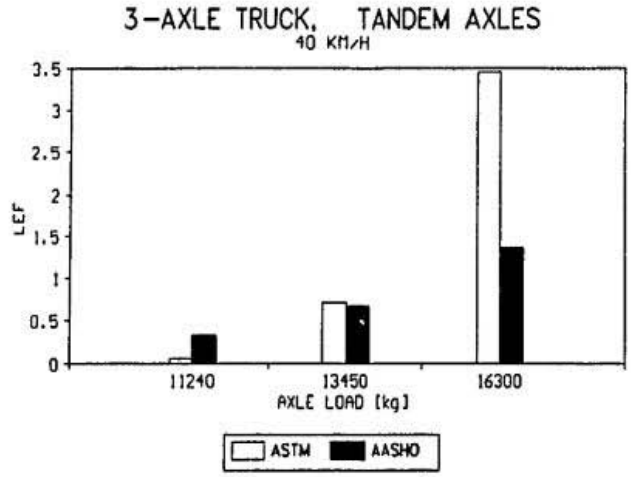

Figure 7.25 : Comparison of ASTM LEF's to AASHO LEF's for 3-Axle Truck, Tandem, Speed 40 km/h

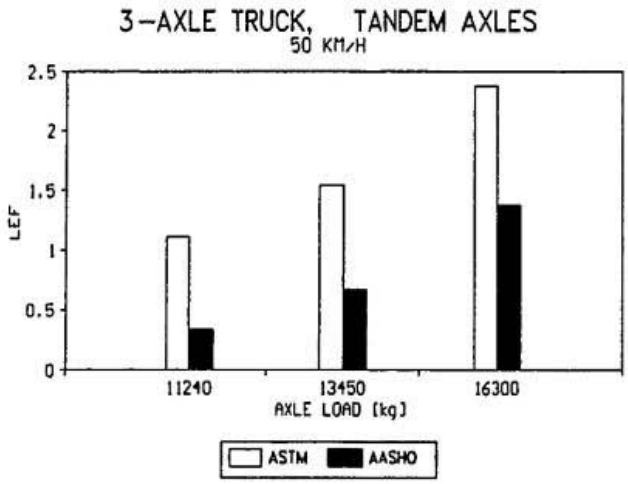

Figure 7.26 : Comparison of ASTM LEF's to AASHO LEF's for 3-Axle Truck, Tandem, Speed 50 km/h

The LEF's for the steering axle of the 5-axle truck are shown in Figures 7.27 to 7.29.

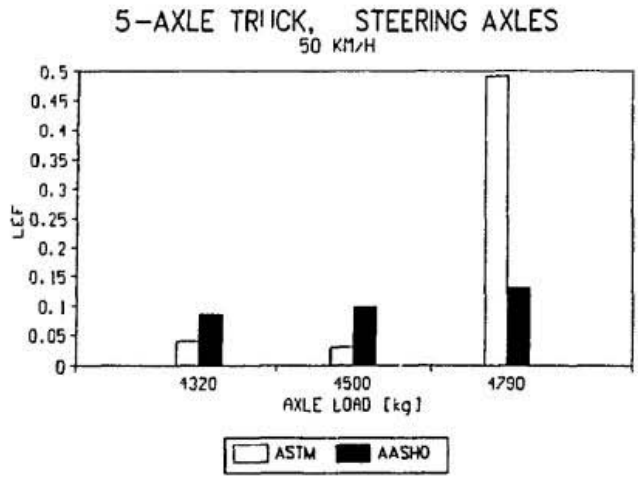

Figure 7.29 : Comparison of ASTM LEF's to AASHO LEF's for 5-Axle Truck, Steering Axle, Speed 50 km/h

For all the speed levels, the sensitivity of mechanistic LEF's to load was shown to be higher than that of empirical LEF's. In general, the ASTM method yielded higher LEF's than the AASHO method.

Figures 7.30 to 7.32 show the LEF's for the tandem of the 5-axle truck, grouped according to speed. At each level of speed, the LEF's of both the first and the second tandem were plotted together versus load.

At 40 km/h, both 16,890 and 17,550 kg tandem load yielded lower than expected LEF's, again a reflection of the lateral placement of the Run 31. However, based on LEF's corresponding to other levels of loading, it was observed that LEF's of heavier axles are less sensitive to speed than LEF's of light

axles.

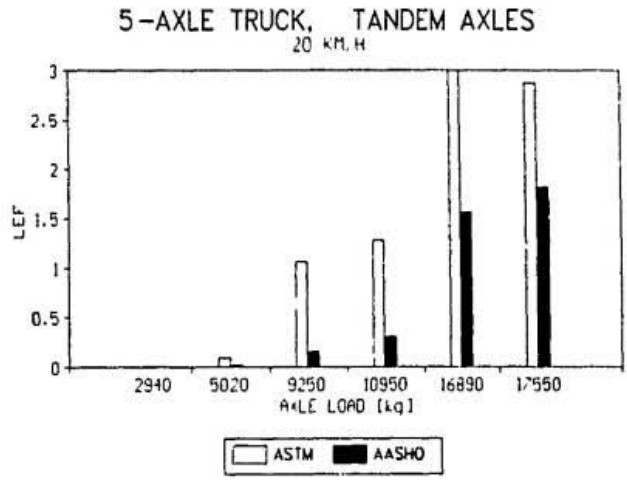

Figure 7.30 : Comparison of ASTM LEF's to AASHO LEF's for 5-Axle Truck, Tandems , Speed 20 km/h

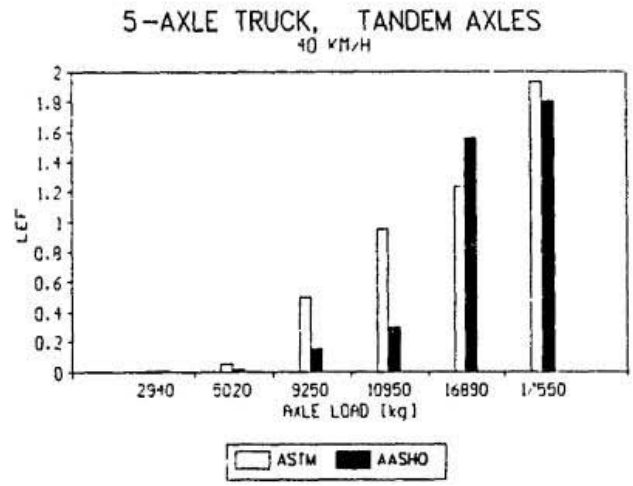

Figure 7.31 : Comparison of ASTM LEF's to AASHO LEF's for 5-Axle Truck, Tandems, Speed 40 km/h

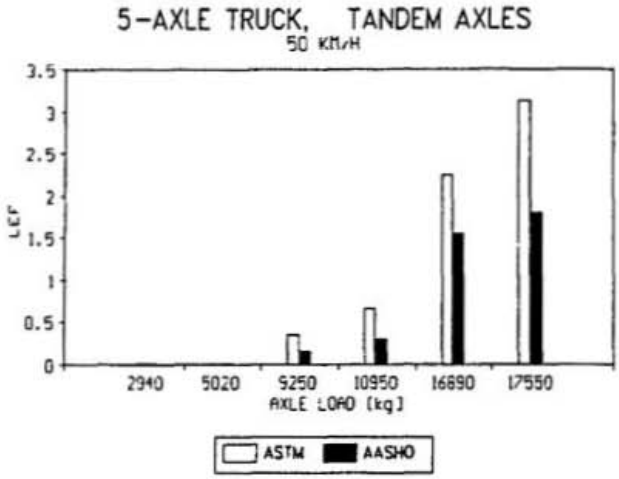

Figure 7.32 : Comparison of ASTM LEF's to AASHO LEF's for 5-Axle Truck, Tandems, Speed 50 km/h

For increased tandem loads, the increase in LEF's of ASTM LEF's was proportional to the increase in LEF's of the AASHO LEF's.

In conclusion, it was observed that LEF's obtained by the Range-Pair Counting Method are typically higher than those obtained by the \ASHO Road Test. In general, a trend of decreasing LEF's with increased speed and decreasing load was observed. Although at lower speeds and loads both ASTM and RTAC yielded higher LEF's than the AASHO Road Test LEF's, at higher loads, the ASTM values are more close to the AASHO ones than the RTAC values. However, given the different nature of mechanistic and empirical methods, it is not conclusive to assess quantitatively a mechanistic method based on empirical

standards.

7.4 LEF's obtained by integrating the strain cycles

In addition to the discrete methods presented earlier, an attempt to devise LEF's calculation methods based on integrals of the strain cycles was made. The introduction of the time variable into the calculation of LEF's can be justified by the visco-elastic behavior of the asphalt concrete. As pointed out by Govind et al. (Section 3.13), fatigue is determined both by load magnitude and its rate of application. Accordingly, the rate of change of force, stress or energy can be considered as representative of damage.

The LEF's were calculated as the ratio of two integral values, namely the integral of the cycle generated by the candidate axle/axle group divided by the integral of the strain cycle generated by the BB axle. The integration was based on Simpson's rule, considering sub-intervals of 0.001 seconds width, corresponding to the sampling interval used during the acquisition of experimental data.

Two approaches were considered initially, first by integrating the entire trough-peak-trough cycles of the strain versus time history, and second, by integrating only the tensile part of the same cycles. These two approaches intended to parallel, in integral terms, the ASTM and RTAC discrete methods. However, it was found that the integral LEF's calculated by

using the tensile part of the strain cycles closely reproduced across speed and load the trends of the RTAC LEF's. In quantitative terms, the integral approach yielded always smaller LEF's. As a result, only the LEF's based on the Trough-Peak-Trough integrals will be discussed bellow.

7.4.1 Trough-Peak-Trough Integrals

The results presented in this section refer to the 3-axle and the 5-axle truck. Table 7.3 presents the LEF's for the 3-axle truck, while Table 7.4 presents the LEF's for the 5-axle truck.

Table 7.3: Integral LEF's for 3-axle Truck

RUN	LOAD CODE	SPEED km/h	STEERING	TANDEM	SUM OF AXLES	VEHICLE
2		20	1.15	2.54	3.69	3.69
6	1	40	0.09	3.16	3.25	3.25
8		50	1.21	1.82	3.03	3.03
11		20	2.90	0.83	3.74	3.74
14	2	40	0.05	0.56	0.56	0.56
18		50	20.54	1.19	21.73	21.73
20		20	0.21	0.47	0.69	0.69
23	3	40	0.07	0.04	0.12	0.12
27		50	3.07	0.87	3.94	3.94

Table 7.4: Integral LEF's for 5-axle Truck

RUN	LOAD CODE	SPEED km/h	STEERING	TANDEM 1	TANDEM 2	SUM OF AXLES	VEHICLE
29		20	2.21	6.75	3.23	12.20	12.66
32	1	40	0.41	3.32	2.00	5.75	5.76
35		50	4.34	3.13	2.99	10.47	10.52
38		20	0.45	1.79	1.58	3.83	4.66
42	2	40	0.26	12.63	0.72	13.62	13.62
44		50	0.04	6.04	0.38	6.47	6.47
48		20	0.05	0.12	0.01	0.18	0.30
50	3	40	0.05	0.08	0.005	0.14	0.16
54		50	0.088	0.001	0.0004	0.09	0.09

LEF's for entire configurations were obtained by adding LEF's for the steering axle and the tandem axles ("axle sum" LEF's), and by adding the LEF's of all the strain cycles, including the strain cycles obtained between the axles ("vehicle" LEF's). The LEF's presented in both tables are discussed subsequently both in terms of individual axles/axle groups and entire vehicles. The following analysis presents the effect of speed and level of loading on integral LEF's based on the entire trough-peak-trough strain cycles. Expected trends are described and inconsistencies explained.

The main limitation of the integral method was encountered

for certain strain versus time histories, where it was not possible to differentiate between the inter-axle strain cycle from the cycles produced by the preceding axle. In such cases, the strain cycle produced by an axle incorporated the following inter-axle cycle, without defining any intermediate trough. Figure 7.33 presents a strain versus time history where the strain cycle produced by the steering axle incorporated the inter-axle cycle, generating a composite cycle characterized by a much longer duration.

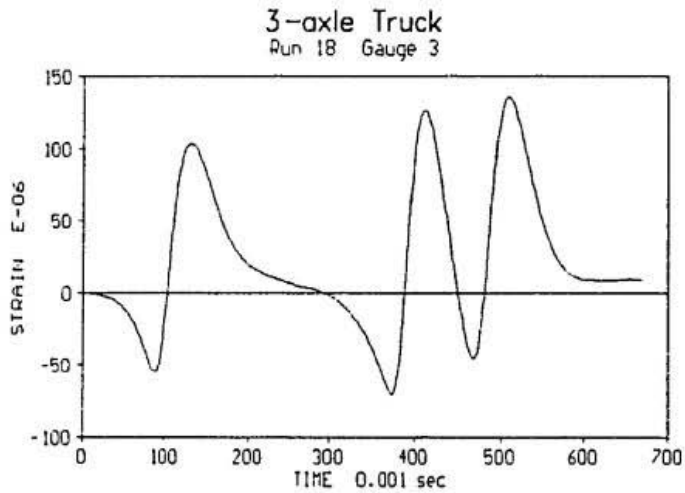

Figure 7.33 : Strain versus Time History Presenting a Composite Steering-Inter-axle Strain Cycle

The integral value of the composite cycle increased significantly, affecting the resulting LEF's. This situation did not affect the discrete LEF's obtained by the ASTM or RTAC

methods, because the peak value of the analyzed cycle was not modified by composite axle-inter-axle cycles.

Figure 7.34 presents the LEF's obtained by using the Trough-Peak-Trough integrals for the steering axle of the 3-axle truck. Besides the high LEF obtained for the second load class at 50 km/h, it was found that the integral method yielded in general higher LEF's (for example at 50 km/h, load class 3, the LEF was 3).

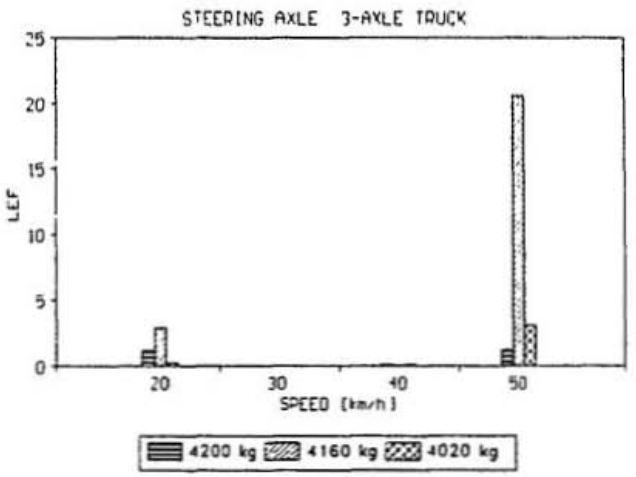

Figure 7.34 : LEF's for 3-Axle Truck, Steering Axle, Calculated using Trough-Peak-Trough Integrals

The tandem LEF's presented in Figure 7.35 have values comparable to LEF's obtained by other methods under the same loading and speed conditions. These LEF's were consistent across classes of loading for the same speed, although they present inconsistences across levels of speed for the same load class.

It was observed that the integral LEF's of the 3-axle truck tandem and the ASTM LEF's for the same axle, shown in Figure 7.2 presented a similar behavior across speed and load classes. However, for the same load-speed combinations, ASTM LEF's were quantitatively higher than integral LEF's.

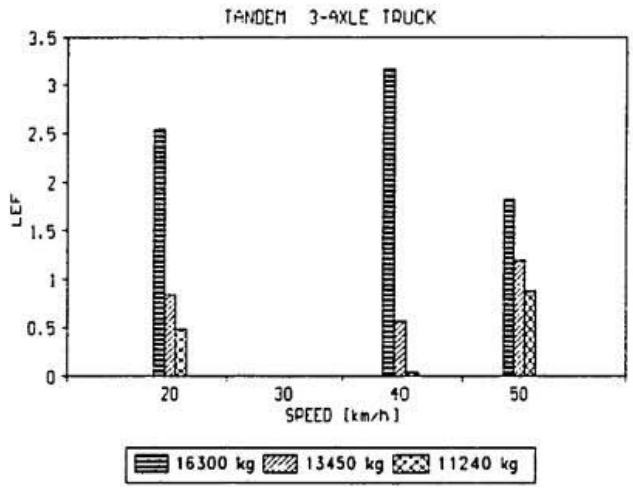

Figure 7.35 : LEF's for 3-Axle Truck, Tandem, Calculated using Trough-Peak-Trough Integrals

Vehicle LEF's calculated as a sum of axle LEF's were highly affected by the integral LEF's of the steering axle (Figure 7.36). The comparison presented in Section 1.1.2, between "axle sum" LEF's and "vehicle" LEF's was also carried out for the integral method. The last two columns of Table 7.3 make clear that both approaches resulted in numerically equal results for the 3-axle truck. All the integral LEF's of the 5-axle truck, at 40 km/h and the highest load class, showed again the

influence of the large lateral placement value described earlier. The influence of the composite axle-inter-axle cycle was observed at 50 km/h, load class 1, for the steering axle (Figure 7.37).

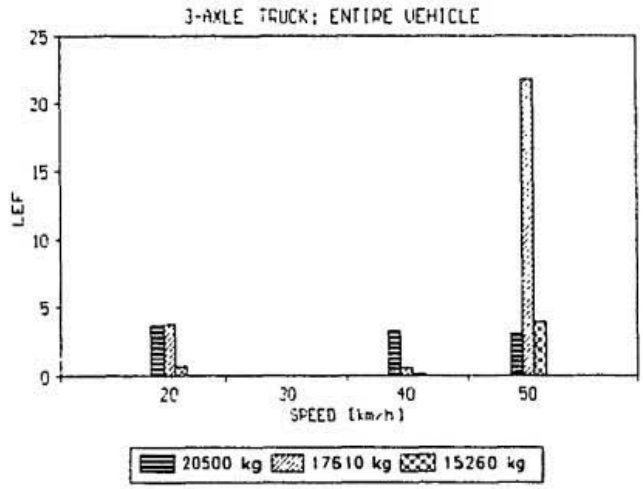

Figure 7.36 : LEF's for 3-Axle Truck, Entire Vehicle, Calculated using Trough-Peak-Trough Integrals

The corresponding LEF exceeded considerably all the LEF's produced by the steering axle. Despite these shortcomings, it was concluded that the integral method yielded higher LEF's than any discrete methods. Without taking into account the LEF's affected by the lateral placement, the maximum LEF was around 2 for the integral method, while the ASTM method yielded a 0.7 value for the same conditions.

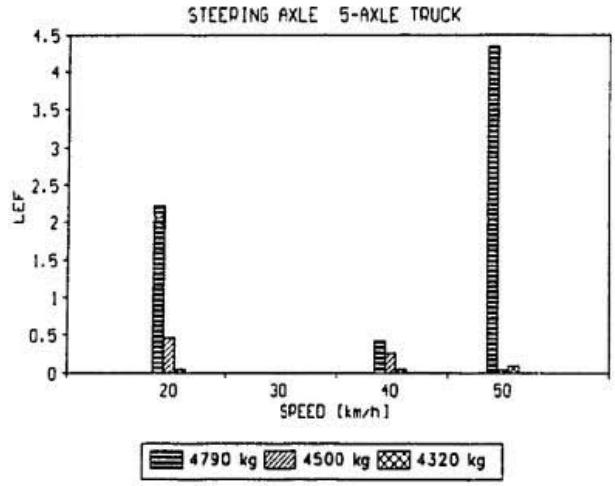

Figure 7.37 : LEF's for 5-Axle Truck, Steering Axle, Calculated using Trough-Peak-Trough Integrals

The first tandem of the 5-axle truck (Figure 7.38) yielded very high LEF's, often two times higher than those produced by the ASTM method. However, the second tandem (Figure 7.39) followed the trend and was compatible to the ASTM LEF's values.

The LEF's for the 5-axle truck, calculated both as "axle sum" LEF's and "vehicle" LEF's are tabulated in the last two columns of Table 7.4 and plotted in Figure 7.40. It was observed that for the strain versus time histories of the 5-axle truck, there was a difference between "axle sum" LEF's and "vehicle" LEF's. However, the contribution of the inter-axle LEF's was in general small, never surpassing a value of one.

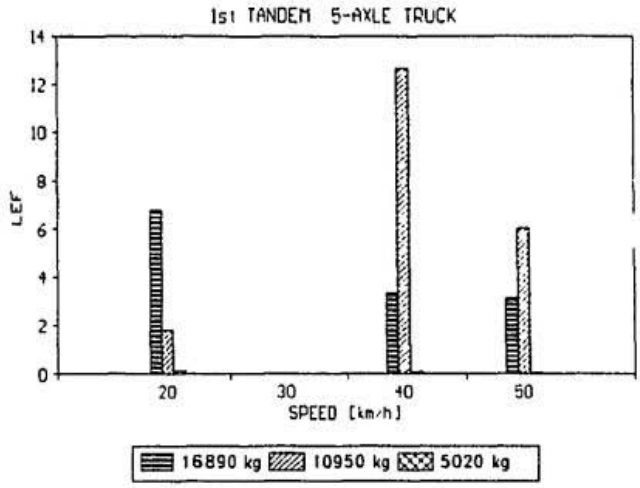

Figure 7.38 : LEF's for 5-Axle Truck, 1st Tandem, Calculated using Trough-Peak-Trough Integrals

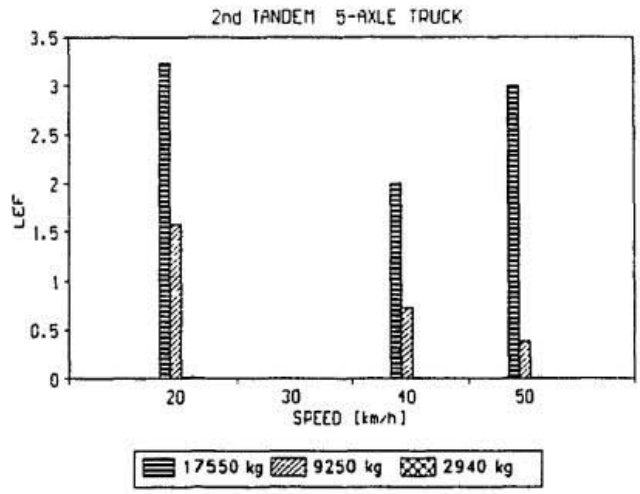

Figure 7.39 : LEF's for 5-Axle Truck, 2nd Tandem, Calculated using Trough-Peak-Trough Integrals

The high variability of LEF's calculated by the integral method was a result of the cycle definition methodology. Apparently the ASTM cycle identification procedure, while being well suited for discrete methods, is not suitable to the integral approach.

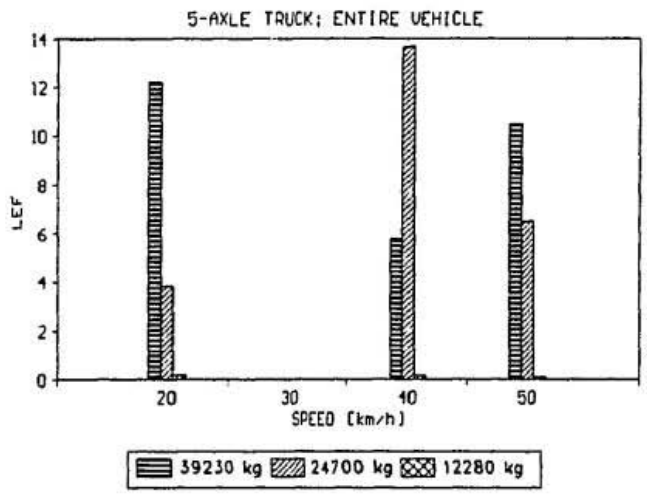

Figure 7.40 : LEF's for 5-Axle Truck, Entire Vehicle, Calculated using Trough-Peak-Trough Integrals

The integral method yielded inconsistent results, such as increased LEF's for lower loads, and much higher than expected LEF's values. Based on these observations, this approach (as it was applied and based on the 3.8 exponent) has to be rejected at this level.

Chapter 8

CONCLUSIONS

The literature review revealed that extensive work has been done on the load equivalence area (LEF), and indicated a recent emphasis on mechanistic methods for LEF's calculation. These methods are characterized by increasing sophistication and generality.

The ASTM E 1049-85, initially introduced for metals, was considered and it was demonstrated that its Range-Pair Cycle Counting method is the most suitable for the analysis of flexible pavements presenting the fatigue cracking type of distress. This method identifies the trough-peak-trough strain cycles of any strain versus time history, taking into account both the part in tension and the part in compression of each cycle.

The LEF's obtained were dependent both on the candidate axle load and vehicle speed. Higher loads produced higher LEF's while increased speeds produced lower LEF's.

It was observed that the values of the LEF's were significantly affected by the relative lateral placement of a given candidate axle versus the lateral placement of the corresponding BB truck standard axle, and by the absolute lateral placement of any axle with respect to the stain gauge monitoring the run. In both cases, larger lateral placement values result in reduced LEF's, based on strain versus time histories having

lower strain magnitudes.

It is recommended to closely monitor the lateral placement of the vehicles during the experimental runs. Quantitative improvements of the lateral placement can be obtained both by attentively driving the experimental vehicles, and/or by increasing the number of run replicates.

In general, runs corresponding to heavier loads and lower speeds, yielded more consistent LEF's, because the external factors (lateral placement, temperature, etc.) usually had lower impact on high amplitude strain versus time histories.

A comparison was made between the LEF's obtained by the ASTM Range-Pair Counting Method and the LEF's obtained by the RTAC Method. It was found that LEF's obtained by the ASTM Range-Pair Counting Method were higher than those obtained by the RTAC Method. The ASTM method was the most sensitive to changes in load, being at the same time less sensitive than the RTAC method to changes in speed. However, the superiority of one method over the other was not demonstrated. It was concluded that this question can be addressed only by laboratory testing, by experimentally determining the fatigue life of asphalt concrete samples.

A qualitative comparison was also made between mechanistic ASTM LEF's and empirical AASHO LEF's, keeping in mind the conceptual differences between the two approaches. It was

observed that LEF's obtained by the ASTM Range-Pair Counting Method were typically higher than those obtained at the AASHO Road Test. Although at lower speeds and loads both ASTM and RTAC yielded higher LEF's than the AASHO Road Test LEF's, at higher loads, the ASTM values were closer in magnitude to the AASHO LEF's than the RTAC LEF's. However, given the different nature of mechanistic and empirical methods, these comparisons cannot be considered.

Another issue raised was the treatment of the trough-peak-trough cycles existing between the axle groups. These cycles, referred to as inter-axle cycles, were found not to be quantitatively significant, although the concept may be theoretically valid.

An attempt was made to devise LEF's calculation methods based on integrals of the strain cycles, by using integral values of the trough-peak-trough cycles of the strain versus time history. The results were unsatisfactory, apparently because of the cycle definition methodology. The ASTM Range-Pair cycle identification procedure proved to be unsuitable for the integral approach, yielding inconsistent results. Based on the quality of the results, the integral method for LEF's calculation had to be rejected.

REFERENCES

American Association of State Highway Officials (1961). **AASHO Interim Guide for Design of Pavement Structures**, Washington D.C.

American Association of State Highway and Transportation Officials (1986). **AASHTO Guide for Design of Pavement Structures**, Washington D.C.

American Society for Testing of Materials (1985). **Standard Practices for Cycle Counting in Fatigue Analysis**, ASTM E1049-85, pp. 836-848.

Barenberg, E.J. (1988). **"Role of Instrumented Pavements in Establishing Load Equivalencies"**, FHWA Workshop on Load Equivalency, McLean, Virginia.

Brown, S.F. and B.V. Brodrick (1981). **"Instrumentation for Monitoring the Response of Pavements to Wheel Loading"**, Sensors in Highway and Civil Engineering, ICE, London.

Christison, J.T., K.O. Anderson and B.P. Shields (1978). **In Situ Measurements of Strains and Deflections in a Full-Depth Asphaltic Concrete Pavement**, Proceedings, Association of Asphalt Paving Technologists, Univ. of Minnesota, Minneapolis, Vol.47, pp. 398-433.

Deacon, J.A. (1969). **"Load Equivalency in Flexible Pavements"**, Proceedings, Association of Asphalt Paving Technologists, Univ. of Minnesota, Minneapolis, Vol.38, pp. 465-494.

ELSYM5 (1985). **"Report No. FHWA-RD-85"**, Federal Highway Administration, McLean, Virginia.

Fernando, E.G., D.R. Luhr and H.N. Saxena (1988). **"Analysis of Axle Loads and Axle Types for the Evaluation of Load Limits on Flexible Pavements"**, National Research Council, Transportation Research Record 1136, pp. 69-78.

Govind S. and C.M. Walton (1989). **"Fatigue Model to Assess Pavement Damage"**, National Research Council, Transportation Research Record 1227, pp. 99-96.

Hajek, J.J. and A.C. Agarwal (1989). **Influence of Axle Group Spacing on Pavement Damage**, Ontario Ministry of Transportation, The Research and Development Branch.

Hallin, J.P., J. Sharma and J.P. Mahoney (1984). **"Development of Rigid and Flexible Pavement Load Equivalency Factors for Various Widths of Single Tires"**, National Research Council, Transportation Research Record 949, pp. 4-13.

Highway Research Board (1962). **The AASHO Road Test: Report 5 - Pavement Research**, Highway Research Board Special Report 61E, HRB, National Research Council, Washington, D.C., 1962

Hutchinson, B.G., R.C.G. Haas, P.Meyer, K. Hadipour and T. Papagiannakis (1987). **"Equivalencies of Different Axle Load Groups"**, Proceedings, 2nd North American Conference on Managing Pavements, Toronto, pp. 3.191-3.202.

Lytton, R.L. (1988). **"Damage Factors"**, FHWA Workshop on Load Equivalency, McLean, Virginia.

Majidzadeh, K. and G.J. Ilves (1988). **"Methods for Determining Primary Response Load Equivalency Factors"**, FHWA Workshop on Load Equivalency, McLean, Virginia.

Michelow J. (1963). **"Analysis of Stresses and Displacements in an N-Layered Elastic System under a Load Uniformly Distributed on a Circular Area"**, Chevron Research Corporation, Richmond, California.

Organization for Economic Co-operation and Development (1982). **Impacts of Heavy Freight Vehicles**, OECD Road Research Group.

Organization for Economic Co-operation and Development (1988). **Heavy Trucks, Climate and Pavement Damage**, OECD Road Transport Research, Paris.

Papagiannakis , T., M.A. Oancea, N. Ali, J. Chan and A.T. Bergan (1991). **Application of ASTM E 1049-85 in Calculating Load Equivalence Factors from In-situ Strains**, Presented at the 70th Annual Meeting, TRB, Washington, D.C., accepted for publication in Transportation Research Record.

Prakash, A. and A.C. Agarwal (?). **"Tri-Axle Study: Proposed Methodology to Study Effect on Pavements"**, Internal Report, Ontario Ministry of Transportation.

Ramsamooj, D.V., K.Majidzadeh and E.M. Kauffmann (1972). **"The Analysis and Design of the Flexibility of Pavement"**, Proceedings, International Conference on the Structural Design of Asphalt Pavements, University of Michigan, Ann Arbor, pp. 692-704.

Rilett, L.R. and B.G. Hutchinson (1988). **LEF Estimation from Canroad Pavement Load-Deflection Data**, National Research Council, Transportation Research Record 1196, pp. 170-178.

RTAC (1986). **Pavement Response to Heavy Vehicle Test Program: Part 2 - Load Equivalency Factors**, Canroad Transportation Research Corporation.

Terrel, R.L. and S. Rimscritong (1976). **"Pavement Response and Equivalencies for Various Truck Axle Tire Configurations"**, National Research Council, Transportation Research Record 602, pp. 33-38.

Treybing, H.J. (1983). **"Equivalency Factor Development for Multiple Axle Configurations"**, National Research Council, Transportation Research Record 949, pp. 32-44.

Treybing, H.J. and H.L. Von Quintus (1977). **"Equivalency Factor Analysis and Prediction for Triple Axles"**, Presented at the 56th Annual Meeting, TRB, Washington, D.C.

Tseng, K.H. and R.L. Lytton (1990). **"Fatigue Damage Properties of Asphaltic Concrete Pavements"**, Paper 890201 presented at The 69th Annual Meeting, Transportation Research Board, Washington, D.C.

Wang, M.C. and R.F. Anderson (1980). **"Load Equivalency Factors for Triaxle Loading"**, National Research Council, Transportation Research Record 810, pp. 42-49.

Appendix A

STRAIN PEAKS AND INTEGRALS VERSUS VEHICLE LATERAL PLACEMENT

The plots presented in this appendix depict the behavior of strain peaks and integrals with modified lateral placement of the Benkelman Beam truck trailing axle.

The peak strain values plotted together were obtained by applying the ASTM Range-Pair Counting Method and the RTAC Method. The X axis of these plots displays the lateral placement in centimeters, while the Y axis displays the strain measured in microstrain. Another category of plots show the integrals of the strain cycles as defined by the ASTM method (trough-peak-trough) and as defined by the RTAC method (zero strain-peak-zero strain) versus lateral placement. For these plots, the X axis displays the lateral placement in centimeters, and the Y axis displays the integral values measured in microstrain * second E-3. Above the marker representing the strain peak or strain integral values, appears the BB run number which generated the strain versus time history.

Besides the processing method, the results are grouped by strain gauge and vehicle speed. Each page of the appendix contains the plots for a specific strain gauge (from S1 to S12a), organized in three rows, corresponding to speeds of 20, 40, and 50 km/h.

Strain gauge 1

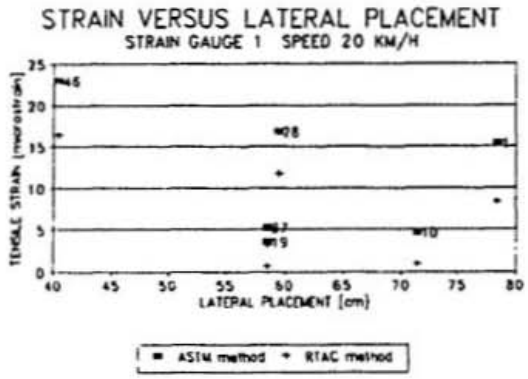

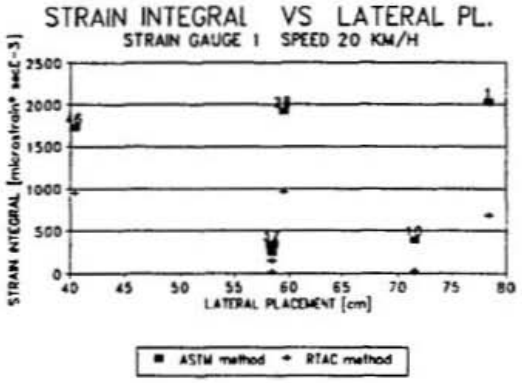

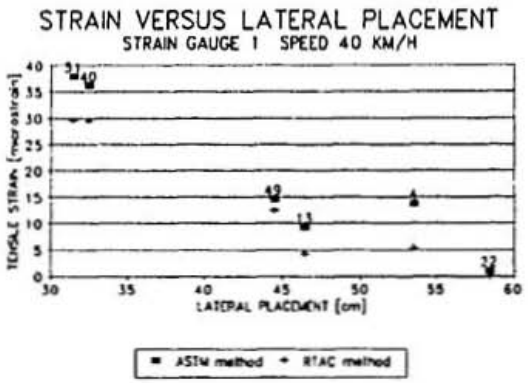

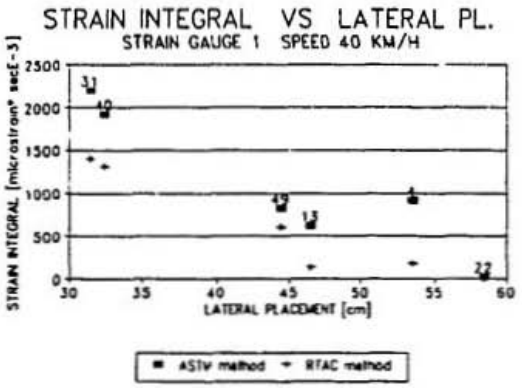

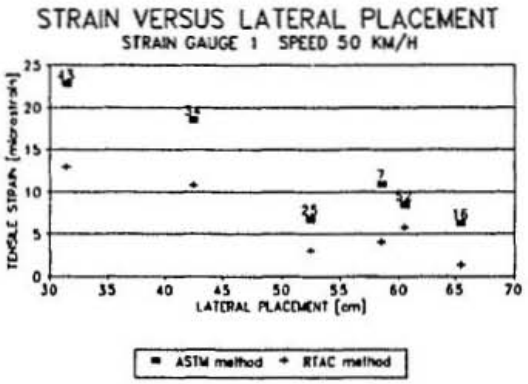

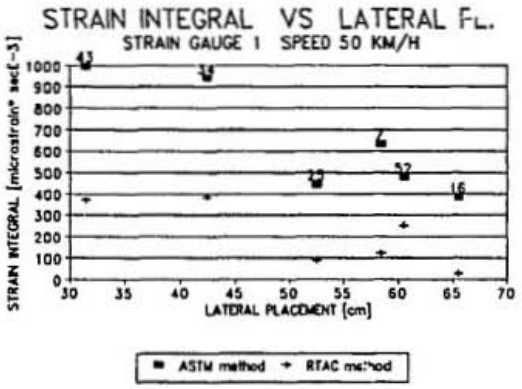

Strain gauge 2

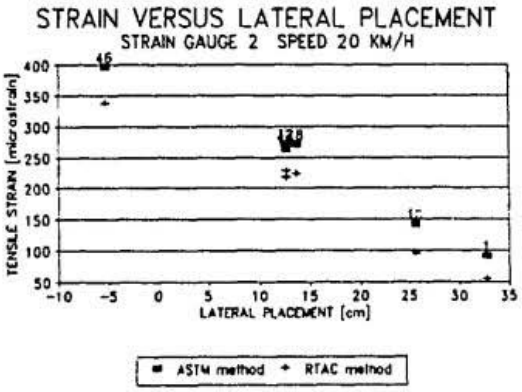

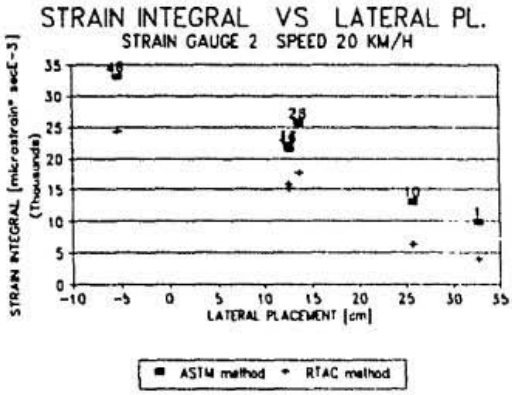

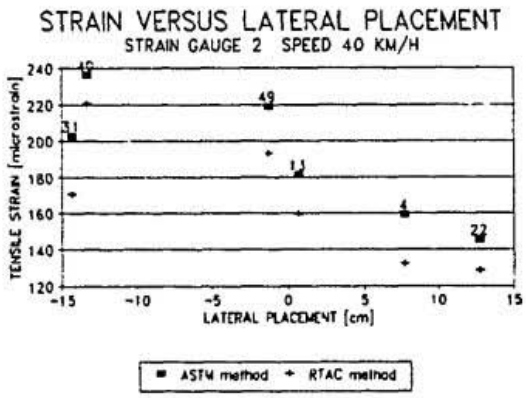

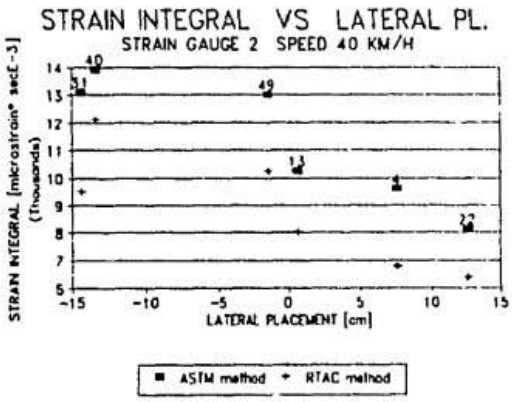

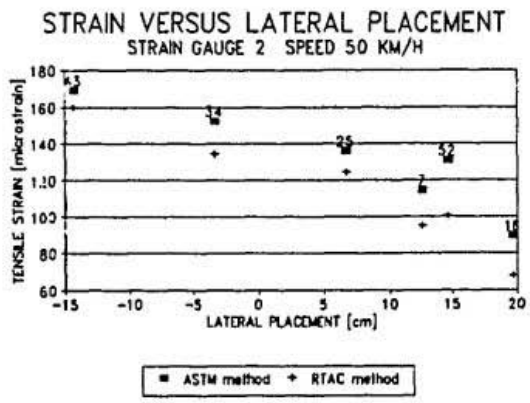

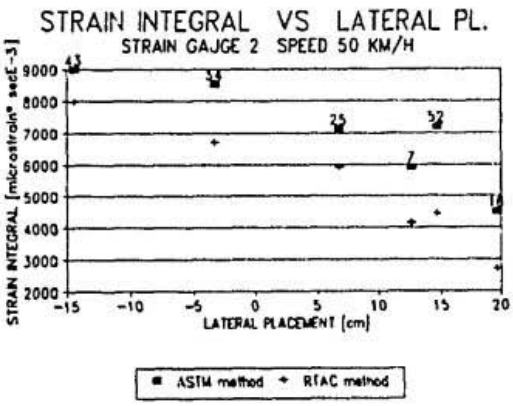

Strain gauge 3

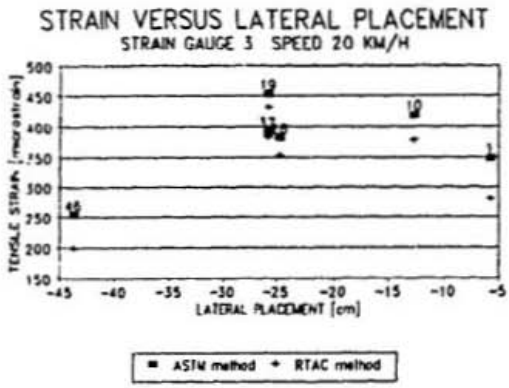

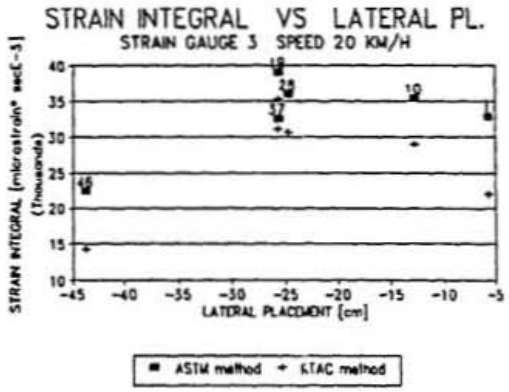

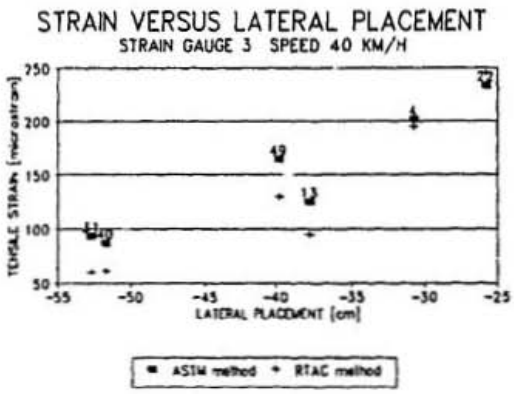

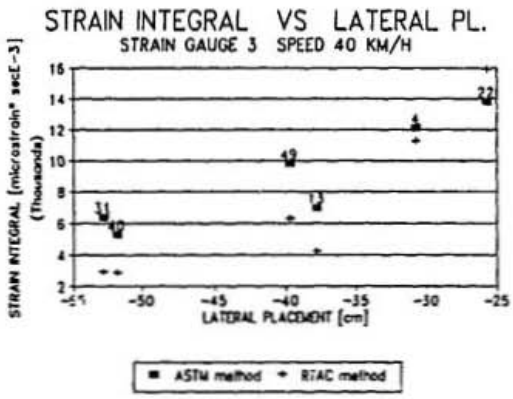

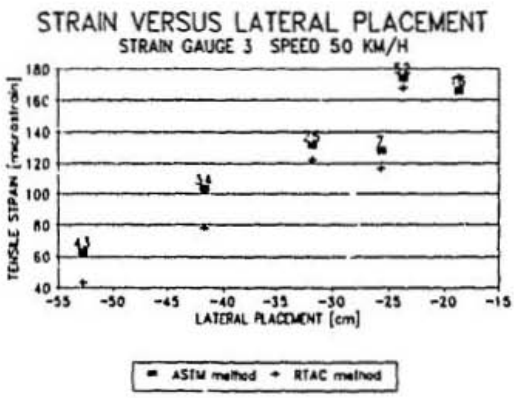

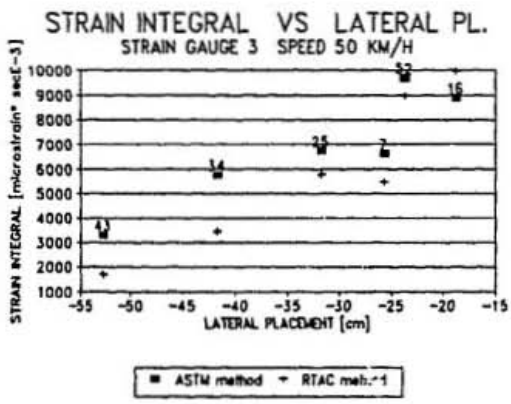

Strain gauge 4

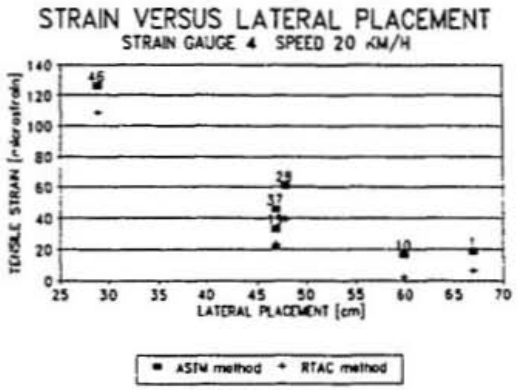

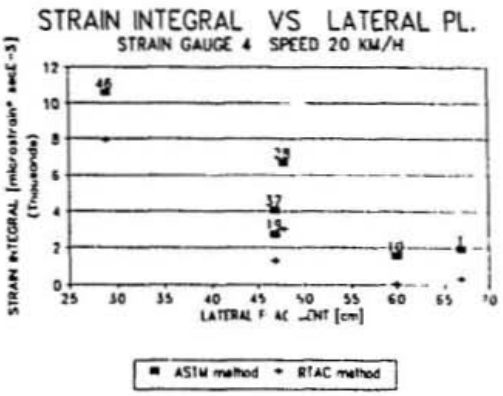

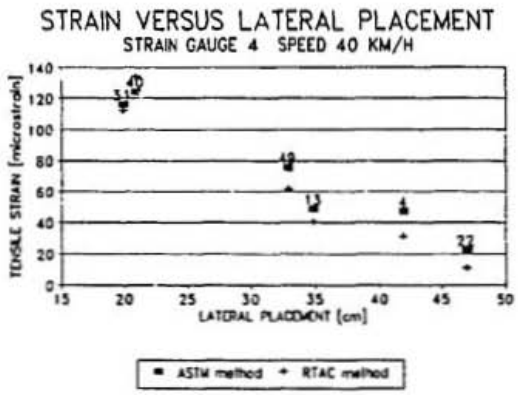

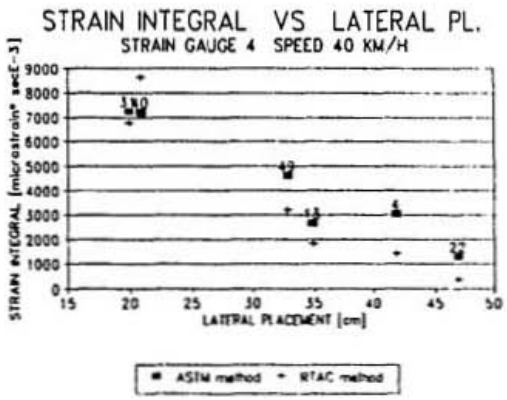

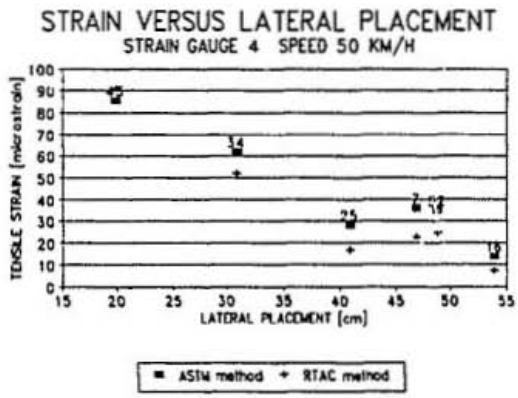

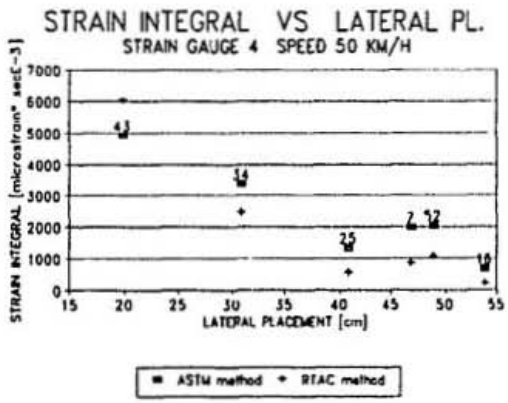

Strain gauge 6

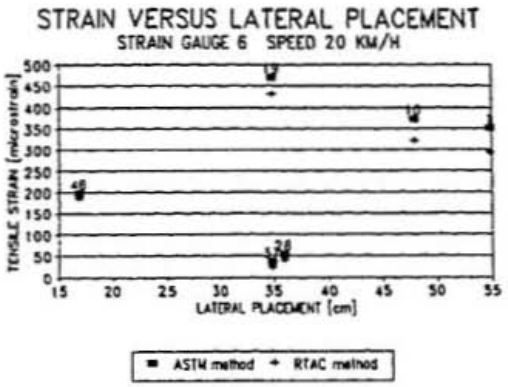

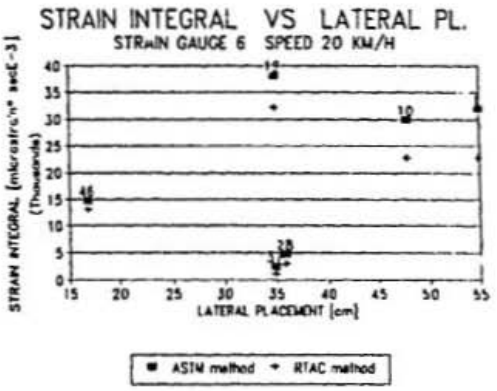

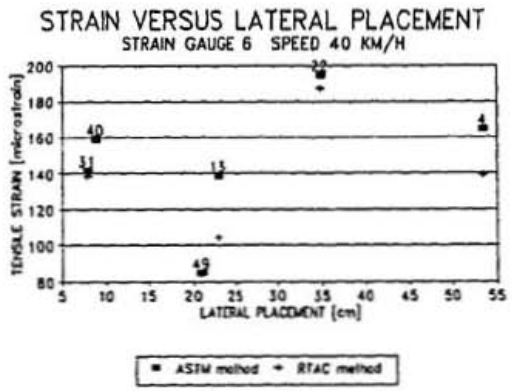

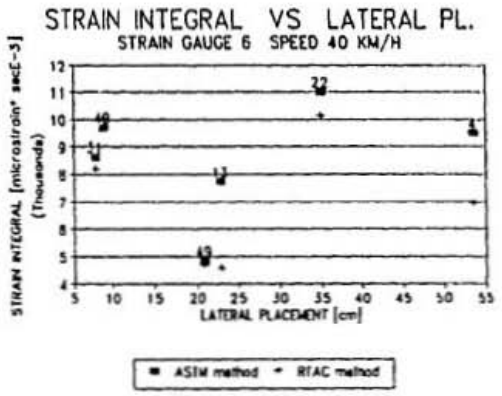

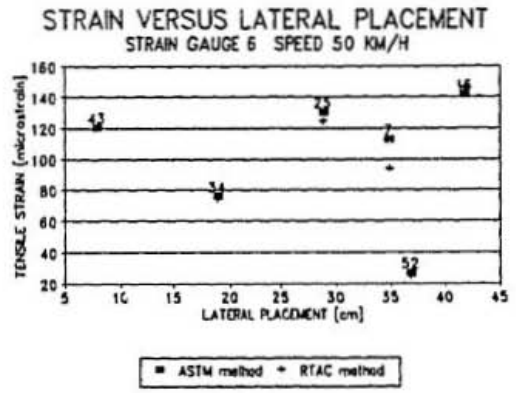

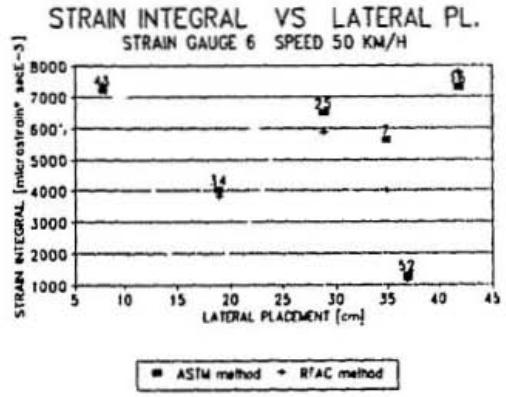

Strain gauge 5

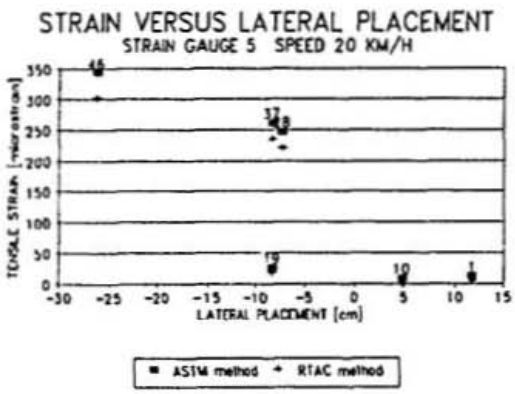

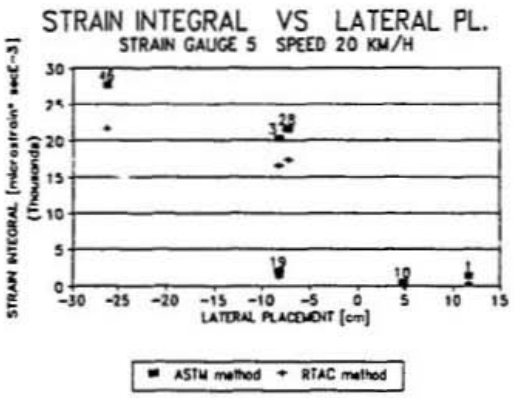

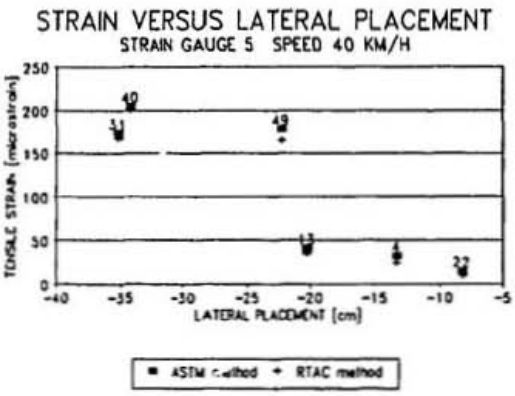

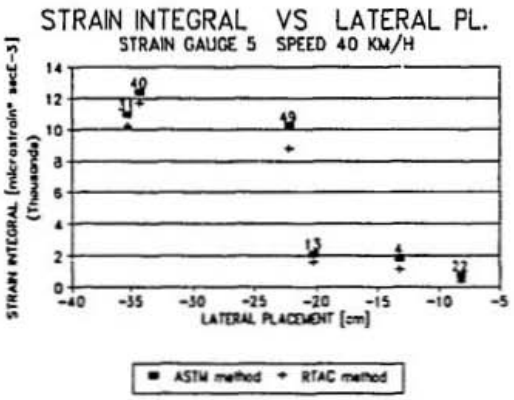

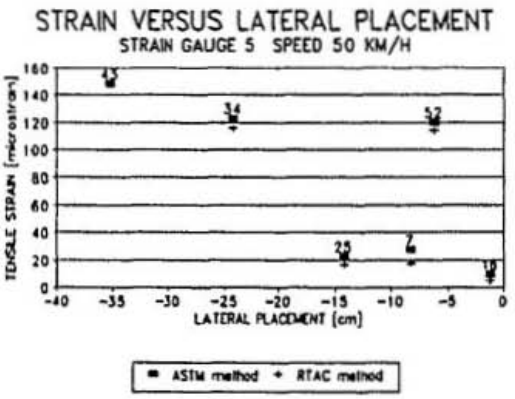

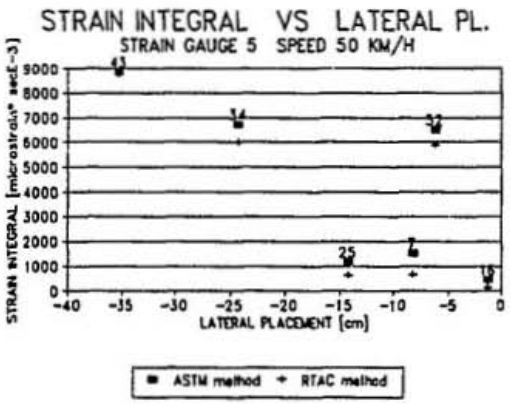

Strain gauge 7

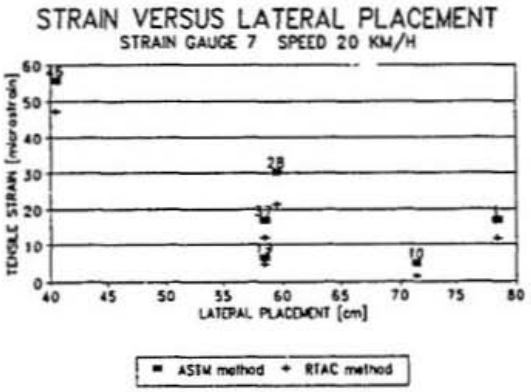

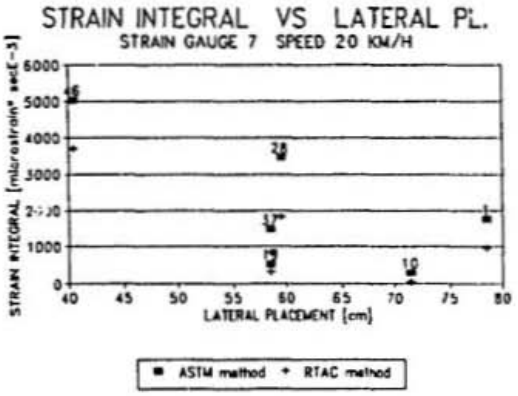

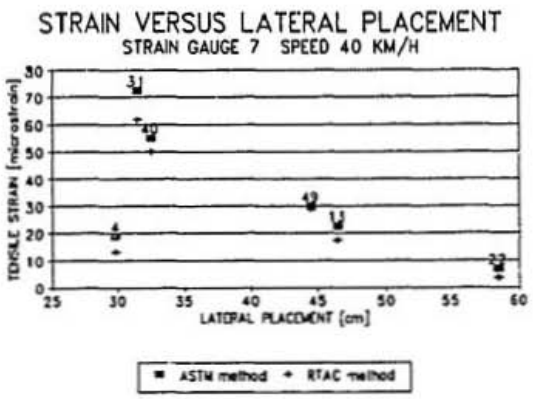

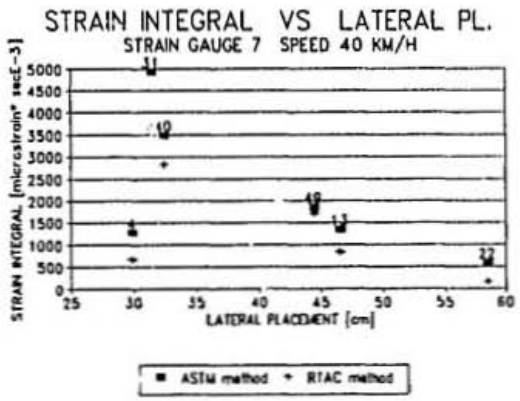

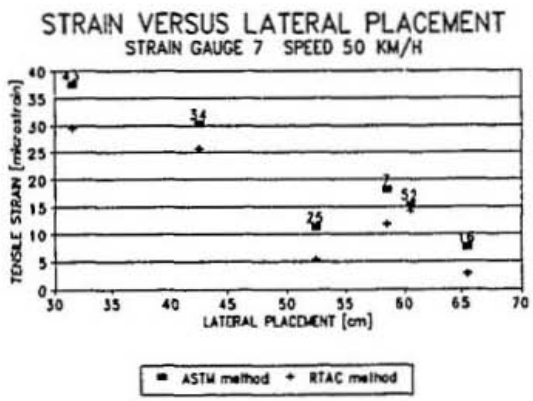

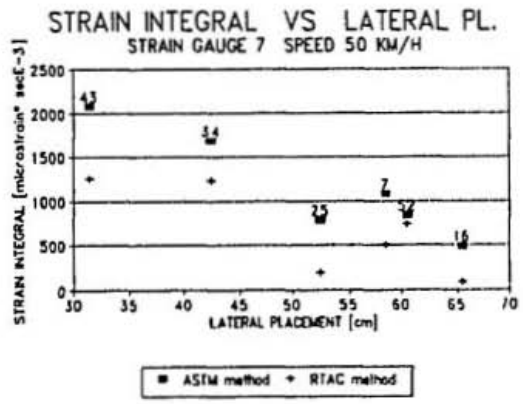

Strain gauge 8

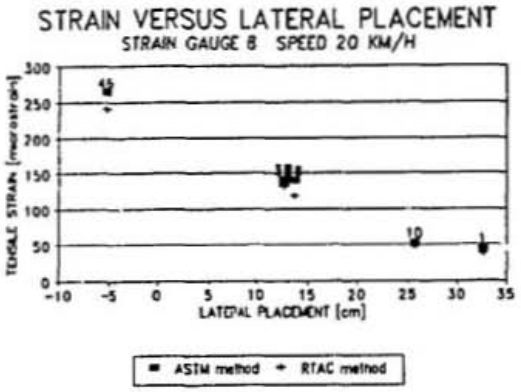

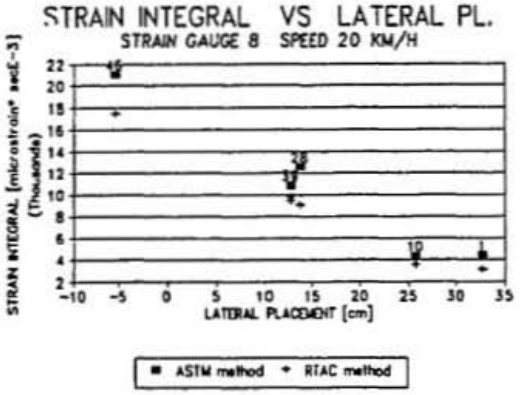

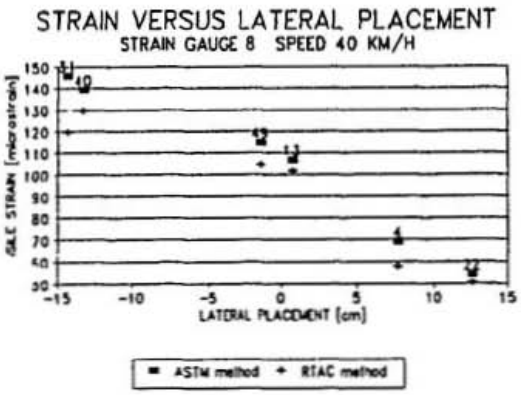

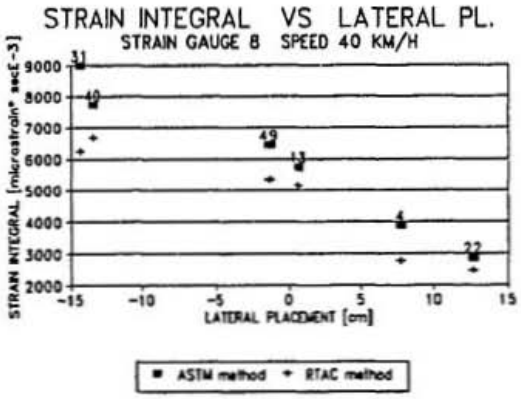

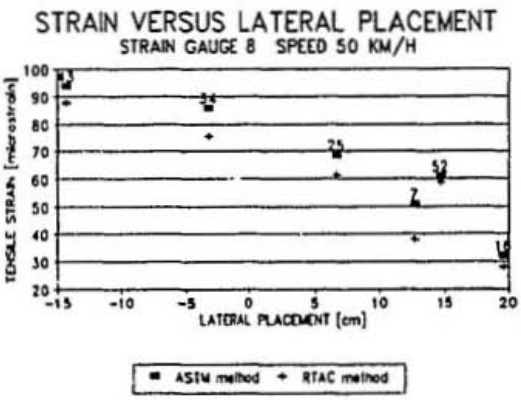

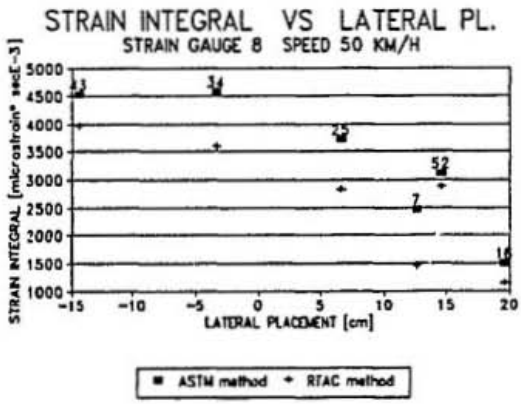

Strain gauge 9

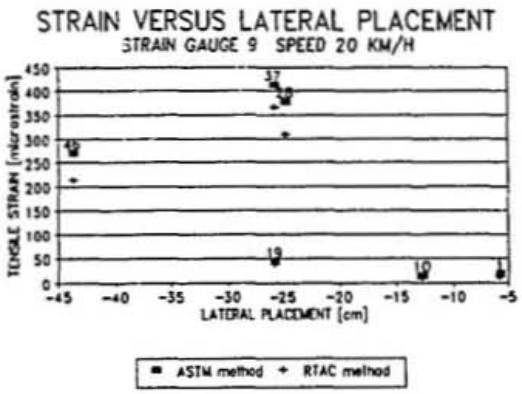

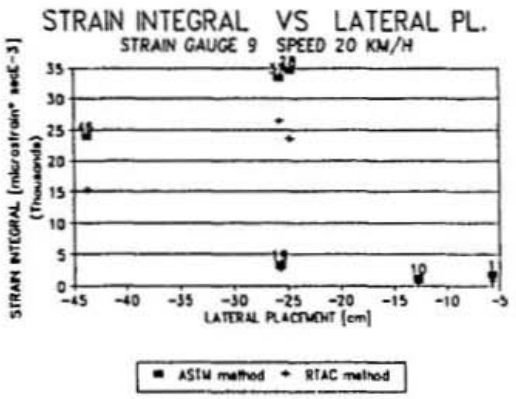

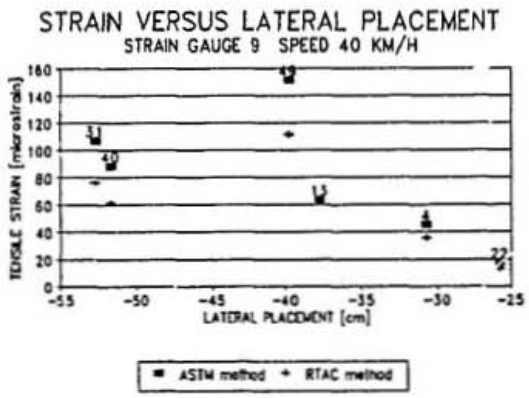

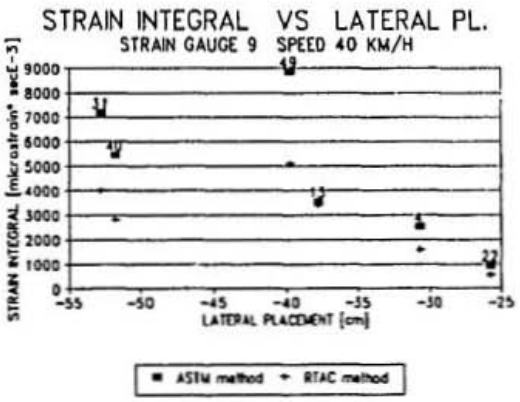

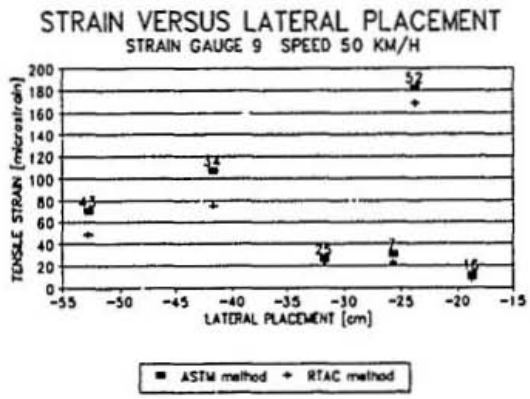

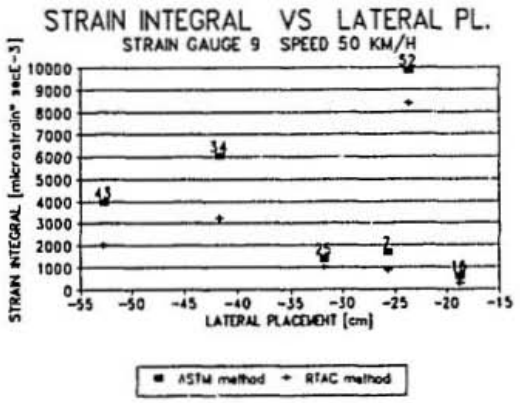

Strain gauge 10

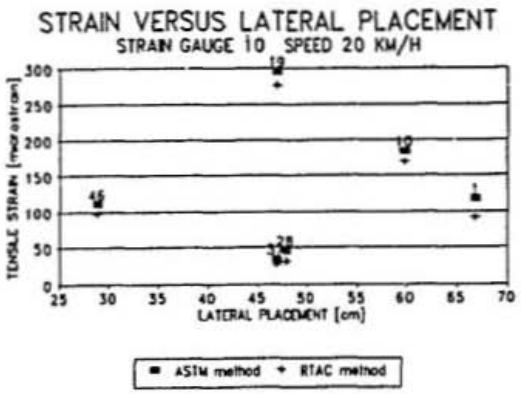

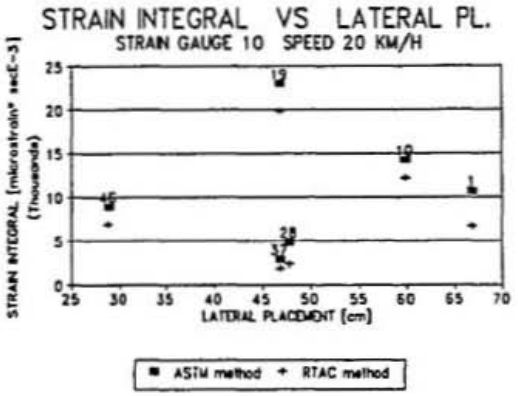

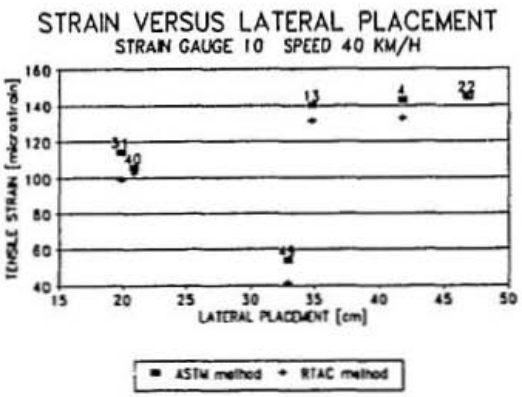

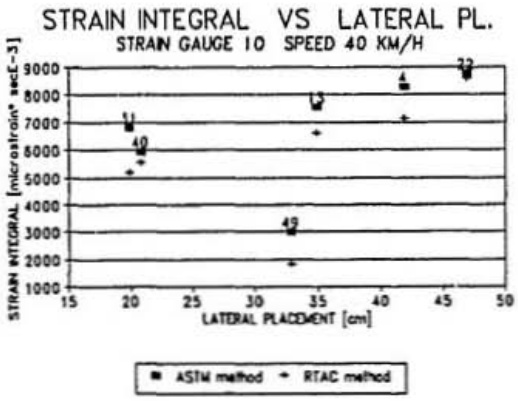

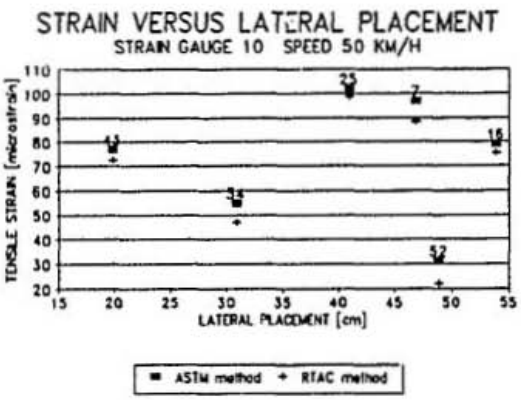

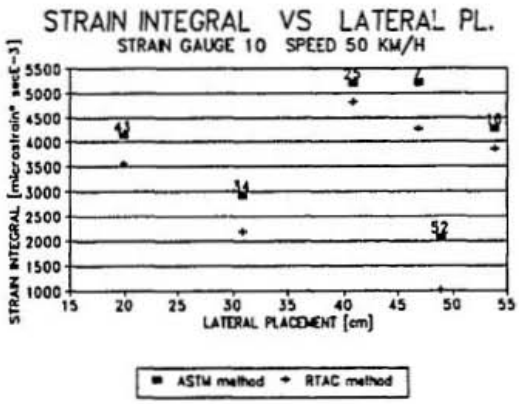

Strain gauge 11

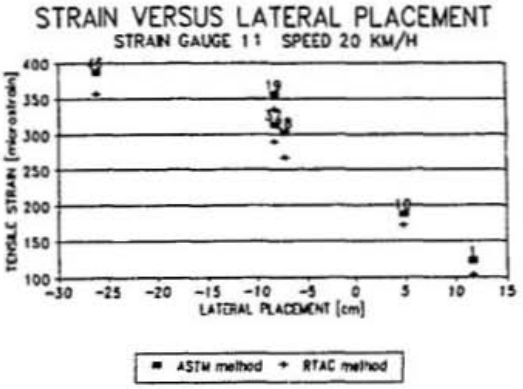

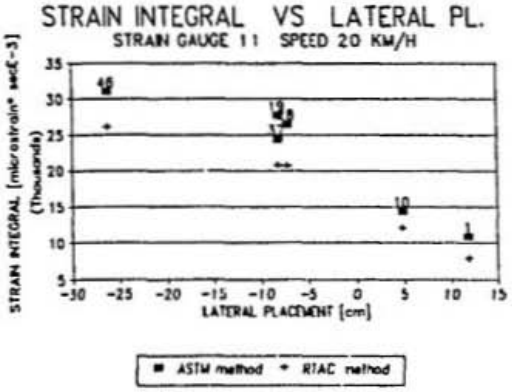

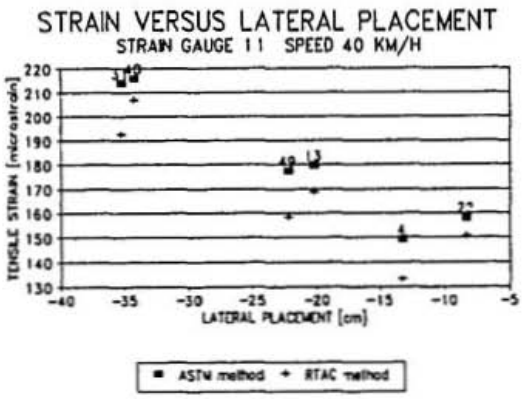

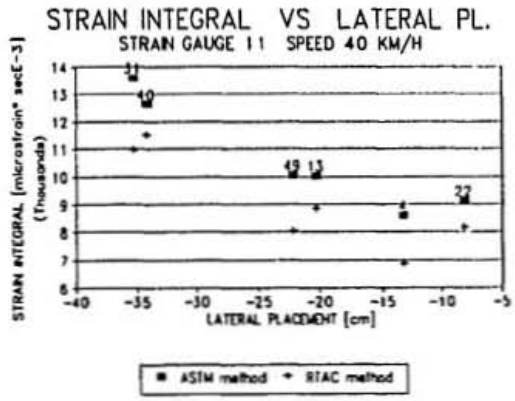

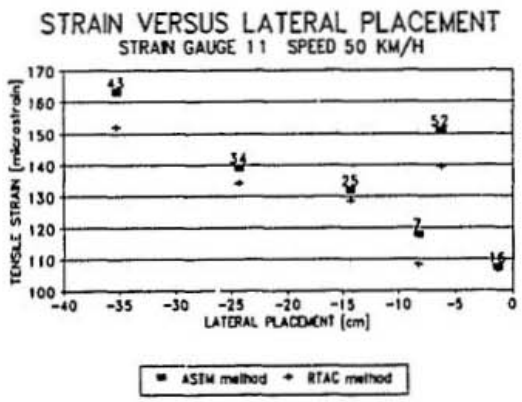

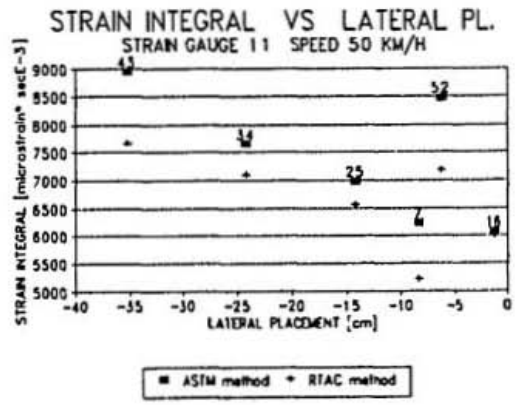

Strain gauge 12

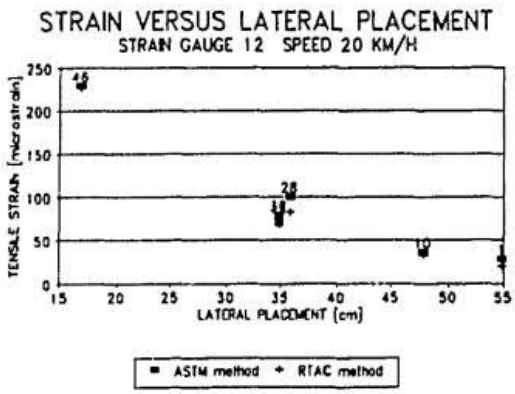

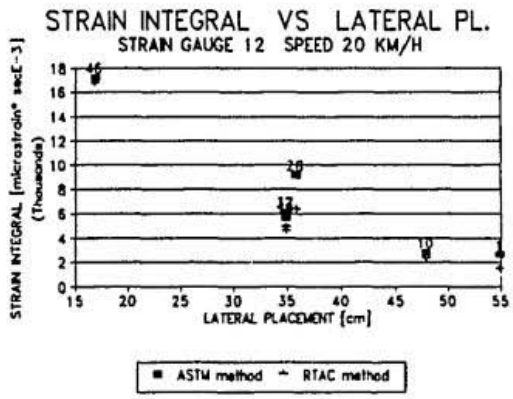

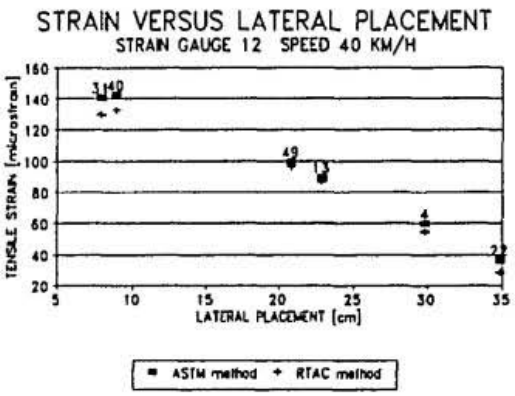

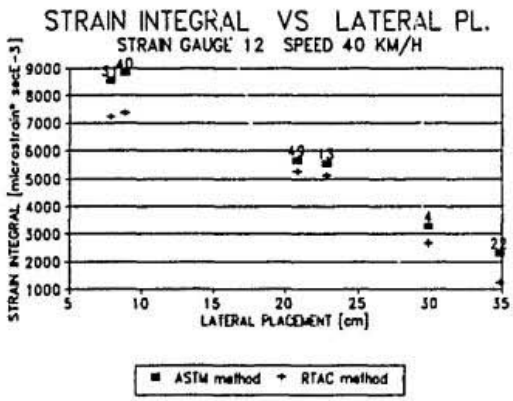

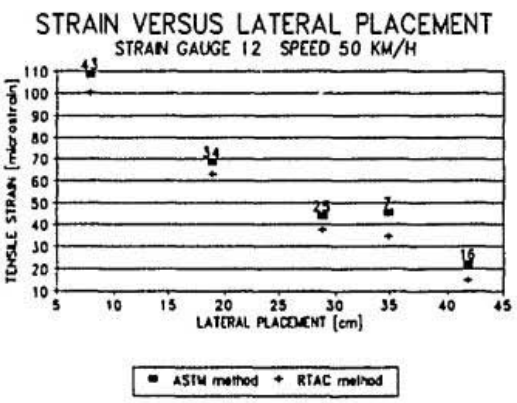

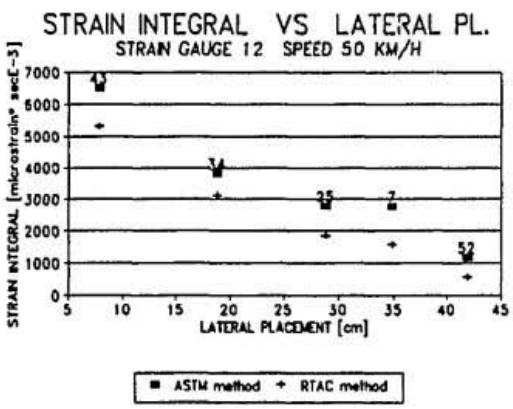

Appendix B

SOFTWARE FOR PROCESSING EXPERIMENTAL DATA

The following section describes the software developed as a work tool during the analysis stage. The computer program was written in Turbo Pascal(R) version 5.5 (Borland International, Inc.).

Given the diversity of strain versus time histories, and the complexity of strain cycle identification, the program was not intended to automatically perform all the pertinent operations. Instead, the main decisions are made by the user, based on numerical information provided at the run time.

Usually, each run was monitored during five seconds, with a sampling rate of 1000 times per second. As a result, after the analog to digital conversion, files recording 5000 strain values were obtained. From a memory management point of view, the use of an array was early discarded, selecting instead pointer related dynamic memory allocation techniques, namely the Doubly Linked List structure. In such a list structure, each record contains data (the strain value in this case), and two pointers linking the current record to the previous and the next records. As a result, the list can be processed backward and forward.

A first step in strain versus time histories processing is the elimination of the noise preceding and following the strain

response produced by an experimental vehicle. This noise corresponds to the "no load" condition, and is irrelevant for the analysis. Figure B.1 presents the complete strain versus time history for Run 2, induced by a 3-axle truck and sensed by the strain gauge S3.

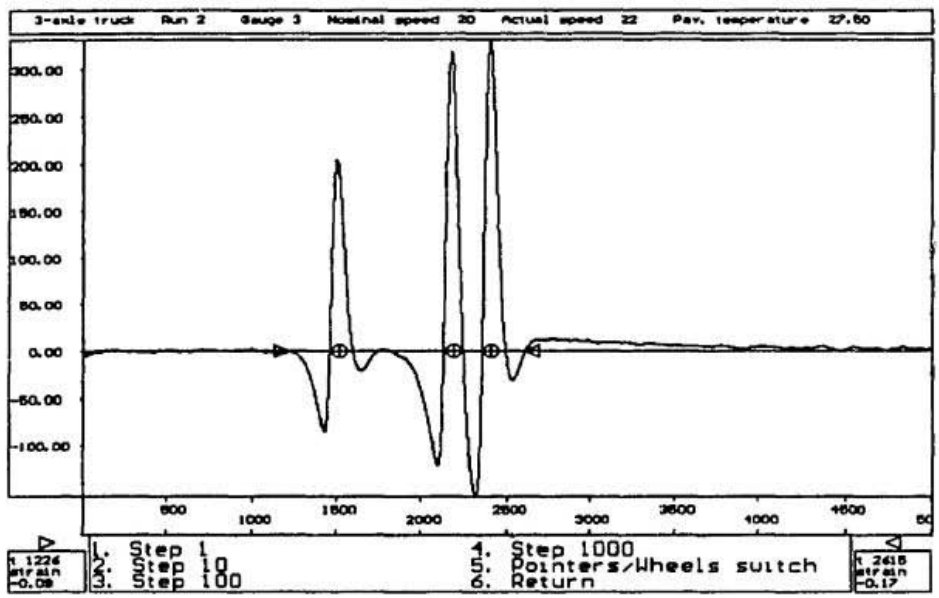

Figure B.1 : Strain versus time history for Run 2, gauge 3.

This strain versus time history had a good quality, with low noise and well defined strain peaks. However, other histories investigated presented high level of noise, and as a result the tensile strain peak produced by the lighter steering axles was difficult to identify. The solution was the simulation of the truck configuration, based on the actual speed of the vehicle and the distance between the axles. The

simulated vehicle, represented by three circles in Figure B.1, can slide along the time axis, using the arrow keys of the keyboard. If the strain peaks generated by the tandem are easy to recognize, the tandem group of the simulated vehicle should be aligned under the tandem peaks. As a result, the position of the strain peak produced by the steering axle should be indicated by the position of the steering axle.

When the main components of the strain versus time history are recognized, its start and end have to be identified, in order to separate and eliminate the noise. This was accomplished by using two screen arrows which can be slide along the strain versus time history. The position of each arrow along the time axis, and the strain corresponding to that position, are indicated in two windows at the bottom of the screen (Figure B.1). The left window reflects the movement of the left arrow, while the right one corresponds to the right arrow. The movement step of both arrows is keyboard controlled, the built-in steps being 1, 10, 100, and 1000 miliseconds. Figure B.1 presents the arrows positioned at the extremes of the strain versus time history.

Figure B.2 presents the same history after the noise elimination. This was the start for identification and processing of individual strain cycles. According to the ASTM Range-Pair Method, after a cycle is processed, the strain

versus time history must be rebuild without the two reversals which defined the first range of that cycle (Section 3.7.4). The Doubly Linked List approach proved to be the most suited for such an operation, realized simply by pointer swapping. The screen arrows in Figure B.2 limit the first strain cycle which had the first range smaller than the second one (for details about the procedure, see Section 3.7.4).

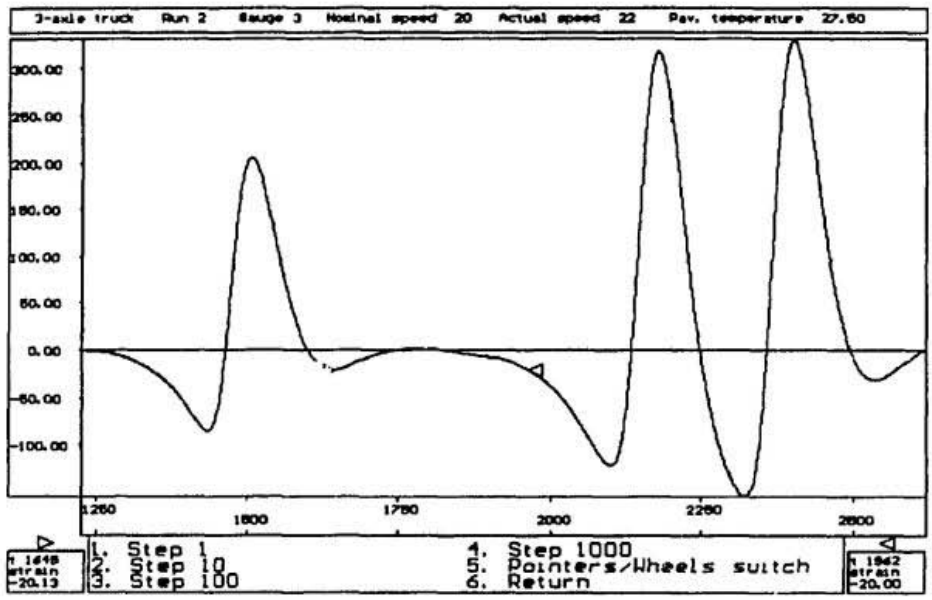

Figure B.2 : Identification of the first strain cycle.

For the example selected, the first cycle was the cycle between the steering axle and the tandem group.

Figure B.3 presents the isolated cycle and numerical values obtained by processing it, namely cycle duration, peak and integral values under both ASTM and RTAC cycle definitions.

Also, the maximum and the minimum strain values are recorded. Figures B.4 and B.5 present the identification of the second cycle to be extracted. Follow Figures B.6 and B.7 for the first tandem axle, and Figures B.8 and B.9 for the second tandem axle. Figure B.10 presents the remaining compressive cycle, which should be discarded according to the mode of failure selected.

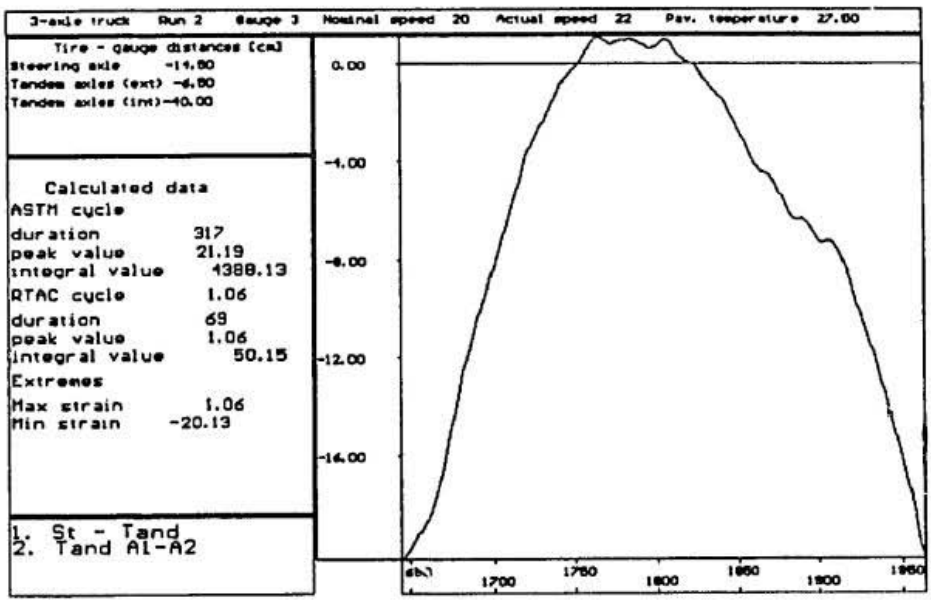

Figure B.3 : Processing of the first strain cycle.

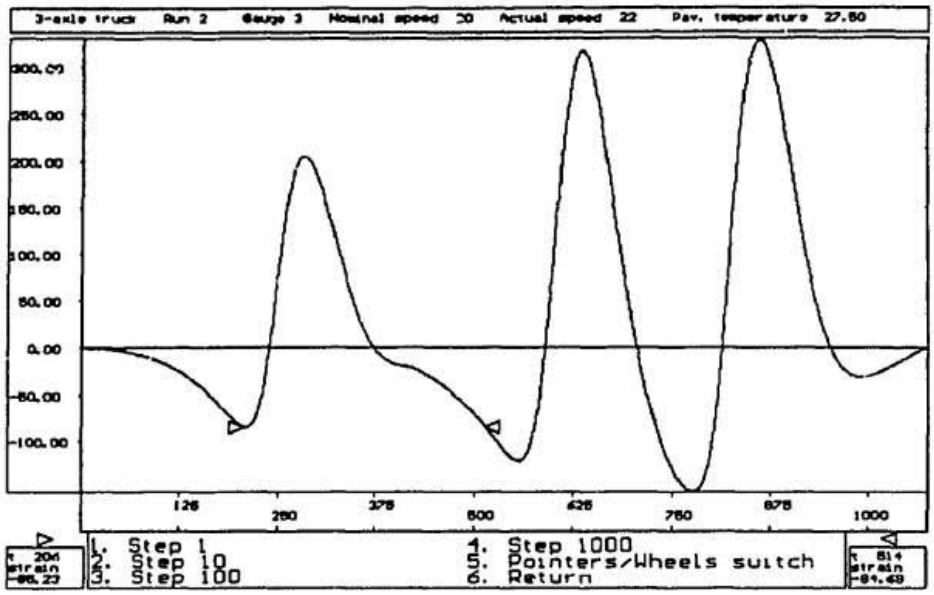

Figure B.4 : Identification of the second strain cycle.

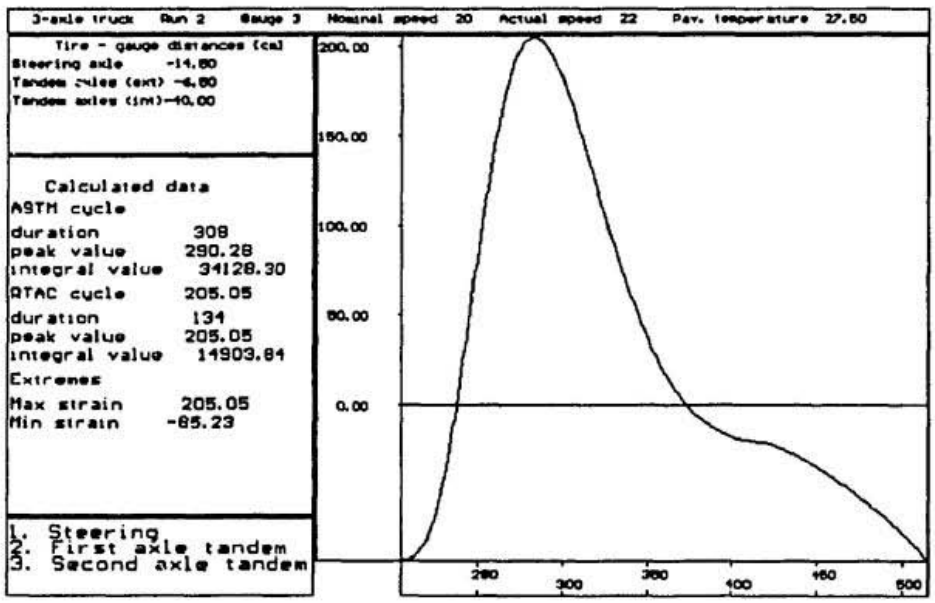

Figure B.5 : Processing of the second strain cycle.

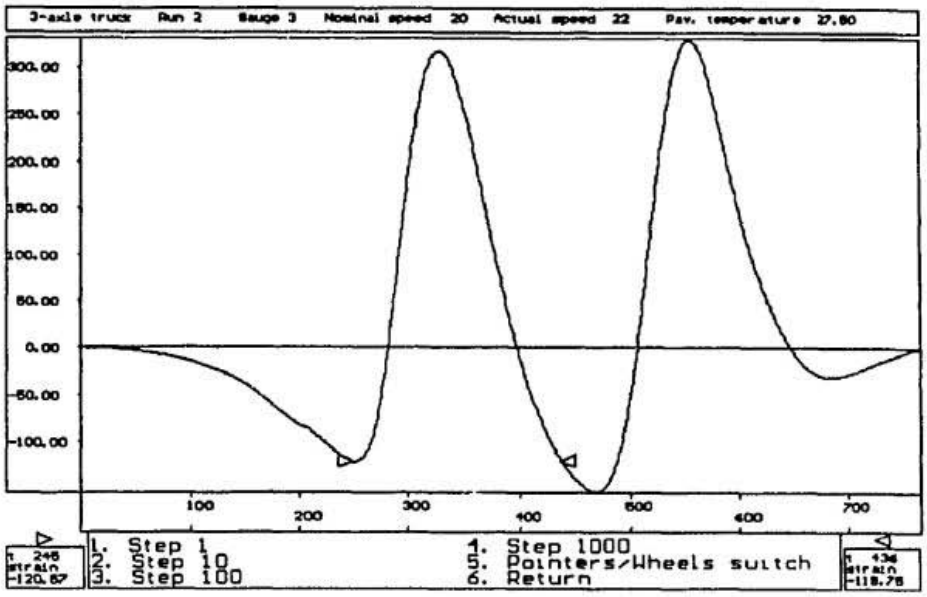

Figure B.6 : Identification of the third strain cycle.

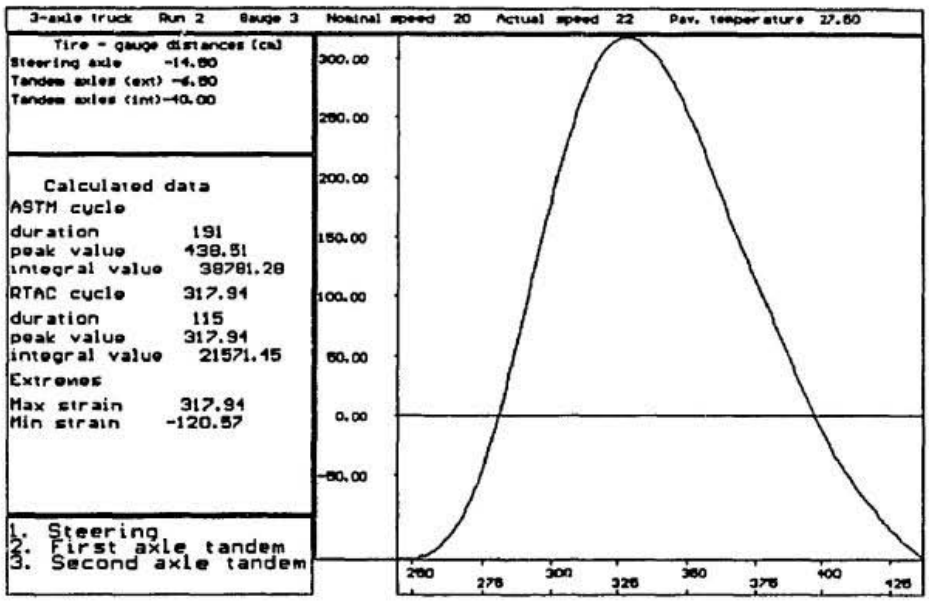

Figure B.7 : Processing of the third strain cycle.

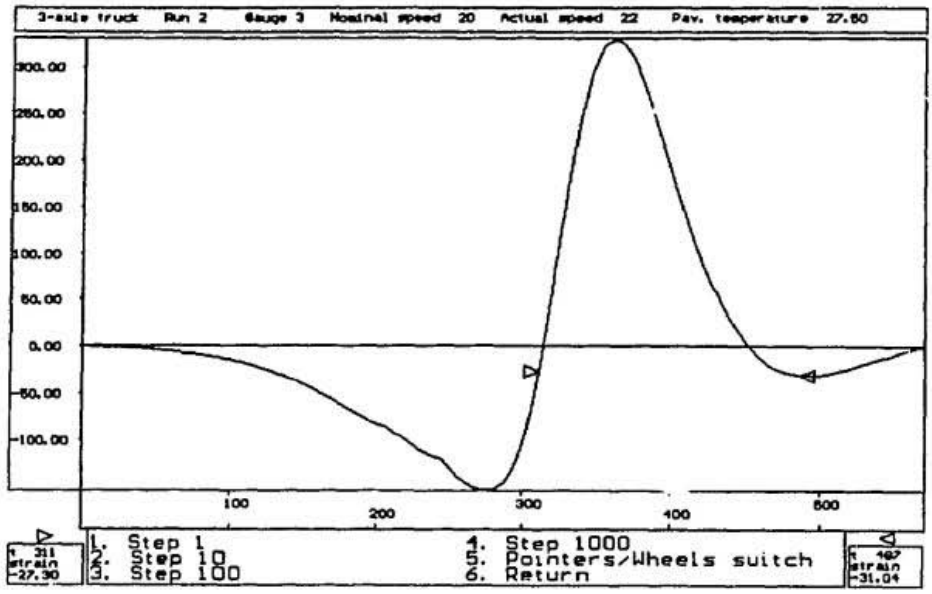

Figure B.8 : Identification of the fourth strain cycle.

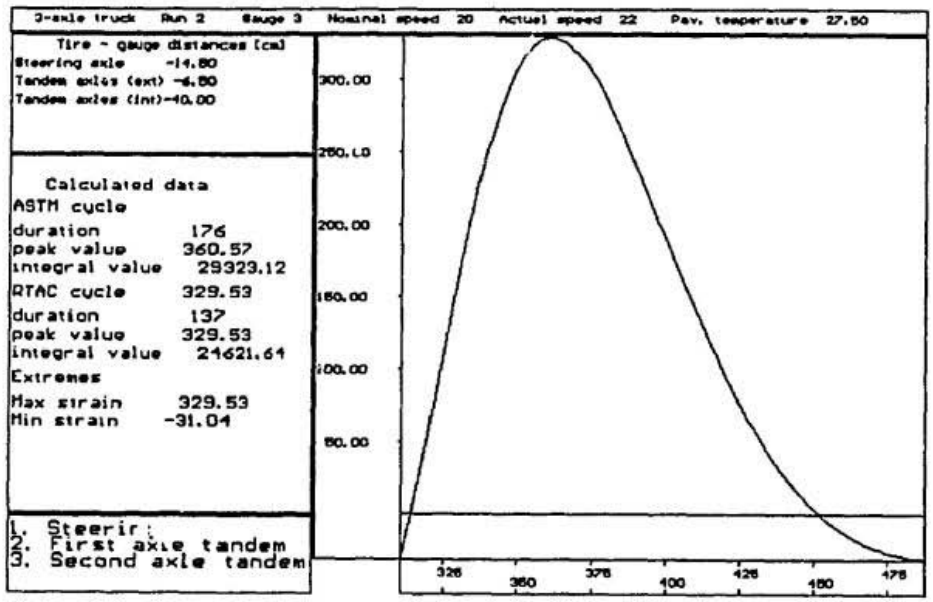

Figure B.9 : Processing of the fourth strain cycle.

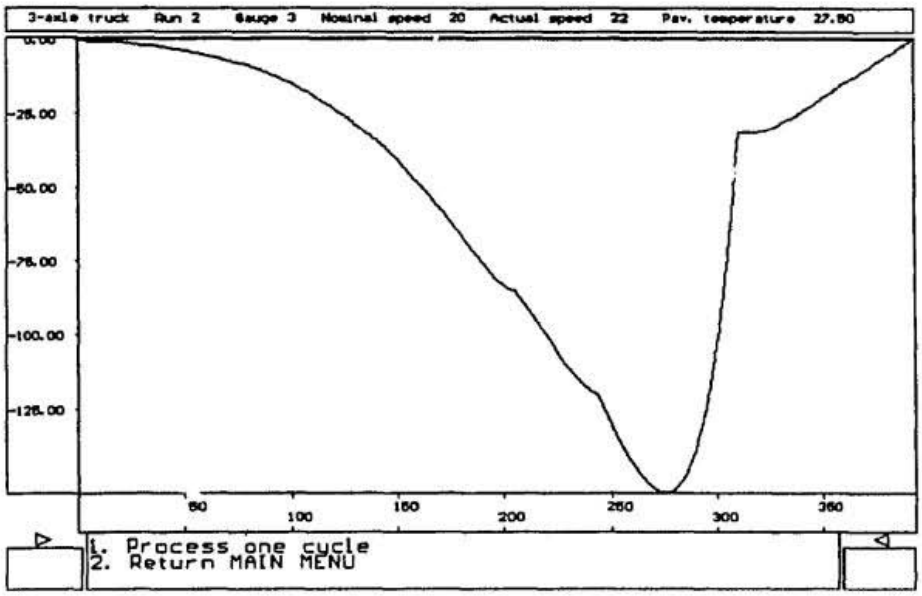

Figure B.10 : Compressive cycle resulted after the processing of the strain versus time history.

Appendix C : Load Equivalency Factors' Tables

C.1 LEF's Obtained by the ASTM Range-Pair Counting and the RTAC Method

Table C.1: LEF's for the 3-Axle Truck, Steering Axle, (ASTM Range-Pair Counting)

Speed [km/h]	Load 1	Load 2	Load 3
20	0.5	0.37	0.06
40	0.05	0.004	0.023
50	0.23	0.83	0.37

Table C.2: LEF's for the 3-Axle Truck, Steering Axle, (RTAC Method)

Speed [km/h]	Load 1	Load 2	Load 3
20	0.3	0.15	0.02
40	0.01	0.001	0.0007
50	0.05	0.13	0.04

Table C.3: LEF s for the 3-Axle Truck, Tandem, (ASTM Range-Pair Counting)

Speed [km/h]	Load 1	Load 2	Load 3
20	3.54	1.04	0.75
40	3.46	0.71	0.06
50	2.38	1.54	1.11

Table C.4: LEF's for the 3-Axle Truck, Tandem, (RTAC Method)

Speed [km/h]	Load 1	Load 2	Load 3
20	3.39	0.62	0.41
40	1.43	0.31	0.004
50	1.19	0.67	0.44

Table C.5: LEF's for the 3-Axle Truck, Complete Configuration, (ASTM Range-Pair Counting)

Speed [km/h]	Load 1	Load 2	Load 3
20	4.04	1.41	0.81
40	3.52	0.71	0.08
50	2.62	2.38	1.49

Table C.6: LEF's for the 3-Axle Truck, Complete Configuration, (RTAC Method)

Speed [km/h]	Load 1	Load 2	Load 3
20	3.7	0.77	0.42
40	1.45	0.31	0.004
50	1.24	0.81	0.48

Table C.7: LEF's for the 5-Axle Truck, Steering Axle, (ASTM Range-Pair Counting)

Speed [km/h]	Load 1	Load 2	Load 3
20	0.69	0.19	0.05
40	0.22	0.13	0.03
50	0.49	0.03	0.04

Table C.8: LEF's for the 5-Axle Truck, Steering Axle, (RTAC Method)

Speed [km/h]	Load 1	Load 2	Load 3
20	0.32	0.1	0.03
40	0.1	0.05	0.013
50	0.13	0.006	0.007

Table C.9: LEF's for the 5-Axle Truck, 1st Tandem, (ASTM Range-Pair Counting)

Speed [km/h]	Load 1	Load 2	Load 3
20	3	1.28	0.09
40	1.23	0.95	0.05
50	2.24	0.66	0.002

Table C.10: LEF's for the 5-Axle Truck, 1st Tandem, (RTAC Method)

Speed [km/h]	Load 1	Load 2	Load 3
20	1.13	0.56	0.05
40	0.41	0.18	0.016
50	0.43	0.11	0

Table C.11: LEF's for the 5-Axle Truck, 2nd Tandem, (ASTM Range-Pair Counting)

Speed [km/h]	Load 1	Load 2	Load 3
20	2.87	1.06	0.011
40	1.93	0.5	0.004
50	3.13	0.34	0.0005

Table C.12: LEF's for the 5-Axle Truck, 2nd Tandem, (RTAC Method)

Speed [km/h]	Load 1	Load 2	Load 3
20	1.56	0.53	0.007
40	1.06	0.14	0.002
50	0.85	0.11	0

Table C.13: LEF's for the 5-Axle Truck, Complete Configuration, (ASTM Range-Pair Counting)

Speed [km/h]	Load 1	Load 2	Load 3
20	6.57	2.54	0.15
40	3.4	1.58	0.09
50	5.86	1.03	0.048

Table C.14: LEF's for the 5-Axle Truck, Complete Configuration, (RTAC Method)

Speed [km/h]	Load 1	Load 2	Load 3
20	3.01	1.2	0.09
40	1.58	0.38	0.03
50	1.42	0.23	0.007

C.2 Comparison between LEF's obtained by different methods

Table C.15: LEF's for the 3-Axle Truck, Steering Axle, Speed 20 km/h

Load Code	Load 3	Load 2	Load 1
Weight [kg]	4020	4160	4200
ASTM	0.06	0.37	0.5
RTAC	0.02	0.15	0.3
AASHO	0.065	0.075	0.077

Table C.16: LEF's for the 3-Axle Truck, Steering Axle, Speed 40 km/h

Load Code	Load 3	Load 2	Load 1
Weight [kg]	4020	4160	4200
ASTM	0.023	0.004	0.05
RTAC	0.07	0.001	0.01
AASHO	0.065	0.075	0.077

Table C.17: LEF's for the 3-Axle Truck, Steering Axle, Speed 50 km/h

Load Code	Load 3	Load 2	Load 1
Weight [kg]	4020	4160	4200
ASTM	0.37	0.83	0.23
RTAC	0.04	0.13	0.05
AASHO	0.065	0.075	0.077

Table C.18: LEF's for the 3-Axle Truck, Tandem Axle, Speed 20 km/h

Load Code	Load 3	Load 2	Load 1
Weight [kg]	11240	13450	16300
ASTM	0.75	1.04	3.54
RTAC	0.41	0.62	3.39
AASHO	0.33	0.67	1.37

Table C.19: LEF's for the 3-Axle Truck, Tandem Axle, Speed 40 km/h

Load Code	Load 3	Load 2	Load 1
Weight [kg]	11240	13450	16300
ASTM	0.06	0.71	3.46
RTAC	0.004	0.31	1.43
AASHO	0.33	0.67	1.37

Table C.20: LEF's for the 3-Axle Truck, Tandem Axle, Speed 50 km/h

Load Code	Load 3	Load 2	Load 1
Weight [kg]	11240	13450	16300
ASTM	1.11	1.54	2.38
RTAC	0.44	0.67	1.19
AASHO	0.33	0.67	1.37

Table C.21: LEF's for the 3-Axle Truck, Complete Configuration, Speed 20 km/h

Load Code	Load 3	Load 2	Load 1
ASTM	0.81	1.41	4.04
RTAC	0.42	0.77	3.7
AASHO	0.398	0.745	1.447

Table C.22: LEF's for the 3-Axle Truck, Complete Configuration, Speed 40 km/h

Load Code	Load 3	Load 2	Load 1
ASTM	0.08	0.71	3.52
RTAC	0.004	0.31	1.45
AASHO	0.398	0.745	1.447

Table C.23: LEF's for the 3-Axle Truck, Complete Configuration, Speed 50 km/h

Load Code	Load 3	Load 2	Load 1
ASTM	1.49	2.38	2.62
RTAC	0.48	0.81	1.24
AASHO	0.398	0.745	1.447

Table C.24: LEF's for the 5-Axle Truck, Steering Axle, Speed 20 km/h

Load Code	Load 3	Load 2	Load 1
Weight [kg]	4320	4500	4790
ASTM	0.05	0.19	0.69
RTAC	0.03	0.1	0.32
AASHO	0.085	0.097	0.13

Table C.25: LEF's for the 5-Axle Truck, Steering Axle, Speed 40 km/h

Load Code	Load 3	Load 2	Load 1
Weight [kg]	4320	4500	4790
ASTM	0.03	0.13	0.22
RTAC	0.013	0.05	0.1
AASHO	0.085	0.097	0.13

Table C.26: LEF's for the 5-Axle Truck, Steering Axle, Speed 50 km/h

Load Code	Load 3	Load 2	Load 1
Weight [kg]	4320	4500	4790
ASTM	0.04	0.03	0.49
RTAC	0.002	0.002	0.1
AASHO	0.085	0.097	0.13

Table C.27: LEF's for the 5-Axle Truck, Tandem Axles, Speed 20 km/h

Load Code	Load 3		Load 2		Load 1	
Tandem	Tand 2	Tand 1	Tand 2	Tand 1	Tand 1	Tand2
Weight [kg]	2940	5020	9250	10950	16890	17550
ASTM	0.011	0.09	1.06	1.28	3.0	2.87
RTAC	0.007	0.05	0.53	0.56	1.13	1.56
AASHO	0.005	0.015	0.153	0.297	1.56	1.80

Table C.28: LEF's for the 5-Axle Truck, Tandem Axles, Speed 40 km/h

Load Code	Load 3		Load 2		Load 1	
Tandem	Tand 2	Tand 1	Tand 2	Tand 1	Tand 1	Tand2
Weight [kg]	2940	5020	9250	10950	16890	17550
ASTM	0.004	0.05	0.5	0.95	1.23	1.93
RTAC	0.002	0.016	0.14	0.18	0.41	1.06
AASHO	0.005	0.015	0.153	0.297	1.56	1.80

Table C.29: LEF's for the 5-Axle Truck, Tandem Axles, Speed 50 km/h

Load Code	Load 3		Load 2		Load 1	
Tandem	Tand 2	Tand 1	Tand 2	Tand 1	Tand 1	Tand2
Weight [kg]	2940	5020	9250	10950	16890	17550
ASTM	0.0005	0.002	0.34	0.66	2.24	3.13
RTAC	0	0	0.11	0.11	0.43	0.85
AASHO	0.005	0.015	0.153	0.297	1.56	1.80

Table C.30: LEF's for the 5-Axle Truck, Complete Configuration, Speed 20 km/h

Load Code	Load 3	Load 2	Load 1
ASTM	0.15	2.54	6.57
RTAC	0.09	1.2	3.01
AASHO	0.353	1.12	4.73

Table C.31: LEF's for the 5-Axle Truck, Complete Configuration, Speed 40 km/h

Load Code	Load 3	Load 2	Load 1
ASTM	0.09	1.58	3.4
RTAC	0.03	0.38	1.58
AASHO	0.353	1.12	4.73

Table C.32: LEF's for the 5-Axle Truck, Complete Configuration, Speed 50 km/h

Load Code	Load 3	Load 2	Load 1
ASTM	0.048	1.03	5.86
RTAC	0.007	0.23	1.42
AASHO	0.353	1.12	4.73

C.3 LEF's Obtained by Integrating the Strain Cycles

Table C.33: LEF's for the 3-Axle Truck, Steering Axle (Trough-Peak-Trough Cycle Integral)

Speed [km/h]	Load 1	Load 2	Load 3
20	1.15	2.9	0.21
40	0.09	0.006	0.073
50	1.21	20.54	3.07

Table C.34: LEF's for the 3-Axle Truck, Steering Axle, (Zero Strain-Peak-Zero Strain Cycle Integral)

Speed [km/h]	Load 1	Load 2	Load 3
20	0.22	0.11	0.009
40	0.007	0.0005	0.00008
50	0.04	0.21	0.025

Table C.35: LEF's for the 3-Axle Truck, Tandem (Trough-Peak-Trough Cycle Integral)

Speed [km/h]	Load 1	Load 2	Load 3
20	2.54	0.84	0.48
40	3.16	0.56	0.04
50	1.82	1.19	0.97

Table C.36: LEF's for the 3-Axle Truck, Tandem, (Zero Strain-Peak-Zero Strain Cycle Integral)

Speed [km/h]	Load 1	Load 2	Load 3
20	2.43	0.32	0.15
40	0.79	0.16	0.0003
50	0.78	0.41	0.26

Table C.37: LEF's for the 3-Axle Truck, Complete Configuration, (Trough-Peak-Trough Cycle Integral)

Speed [km/h]	Load 1	Load 2	Load 3
20	3.69	3.74	0.69
40	3.26	0.57	0.12
50	3.03	21.73	3.94

Table C.38: LEF's for the 3-Axle Truck, Complete Configuration, (Zero Strain-Peak-Zero Strain Cycle Integral)

Speed [km/h]	Load 1	Load 2	Load 3
20	2.66	0.43	0.16
40	0.79	0.16	0.0004
50	0.82	0.62	0.28

Table C.39: LEF's for the 5-Axle Truck, Steering Axle, (Trough-Peak-Trough Cycle Integral)

Speed [km/h]	Load 1	Load 2	Load 3
20	2.22	0.46	0.05
40	0.42	0.26	0.05
50	4.34	0.04	0.09

Table C.40: LEF's for the 5-Axle Truck, Steering Axle, (Zero Strain-Peak-Zero Strain Cycle Integral)

Speed [km/h]	Load 1	Load 2	Load 3
20	0.25	0.09	0.026
40	0.06	0.04	0.008
50	0.1	0.002	0.002

Table C.41: LEF's for the 5-Axle Truck, 1st Tandem,

(Trough-Peak-Trough Cycle Integral)

Speed [km/h]	Load 1	Load 2	Load 3
20	6.75	1.79	0.12
40	3.32	12.63	0.08
50	3.13	6.04	0.001

Table C.42: LEF's for the 5-Axle Truck, 1st Tandem,

(Zero Strain-Peak-Zero Strain Cycle Integral)

Speed [km/h]	Load 1	Load 2	Load 3
20	0.7	0.32	0.03
40	0.24	0.12	0.009
50	0.13	0.06	0

Table C.43: LEF's for the 5-Axle Truck, 2nd Tandem,

(Trough-Peak-Trough Cycle Integral)

Speed [km/h]	Load 1	Load 2	Load 3
20	3.23	1.58	0.013
40	2.0	0.72	0.005
50	2.99	0.38	0.0004

Table C.44: LEF's for the 5-Axle Truck, 2nd Tandem, (Zero Strain-Peak-Zero Strain Cycle Integral)

Speed [km/h]	Load 1	Load 2	Load 3
20	0.99	0.34	0.004
40	0.71	0.07	0.005
50	0.32	0.08	0

Table C.45: LEF's for the 5-Axle Truck, Complete Configuration, (Trough-Peak-Trough Cycle Integral)

Speed [km/h]	Load 1	Load 2	Load 3
20	12.2	3.83	0.18
40	5.75	13.62	0.14
50	10.47	6.47	0.09

Table C.46: LEF's for the 5-Axle Truck, Complete Configuration, (Zero Strain-Peak-Zero Strain Cycle Integral)

Speed [km/h]	Load 1	Load 2	Load 3
20	1.94	0.75	0.06
40	1.02	0.24	0.02
50	0.56	0.15	0.002